To the Graduate Council:

I am submitting herewith a thesis written by Amy L. Halleran entitled "Comparison of hydrologic cycle components for pre-storm and storm conditions, Walker Branch Watershed, Oak Ridge Reservation". I have examined the final copy of this thesis for form and content and recommend it be accepted in partial fulfillment of the requirements for the degree of Master of Science, with a major in Geology.

Claudia I. Mora, Major Professor

We have read this thesis
and recommend its acceptance:

Ronit Nativ

Accepted for the Council:

Associate Vice Chancellor and
Dean of the Graduate School

Statement of Permission to Use

In presenting this thesis in partial fulfillment of the requirements for a master's degree at The University of Tennessee, Knoxville, I agree that the Library shall make it available to borrowers under rules of the library. Brief quotations from this thesis are allowable without special permission, provided that accurate acknowledgment of the source is made.

Permission for extensive quotation from or reproduction of this thesis may be granted by my major professor, or in her absence, by Head of Interlibrary Services when, in the opinion of either, the proposed use of the material is for scholarly purposes. Any copying or use of the material in this thesis for financial gain shall not be allowed without my written permission.

Signature Amy L. Hallman

Date 1/2/95

Comparison of Hydrologic Cycle Components for Pre-storm and Storm Conditions, Walker Branch Watershed, Oak Ridge Reservation

A Thesis

Presented for the

Master of Science

Degree

The University of Tennessee, Knoxville

Amy L. Halleran

May 1995

Dedication

This thesis is dedicated to

my parents

Mr. & Mrs. John H. Halleran,

my fiance

Mr. Brian T. Sheldon

and Molson Sheldon, the cat,

who have given me invaluable support.

Acknowledgments

I would like to thank my major professor, Claudia I. Mora, for her guidance, patience, and tolerance. She gave me enough freedom to explore without letting me get lost. I would also like to thank my committee members, Dr. Ronit Nativ, Dr. Robert D. Hatcher Jr., and Dr. Patrick J. Mulholland, for their guidance and assistance over the past three years. Dr. Ronit Nativ was especially helpful in providing a Research Assistantship with the Environmental Sciences Division at the Oak Ridge National Laboratory. I would like to thank the secretaries in the Geology Department, Cindy Turner, Denise Stansberry, and Melody Branch, for their assistance in many thankless oddities and the occasional good laugh. Dr. Bill Dunne was very kind in allowing me to use his computers for nearly every deadline I faced.

There were several people at the Oak Ridge National Laboratory that assisted in one way or another towards the completion of this thesis. I would like to thank Lee Cooper, Dave Wesolowski, Juske Horita, and Dave Cole for their kindness and the use of their laboratory facilities. I am grateful to Bonnie Lu for collecting weekly stream and spring samples. Don Todd was gracious to lend me soil coring devices and other field and lab instruments. Phil Jardine, although he doesn't realize it, answered many questions and was always cheerful when I came pondering.

I am especially grateful to Robert Gregory of the Geology Department at Southern Methodist University, and Charles B. Douthitt at Oztech Trading Corporation, for "lending" a hydrogen standard to Ian Richards so that my thesis could be completed. Without this standard, the hydrogen line at the University of Tennessee might still be "out to lunch."

I would also like to thank the many friends I met in Tennessee who made this town enjoyable to a Yankee gal. You know who you are. Ian Richards' sense of humor, guidance in the Isotope Lab, and bodily sacrifices made for the sake of this thesis are especially appreciated. To Arnold Hunley and Charlie Lamb I am "tickled" with the new southern vocabulary. I am always grateful to Brian T. Sheldon for putting up with me, and to Molson the Cat, a.k.a. Miss Molly, who is always happy to see me. Miss Molly could always cheer me.

Abstract

The hydrology of the West Fork of Walker Branch Watershed, a 38.4 ha forested experimental watershed located on the Oak Ridge Reservation in the Valley and Ridge Province of eastern Tennessee, has been studied using oxygen and hydrogen isotopes, and silica as tracers of stream water source. To assist in characterization of water recharging the watershed, the local meteoric water line was determined to be equivalent to the global meteoric water line. The global meteoric water line describes local precipitation and potential groundwater recharge on the Oak Ridge Reservation and surrounding region.

Within the watershed, several possible storm flow components have previously been identified including groundwater within the bedrock and at the soil/bedrock interface, saturated soil water occurring at shallow depths (storm flow zone), and precipitation. A December 15 - 19, 1992 storm event was examined to determine sources of stream flow. Two component ("new" water and "old" water) and three component (precipitation, soil water, and groundwater) end-member mixing models using oxygen isotopes and silica as tracers have been applied. The two end-member separations yielded a "new" water (event precipitation) contribution of 1 - 16% of total stream storm flow at the base of the watershed, and 3 - 19% of total stream flow at one ephemeral stream site. The three component model applied to stream flow at the base of the

watershed indicates that "new" water contributed 1 - 5%, soil water 48 - 52%, and groundwater 45 - 52% of the total stream storm flow. "New" water was determined to contribute 2 - 10%, soil water 40 - 96%, and groundwater 15 - 50% of stream storm flow at the ephemeral stream site. Old soil water and groundwater dominated storm flow at both stream sites. The significant contribution of soil water to storm flow at both stream sites and flow through a subsurface weir support previous suggestions of the importance of a shallow storm flow zone developing within the upper 2 m of the soil column during a storm event. The large role of groundwater in storm stream flow indicates a rapid deeper subsurface flowpath through the soil column.

Table of Contents

List of Tables

List of Figures

I. Introduction

The response of a watershed to precipitation events has been the focus of many investigations of stream hydrology, water resource management, and contaminant migration. This study details the response of the West Fork of Walker Branch, a well-studied 38.4 ha watershed within the Oak Ridge Reservation, eastern Tennessee, to precipitation events ("storms"). Identification of the dominant sources of storm flow, their relative importance in producing stream flow, and timing of appearance are critical in deciphering catchment hydrology. Hydrologic budgets for all of Walker Branch Watershed have indicated that stream flow is approximately 52% of annual precipitation, with storm flow accounting for about 23% of the annual stream flow (Luxmoore and Huff, 1989).

The objectives of this study were to assess the various contributions to storm flow and identify the methods and timing of groundwater recharge and discharge in this watershed. This was accomplished by: 1) hydrologic, chemical and isotopic monitoring of all the components of the hydrologic cycle, and 2) determining the hydrologic end-members and their relative proportions in storm flow using stable isotope and chemical tracers. To assist in determining sources and timing of aquifer recharge, a local meteoric water line was established. Seasonal variations in groundwater recharge and discharge were identified.

Defining the hydrologic response of the Walker Branch Watershed to precipitation events enables a better understanding of the mechanisms of the subsurface recharge and flow and solute migration. The Walker Branch Watershed is underlain by carbonate rocks of the Knox Group, a major aquifer for much of eastern Tennessee in the Valley and Ridge Province. Understanding the recharge to this aquifer and its role in producing surface storm flow would be helpful in assessing the pathways and rates of contaminant migration in the Knox Group residuum. The fate of groundwater contaminants from shallow organic and inorganic waste burial sites in the vadose zone has been the focus of several ongoing projects on the Oak Ridge Reservation. The results of this study are also relevant to other watersheds in the Valley and Ridge, and Piedmont Provinces, which share similar low-permeability, fracture-dominated geologic media.

II. Controls on Storm Flow Components

Stable oxygen and hydrogen isotopes and solutes (i.e. Si) have been used extensively as conservative tracers to determine the proportions of storm flow components (i.e. vadose waters, groundwater, and precipitation). The individual contributions of these components to storm flow can be estimated using mixing models previously developed to explain the response of various watersheds to precipitation events (McKeague and Cline, 1963; Kennedy, 1971; Sklash and Farvolden, 1979; Bottomley et al., 1986; Hooper and Shoemaker, 1986; Kennedy et al., 1986; Pearce et al., 1986; Sklash et al., 1986; DeWalle et al., 1988; Ingraham et al., 1991; Space et al., 1991; Stewart and McDonnell, 1991). The end-member proportions contributing to surface flow during storms depend on numerous factors, including pre-storm soil moisture conditions, watershed relief, stream channel width, and depth to soil/rock interface (Kennedy et al., 1986). For a particular watershed, all elements of the hydrologic cycle must be considered to determine their relative contribution to storm surface and subsurface flow. The following section addresses each of the possible storm flow components, and the effects evaporation has on their isotopic signatures.

Evaporation effects on precipitation, soil and surface waters

The isotopic composition of rainfall may vary seasonally because of evaporation followed by fractionation. Increased evaporation may cause isotopic enrichment of summer precipitation compared to winter precipitation (Nativ and Riggio, 1990; Ingraham et al., 1991). Previous studies (Pearce and Rowe, 1981; Stewart and McDonnell, 1991; Pearce et al., 1986) have indicated that evaporation of precipitation on a watershed canopy may occur at rates of 0.1-0.5 mm/hr, resulting in ^{18}O and ^{2}H enrichment of the throughfall. Gat and Tzar (1967) determined that the enrichment of ^{18}O in throughfall caused by evaporation of rainfall on the forest canopy does not exceed 0.5‰. More recently, Kendall and McDonnell (1993) studied the oxygen and hydrogen isotope compositions of throughfall and rainfall for 30 storm events in Georgia. For an average interception loss of 15%, the volume-weighted average throughfall signature was enriched by 0.5‰ in ^{18}O and 3‰ in deuterium relative to open rainfall. Additionally, they found a 0.1‰ average enrichment in ^{18}O of throughfall at conifer sites relative to deciduous sites. Other studies have shown these and other such variations are insignificant compared to the analytical precision of isotope measurement (Pearce and others, 1986). If their is a significant difference between the isotopic signatures of rainfall and throughfall for a given area, then throughfall, the portion of

precipitation that reaches the ground surface should be sampled to represent precipitation recharging the groundwater system (DeWalle et al., 1988). Kendall and McDonnell (1993) suggested using either one open rainfall collector that can later be corrected for canopy evaporation, or using several throughfall collectors, one placed under each tree type present in the forested watershed.

Evaporation of stream water and soil water may also occur prior to or during a precipitation event. This would cause isotopic enrichment of the remaining ("old") waters, and affect the isotopic signature of water contributed to storm flow. Zimmermann and others (1967), determined that plant transpiration resulted in no detectable isotopic enrichment of soil water.

Precipitation

Precipitation constitutes "new" water added to existing water in the watershed. Because silica usually occurs in only trace amounts in precipitation (Likens et al., 1977; Mulholland et al., 1990; Hirata and Muraoka, 1993; Shimada et al., 1993), the "new" water storm flow component can be easily identified using silica as a tracer. The silica concentration of "new" water may change when the water is introduced to

soil, where additional dissolved silica may be added (Kennedy et al., 1986; Hinton et al., 1994).

Oxygen and hydrogen isotope ratios of precipitation are affected by several variables, such as elevation, moisture source, distance traveled, altitude of travel, and topography, which are all temperature related (Dansgaard, 1964). In addition, the isotopic composition of precipitation may vary during an event (Sklash and Farvolden, 1979; Kennedy et al., 1986). Comparison of the isotopic ratios ($^{18}O/^{16}O$ or $^{2}H/^{1}H$) of local precipitation to the world meteoric water line (Craig, 1961a) may reveal the relative isotopic enrichment or depletion of the local precipitation. This approach has been useful in determining the timing, methods, and locations of groundwater recharge (Nativ and Smith, 1987; Dutton and Sympkins, 1989).

The proportion of precipitation contributing to storm flow varies due to precipitation amount and intensity, watershed dimensions, pre-storm soil moisture, depth to soil/rock interface and climate (Sklash and Farvolden, 1979; Pearce et al., 1986; Sklash et al., 1986; DeWalle et al., 1988; Ingraham et al., 1991). Sklash and Farvolden (1979) generalized that a relatively dry drainage basin receiving intense precipitation would result in storm flow dominated by precipitation (new water). A precipitation event with moderate intensity in a relatively wet, humid basin would result in

groundwater ("old" water) dominated storm flow. These responses may depend on the development of groundwater "ridging" (Ragan, 1968), which will be further explained within the **Groundwater** section.

Surface water

Surface water, or storm runoff, has been examined in many studies to determine if storm flow is dominated by "new" water derived from that event's precipitation or "old" groundwater and/or vadose zone water. There are several possible sources of storm runoff: 1) direct channel precipitation (Hewlett, 1982); 2) overland or Hortonian flow of precipitation that fails to infiltrate the soil (Horton, 1933); 3) subsurface storm flow, defined as water following subsurface flowpaths that arrives at the stream channel fast enough to become a part of the storm hydrograph (Hewlett and Hibbert, 1963; Whipkey, 1965; Mosley, 1979); and 4) groundwater (Fritz et al., 1976; Sklash et al., 1976). Overland flow may occur near the stream channels when raised water table levels reach the land surface or expansion of the stream channel during a storm event (Hewlett and Hibbert, 1967; Freeze, 1974).

Vadose water

Vadose water may contribute significantly to storm flow as parts of the vadose zone become temporarily saturated. Suggested mechanisms responsible for the appearance of vadose water in storm flow include: 1) overland flow caused rises in the water table (Sklash et al., 1979); 2) macropore flow in which a portion of the soil water bypasses the bulk soil matrix (Pearce et al., 1986; Hooper et al., 1990; McDonnell, 1990; Wilson et al., 1991a, b); 3) piston or saturated matrix flow whereby "old" water is displaced by "new" water (Zimmermann et al., 1966; Kennedy et al., 1986; DeWalle et al., 1988; Hooper et al., 1990); and 4) transient perched water tables (Wilson et al., 1991a).

The isotopic and/or chemical compositions of water in the unsaturated zone and groundwater were assumed to be relatively similar in previous studies (Sklash and Farvolden, 1979; Pearce et al., 1986; Sklash et al., 1986; Bottomley et al., 1986). Later studies (Kennedy et al., 1986; DeWalle et al., 1988; Shimada et al., 1993) indicated that these waters may have different chemical and isotopic signatures and therefore should not be lumped together. For example, DeWalle and others (1988) found that vadose zone water contributed 24.1% of storm flow whereas 75% was contributed by groundwater.

Parent geology and soil chemistry determines the silica concentration

of soil waters (Hirata and Muraoka, 1993). Soil water silica concentrations may vary temporally and spatially (both vertically and laterally) with changing geology and soil type. The silica concentration of soil waters along a flowpath continuously evolves as soil chemistry changes (Shimada et al., 1993; Hirata and Muraoka, 1993). The resulting silica concentration of groundwater recharged by vadose water is thus dependent on the evolution of silica along the flowpath. However, in general, the silica concentration of groundwater is greater then that of soil water, unless large evaporative concentration occurs.

Groundwater

Groundwater is generally considered "old water" and, in varying proportions, contributes to storm flow (Sklash and Farvolden, 1979; Pearce et al., 1986; DeWalle et al., 1988). Mechanisms which cause an increase in groundwater contribution include: 1) infiltrating precipitation displacing groundwater within pores of the saturated soil matrix (Freeze, 1974), and 2) infiltrating waters causing rises in water tables and thus an increase in hydraulic head. Groundwater levels may rise during a storm event, particularly near a stream (Sklash and Farvolden, 1979). Sklash and Farvolden (1979) determined that a moderately intense rain storm in a very wet basin would result in groundwater-dominated storm flow due to the

increase in hydraulic head in the vicinity of the stream channel ("ridging"). Groundwater ridging is believed to develop as a result of the rapid conversion of near-surface tension-saturated capillary fringe into phreatic water soon after a precipitation event begins. Expansion of the stream channel as a result of groundwater ridging creates a larger groundwater discharge area, thereby increasing the amount of groundwater capable of becoming a part of the storm flow

III. The Study Area

Location and topography

The study was conducted in the West Fork of the Walker Branch Watershed, a 38.4 ha forested watershed located on the Oak Ridge Reservation in the Valley and Ridge Province of eastern Tennessee (Fig. 1). The topography of Walker Branch Watershed is characterized by broad ridges with moderate slopes and narrow stream valleys (Fig. 2), typical of the Knox Group in the Valley and Ridge Province. Total relief within the watershed is approximately 80 m, with the highest point occurring along the northern ridge crest.

Climate and vegetation

The mean annual temperature is 14.5 °C and the mean annual precipitation is approximately 1400 mm, with significantly greater precipitation occurring during the winter and summer months than spring and fall (Luxmoore and Huff, 1989). Vegetative cover consists primarily of oak and hickory with lesser amounts of pine on the ridges and tulip poplar and beech near the stream (Luxmoore and Huff, 1989; Genereux et al., 1992). Evapotranspiration has been estimated at 730 mm/yr based on differences in precipitation and runoff for several watersheds on the Oak

Figure 1. Geologic map of the Oak Ridge Reservation (after Hatcher et al., 1992), showing the general locations of the reservation and the Walker Branch Watershed.

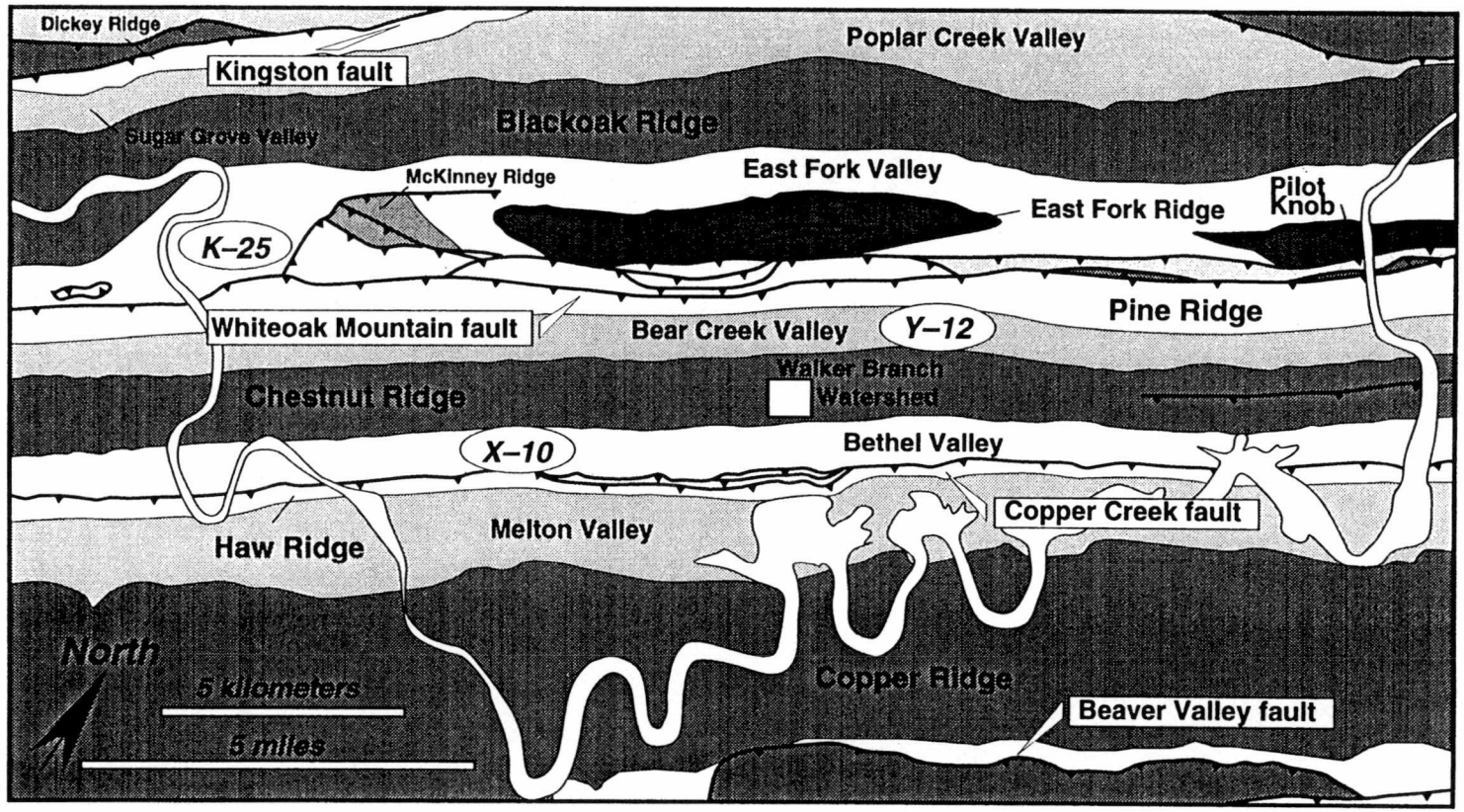
Dickey Ridge
Poplar Creek Valley
Kingston fault
Blackoak Ridge
Sugar Grove Valley
McKinney Ridge
East Fork Valley
East Fork Ridge
Pilot Knob
K-25
Pine Ridge
Whiteoak Mountain fault
Bear Creek Valley
Y-12
Walker Branch Watershed
Chestnut Ridge
X-10
Bethel Valley
Copper Creek fault
Haw Ridge
Melton Valley
North
5 kilometers
5 miles
Copper Ridge
Beaver Valley fault
Rome Formation
Conasauga Group
Knox Group
Chickamauga Group
Reedsville Shale & younger Rocks
ORR
Knoxville

Figure 2. The West Fork of Walker Branch Watershed. Geologic units labeled represent the following: Ccr = Cambrian Copper Ridge Dolomite; Oc = Ordovician Chepultepec Dolomite; Olv = Ordovician Longview Dolomite; Ok = Ordovician Kingsport Formation. Geology by Hatcher and others, 1992.

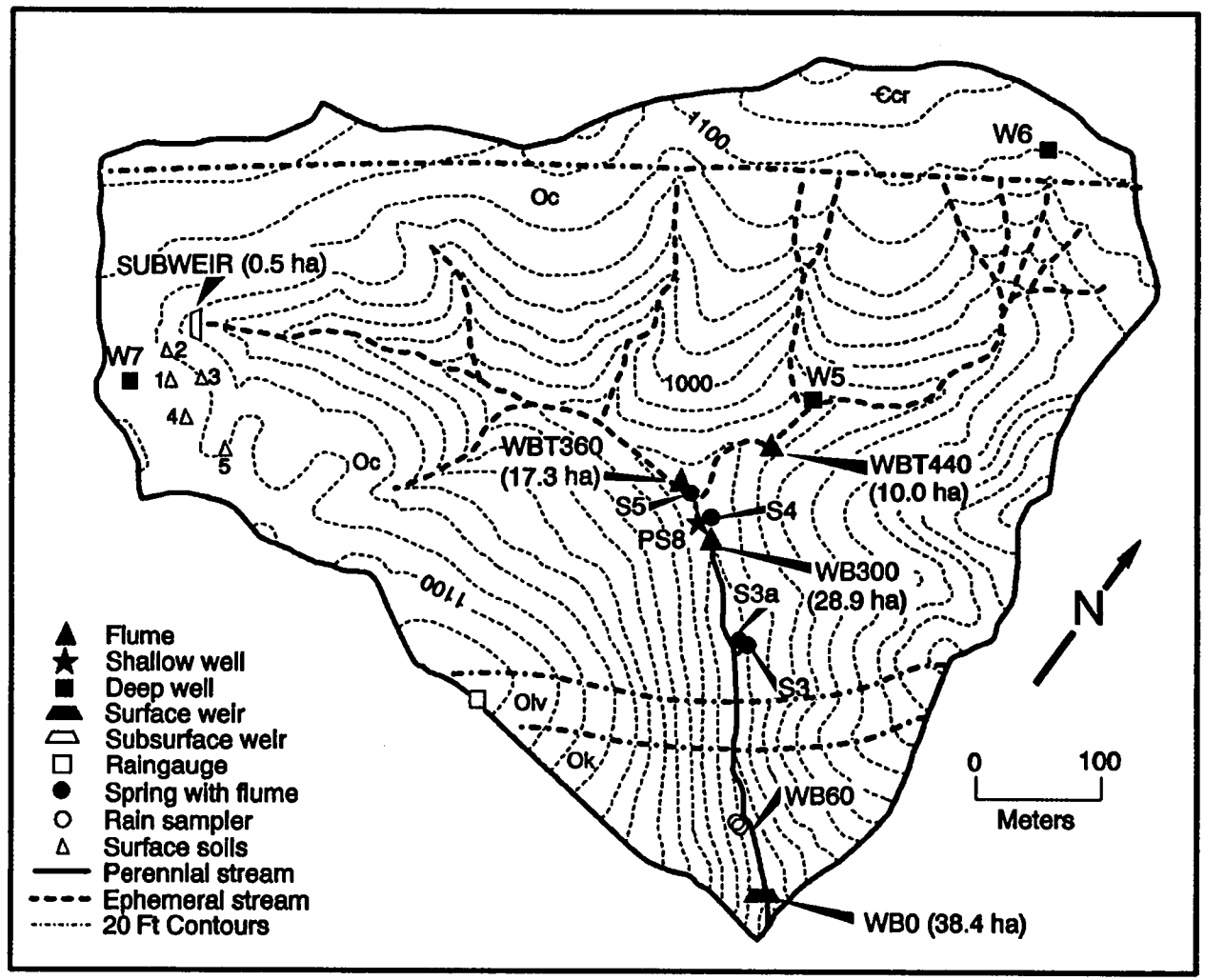
Ccr
1100
W6
Oc
SUBWEIR (0.5 ha)
W7
Δ2
1Δ
Δ3
4Δ
Δ5
1000
W5
WBT360
(17.3 ha)
Oc
WBT440
(10.0 ha)
S5
S4
PS8
WB300
(28.9 ha)
1100
S3a
S3
Olv
Ok
WB60
WB0 (38.4 ha)
N
0
100
Meters
Flume
Shallow well
Deep well
Surface weir
Subsurface weir
Raingauge
Spring with flume
Rain sampler
Surface soils
Perennial stream
Ephemeral stream
20 Ft Contours

Ridge Reservation (McMaster, 1967; TVA, 1972, Luxmoore and Huff, 1989).

Stratigraphy

The bedrock of the Walker Branch Watershed consist of a sequence of Upper Cambrian and Lower Ordovician siliceous dolomite and limestone comprising the Knox Group. The Knox Group is approximately 610 m thick in the watershed, and consists of the Copper Ridge Dolomite, Chepultepec Dolomite, Longview Dolomite, and Kingsport Formation. The Copper Ridge is a massive dolomite of many textures with chert beds 20 - 70 cm thick as well as nodular and porous secondary chert. Within the upper portion, it is a medium- to light-gray, fine-grained, and medium- to thick-bedded dolomite (Hatcher et al., 1992). The Copper Ridge is therefore a ridge former that contains the headwaters of higher order streams. Its uppermost boundary is marked by a well-cemented sandy dolomite (1 - 5 m thick) in the basal Chepultepec Dolomite. The overlying Chepultepec is a light-gray, fine-grained, medium-bedded dolomite with a lesser amount of chert present (Hatcher et al., 1992) so it forms valleys containing higher order streams. The Longview Dolomite is the thinnest of the Knox Group units. Its higher chert content causes it to be more resistant to weathering (Lietzke et al., 1989; Lietzke, 1990). It is a medium- to light-gray, thin- to

medium-bedded siliceous dolomite (Hatcher et al., 1992). The base of the Longview Dolomite lies on tan to white oolitic chert beds of the Chepultepec Dolomite (Hatcher et al., 1992). The overlying Kingsport Formation is a medium- to light-gray, fine- to medium-grained dolomite with nodular and bedded chert and sandstone present near the base (Hatcher et al., 1992). Limestone is an important constituent of the Kingsport Formation, particularly in the lower third of the unit.

Structural geology

The Knox Group is a competent unit that produces the ramp zones of the low-angle imbricate thrust sheets throughout the Valley and Ridge and Cumberland Plateau Provinces (Hatcher et al., 1992). The Knox Group comprises Chestnut Ridge, a NE-SW trending ridge sub-parallel to the NE-SW ridges of the southern Appalachians. The strike of the Knox Group units within the watershed follows the axis of Chestnut Ridge, approximately N55°E. The units dip SE35°. The Knox Group at this locality was emplaced along the White Oak Mountain fault (Fig. 1).

Bedrock fracture orientations are perpendicular and parallel to strike (Crider, 1981). Ground water flow within bedrock fractures is responsible for contributing ground water from outside the surface watershed boundaries (Crider, 1981). The rate of flow into the West Fork of Walker

Branch Watershed across its topographic boundaries is estimated at 1.5 X 10^5 m^3/yr, or about 30% of total annual flow (Genereux et al., 1992).

Soil and saprolite

The weathered zone overlying bedrock within the Walker Branch Watershed varies in depth from about 1 m near the stream to about 30 m at the basin divide (Mulholland et al., 1990). The hydraulic conductivity of surface soils is very high due to abundant macropores, ranging from 0.04 to >0.39 mm/s (Wilson and Luxmoore, 1988), and decreases with depth due to increasing clay content (Wilson et al., 1989).

The soils, 1 - 3 m thick, are dominantly ultisols with a lesser amount of alfisols occurring on the eastern side of the stream, along the lower 150 m (Genereux et al., 1992). Clay minerals present include kaolinite, vermiculite and mica (10 - 40% and 5 - 20% of the clay fraction, respectively) (Lietzke, 1990). A thick layer of saprolite underlies the soils on the western and northern ridgetops, where it reaches thicknesses of up to 30 m. It consists of kaolinite (30 - 55%), mica (10 - 25%), vermiculite (5 - 20%), and iron oxide (2 - 8%)(Lee et al., 1984). Where chert beds have been weathered, fragments remain, as do dolomite and limestone fragments. The clay content of the saprolite causes it to behave as a temporary barrier to infiltration during precipitation events and a perched

saturated zone develops at the saprolite/soil interface (Wilson et al., 1990).

Hydrology

The West Fork of Walker Branch Watershed is drained by several ephemeral streams (WBT360, WBT440) in its upper portions (Fig. 2). Flow in these channels is activated only by large storm events and usually persists for only a few days (Mulholland et al., 1990). In the middle of the watershed there are two perennial springs (S4 and S5) which form the headwaters of the perennial stream and are joined by two other springs (S3 and S3a) further downstream to drain the entire watershed.

Both conductivity and transmissivity have been separately measured in the soil column (0 - 3 m depth) and underlying saprolite (3 - 30 m depth). The maximum potential transmissivity of the soil column under saturated conditions ranges from 6×10^{-5} to 1.5×10^{-4} m^2/s (Genereux et al., 1992). The A (0.5 m thick) and B horizons (1 m thick) have hydraulic conductivities of 10^{-4} m/s (Peters et al., 1970) and 10^{-5} to 10^{-4} m/s (Luxmoore et al., 1981), respectively. Ketelle and Huff (1984) measured the hydraulic conductivity and transmissivity within the saprolite along Chestnut Ridge 6 km southwest of Walker Branch Watershed. The 2.5 - 3 m, 6 - 12 m, and 21 - 30 m depth intervals yielded maximum potential transmissivities much lower than the overlying soils, and conductivity values of 6.1×10^{-8} m/s (21 field measurements),

2.0×10^{-8} m/s (19 field measurements), and 6.3×10^{-10} m/s (8 lab measurements), respectively. The difference in the scale between field and laboratory measurements may account for some of the documented reduction in hydraulic conductivity with depth.

An ephemeral perched saturated zone develops near the soil - saprolite interface (~1.2 m depth) during large storm events because of the large differences in hydraulic conductivity (Wilson et al., 1990). This perched water table occurs primarily near the ridge crests and was identified by transient flow in a subsurface weir, differences in groundwater levels in shallow and deep wells, and its surface expression in ephemeral streams (Luxmoore et al., 1990; Wilson et al., 1990; Mulholland et al., 1990; Mulholland, 1993). As infiltration of precipitation continues during an event, the perched zone saturates upwards towards the surface (Luxmoore et al., 1990). Wilson and others (1990) determined that there is little tendency for perched water table development to occur at the midslope region as opposed to the ridge crest. Macropores (root channels, worm borrows, fractures, etc), act as conduits for water flow from the perched saturated zones, quickly transporting water downslope.

In earlier studies (Mulholland et al., 1990; Mulholland, 1993), it was determined that perched saturation within the soil column accounts for up to 60% of storm runoff at an upstream location, and 53% of storm runoff

at the base of the Walker Branch Watershed. One possible explanation for the smaller contribution of perched water downstream is that near surface bedrock in the lower portions of the watershed results in a greater contribution of groundwater. At upstream sites, where bedrock is substantially deeper, the perennial water table generally remains below the stream and groundwater contributes much less to stream flow. However, Mulholland and others (1990) have also attributed some of this difference to the increasing role of a deeper preferred flowpath through the soil column at the lower watershed sites.

The perched water table that develops near the ridge crest and subsurface flow through macropores within the surface 1 - 2 m of soil are collectively referred to as the shallow storm flow zone within the Oak Ridge Reservation (Wilson et al., 1990; Solomon et al., 1992). This zone transmits up to 90% of the active subsurface flow in catchments on the Oak Ridge Reservation (Solomon et al., 1992). Results of studies within 0.47 ha of the Walker Branch Watershed indicate that subsurface flow occurs primarily through mesopores and macropores within the storm flow zone, bypassing the soil matrix (Luxmoore et al., 1990; Wilson et al., 1991a; 1991b). It is believed that some water is lost to deeper soil horizons through macro- and meso-pores, initiating an additional deeper flowpath (Mulholland et al., 1990; Wilson et al., 1991a). Flow through the

deeper flowpath is believed to continue after precipitation infiltration ceases and the perched water table disappears(Wilson et al., 1991a).

Wilson and others (1991b) examined subsurface solute transport processes occurring as a result of storm events within a 0.47 ha upper slope subcatchment of the Walker Branch Watershed. Silica concentrations decrease with increasing subsurface flow, and then increase after the event. During the event, the silica concentration within small pores of the soil matrix is the same as that of subsurface flow. This is attributed to the capacity of smaller meso- and micro- pores to provide a semi-infinite source of solutes to larger pores through which flow occurs.

IV. Field and Analytical Methods

Sampling strategy

Storm event responses must be compared to antecedent watershed conditions to accurately evaluate storm flow components. The isotopic composition and chemical concentration of each component may vary prior to and/or during an event. The isotopic composition of precipitation may vary during an event (Kennedy et al., 1986); therefore, precipitation samples should be taken sequentially throughout the event. Surface and soil water isotopic ratios may vary temporally due to evaporation. Water solute concentrations may become more or less concentrated depending on the rate of dissolution with changing water supply. For these reasons, pre-storm surface and subsurface waters should be sampled frequently for isotopic (Kennedy et al., 1986) and solute analyses.

Groundwater isotopic ratios and solute concentrations may or may not be directly affected evaporation. Since throughfall, surface, and soil waters are believed to recharge groundwater, the isotopic composition and water chemistry of groundwater may reflect changes in these source waters. The antecedent hydrologic and isotopic conditions of the vadose zone, saturated zone, and surface water were established from routine sampling over a one-year period. In addition, pre-storm measurements were used as a reference to evaluate changes in storm event waters.

Sampling techniques

Sampling of the storm flow components to determine the antecedent watershed conditions consisted of the following. Bulk throughfall samples were collected within 24 hours after most rain events during one year. Stream runoff was monitored and sampled every week at sites WB0 and WB60, respectively (Fig. 2). Soil samples were obtained in December, 1991, at several depths from a 30 m deep borehole (W7; Fig. 2), which penetrated the entire vadose zone to the water table. Soil moisture was measured and oxygen isotope ratios were analyzed for these samples. Pre-storm soil samples were also obtained from the A and B soil horizons, distinguished visually, from five locations near the 30 m deep bore hole (Surface Soils 1 - 5; Fig. 2). Groundwater levels and samples from two deep wells (W5, W6) and one shallow well (PS8) were taken on a monthly basis, and two major springs (S3, S4) were sampled weekly (Fig. 2). Pre-storm and storm bulk throughfall samples (49) were analyzed for O and H isotopic compositions. Surface water (12), soil water (12), and groundwater (24) samples were analyzed for O isotopes, and silica concentration (Appendix A, B, and C, respectively).

One storm event (December 15 - 19) was intensively monitored and sampled. Storm sampling and monitoring consisted of: 1) continuous sampling and monitoring of throughfall for intensity and total volume;

2) automatic sampling and flow monitoring at one perennial and one ephemeral stream site (WB60, WBT440; Fig. 2); 3) automatic sampling at one perennial and one ephemeral stream site (WB300, WBT360); 4) automatic sampling of shallow lateral vadose zone flow using a subsurface weir (SUBWEIR; Fig.2); and 5) pre- and post-event sampling of soil horizons at five locations near W7. Additionally, three groundwater wells (PS8, W5, W6) were sampled prior to and after the event, and four groundwater springs (S3, S3a, S4, S5) were sampled manually each day during the event. All samples (5 throughfall, 34 surface water, 18 soil water, and 23 groundwater) were collected for isotopic and chemical analyses.

Instrumentation

The West Fork of Walker Branch Watershed has been instrumented with a multitude of monitoring and sampling equipment (Fig. 2). Cumulative event precipitation was monitored at two sites on the ridgetop using a weighing recorder. A bulk throughfall collector, consisting of a bucket and funnel, was located near the stream at the base of the watershed (rain sampler; Fig. 2). A sequential throughfall sampler was installed adjacent to the bulk throughfall collector for storm events. The sequential sampler consisted of 9 sequentially-filling plastic bags connected with plastic tubing (after Adar et al., 1991). The nine bags were calibrated

to contain all of the precipitation associated with a large storm event (7.62 cm). When the first bag filled to a calibrated weight/volume, a knife blade was engaged to seal the tubing to that bag and force precipitation to flow into the following bag.

Stream runoff was monitored at the base of the watershed with a 120° V-notch weir (site WB0; Fig. 2). Stage height was measured and recorded at 5 min intervals using a Fisher and Porter model 1542 punched-tape water level recorder. A Manning Technologies model 6000 automatic sampler was used to collect storm related runoff 60 m upstream from the weir to avoid potential effects due to ponded water at the weir. Previous studies indicate that runoff at both WB0 and WB60 has similar chemical composition (Mulholland et al., 1990), therefore site WB60 was accepted as being representative of total stream flow at site WB0. Stage height at the ephemeral stream site WBT440 (Fig. 2) was measured at 30 min intervals at a Parshall flume with a Druck Model 900 pressure transducer and recorded by a Campbell Scientific data logger. Additional flumes located at one perennial and one ephemeral stream sites (WB300 and WBT360, respectively; Fig. 2) were used to manually measure stage height for flow computation. ISCO (Model 2700) battery-powered automatic samplers were used to collect hourly storm runoff at WB300 and

at the two ephemeral tributary stream sites WBT360, and WBT440 (Fig. 2).

A subsurface weir (SUBWEIR; Fig. 2) monitors subsurface storm flow within the upper 2.5 m (8.2 ft) of the vadose zone within a 0.5 ha subcatchment of the Walker Branch Watershed (Luxmoore and Abner, 1987; Wilson et al., 1990). The weir is 13 m long and consists of six pans: three pans collecting drainage within the upper 1 m consisting of the A, E, and Bt1 soil horizons; and three pans collecting drainage from 1 to 2.5 m depth within the Bt2 soil horizon. Drainage from the upper and lower pans is diverted through separate H flumes. The lower flume was equipped with a battery-powered, ISCO Model 2700 automatic sampler collecting at one hour intervals.

Groundwater monitoring and sampling was performed at three wells and four springs. One of the wells is shallow (<1.5 m depth) and located next to the perennial stream (PS8; Fig. 2). Two deeper (20 - 30 m) wells (W5 and W6; Fig. 2) are located near an ephemeral stream channel and near the ridge crest, respectively. Additionally, grab samples were obtained from the borehole (W7) after it was cased (total depth = 28.3 m). All groundwater measurements and sampling were performed manually. With the exception of W7, several well volumes were purged from all the wells before sampling. Stage was measured in flumes at the

four springs (S3, S3a, S4, S5) to measure instantaneous flow rates.

Soil moisture, chemical and isotopic analyses

Soil moisture content was obtained gravimetrically by oven drying the samples, according to the methods described by Gardner (1965). Soil moisture was extracted by centrifuge in the Environmental Sciences Division at Oak Ridge National Laboratory for Si analyses. Samples were placed in a 1 L bucket which had a perforated bottom, allowing soil moisture to escape to an empty bucket below during centrifugation. Soil water was extracted for isotopic analysis by azeotropic distillation using toluene (Revesz and Woods, 1990).

Solute analyses (20 elements) were performed by inductively coupled plasma emission spectroscopy at the University of Georgia Chemical Analysis Laboratory, Athens, Georgia. The precision of these analyses is ±0.01%. The sampling error for these analyses was 0.01 ppm. Vacuum extraction of gases for measurement of D/H and $^{18}O/^{16}O$ ratios were conducted in the Department of Geology at the University of Tennessee. Hydrogen gas was obtained by combustion of water samples with Indiana zinc at 500 °C for 30 minutes (Vennemman and O'Neal, 1993). Oxygen isotopic ratios in water samples were obtained using the CO_2 equilibration method of Epstein and Mayeda (1953). Isotopic ratios

were measured on a fully automated, triple collector, VG903 gas ratio mass spectrometer and are reported in standard δ-permil notation relative to Standard Mean Ocean Water (SMOW; Craig, 1961b). The precision of these analyses is $\pm 0.5‰$ for oxygen and $\pm 2‰$ for hydrogen. Selected D/H gas samples were run on the VG903 mass spectrometer at the Chemical and Analytical Sciences Division, Oak Ridge National Laboratory.

V. Results

Annual conditions

Throughfall

Bulk throughfall samples were collected within 24 hours after each rain event beginning in February 1992 and continuing through May 1993. Analytical results are listed in Appendixes A and B and shown in figure 3. Forty nine throughfall events were collected for oxygen and hydrogen isotope compositions, only forty three were analyzed for deuterium. The samples chosen for deuterium analyses were chosen to represent the range of corresponding oxygen isotope compositions. The average δD and δ^{18}O signatures of water recharging the Walker Branch Watershed are -33‰ (-94‰ to 7‰; standard deviation, SD = 22‰) and -5.7‰ (-12.3‰ to -2.2‰; SD = 2.4‰), respectively. Winter precipitation occurring during the months of October through March recharges groundwater with average δD and δ^{18}O of -47‰ (n = 21) and -7.0‰ (n = 23), respectively. Summer precipitation has an average signature of δD = -20‰ (n = 22), δ^{18}O = -4.2‰ (n = 26). Differences in winter and summer signatures reflect their different source areas and related temperature effects. Winter arctic air masses are more depleted in deuterium and ^{18}O than air masses from the Gulf of Mexico during the summer months. During the transition from one season to another, a storm of one source may be followed by precipitation

originating from the other source area, and vice versa. Thus, some winter precipitation events are more enriched than others; some summer events are more depleted (Fig. 3).

A local meteoric water line has been established ($\delta D = 9.08\delta^{18}O + 17.5$; Fig 3) from the 43 throughfall samples collected over 16 months (February 1992 through May 1993). The sampling period was extended beyond the planned 12 months to compensate for the relatively dry winter months of 1991. Sampling over 16 months allowed for a more equal representation of winter and summer throughfall and prevented favoring of one season when delineating the local meteoric water line. The difference between this line and one derived from samples collected over one year ($\delta D = 9.26; \delta^{18}O + 19.1$) is insignificant. Because of the similarity between the local and global meteoric water lines, the global line should be used to describe local precipitation and groundwater recharge.

Surface water

Discharge was computed from stage height measured at stream site WB0 once a week for over two years (Fig. 4). These weekly measurements provide a clear indication of the seasonality of discharge within the watershed. Discharge from the watershed is greater during the winter months, and lower during the summer months. Storm events,

Figure 3. A local meteoric water line describing throughfall that fell between February 1992 and May 1993 on the Oak Ridge Reservation is compared to the global meteoric line. Winter and summer throughfall samples are highlighted. River samples collected during the years 1984 - 1987 by the U. S. Geological Survey (Kendall, unpublished data) are compared to local throughfall samples.

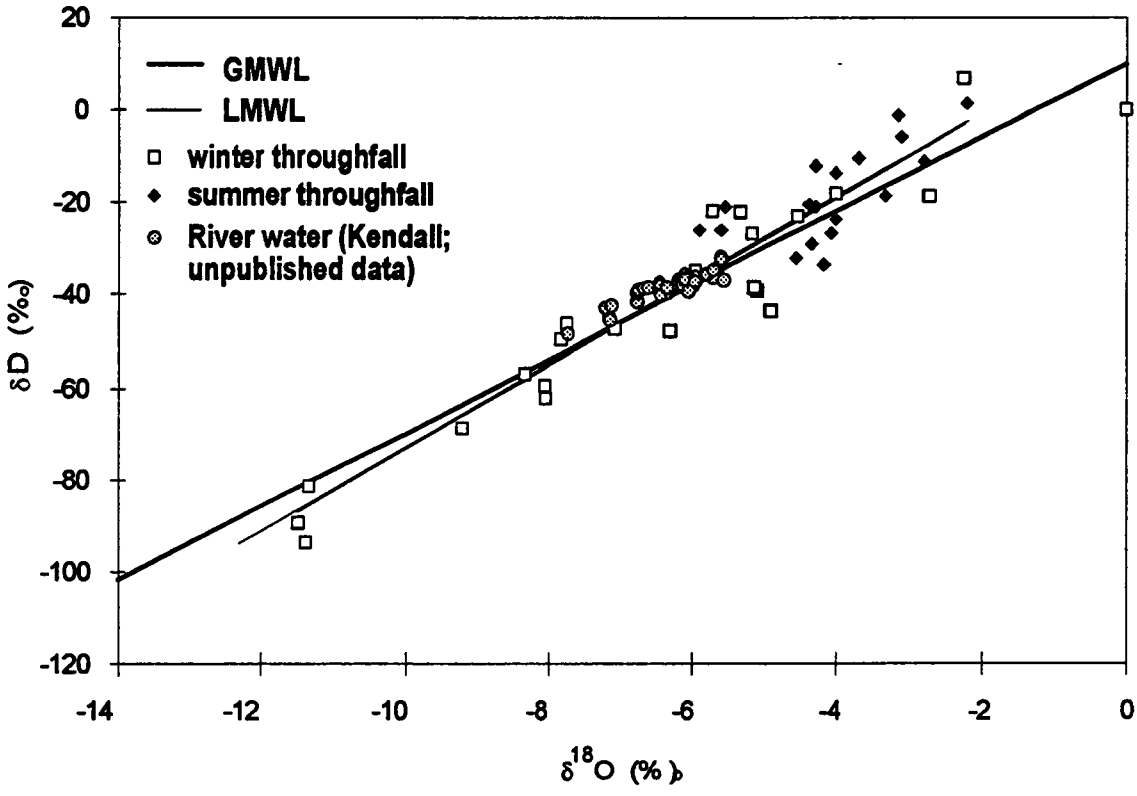
GMWL
LMWL
winter throughfall
summer throughfall
River water (Kendall; unpublished data)
δD (‰)
δ18O (‰)
20
0
-20
-40
-60
-80
-100
-120
-14
-12
-10
-8
-6
-4
-2
0

Figure 4. Stream discharge measured once a week at the base of the West Fork of the Walker Branch Watershed, from January 1992 through December 1993. The storm which is the focus of this report is not represented on the plot due to the sampling interval. Discharge measured for any given day represents the discharge at stream site WB0 when a stream sample was collected from site WB60 for oxygen isotope ratio analyses.

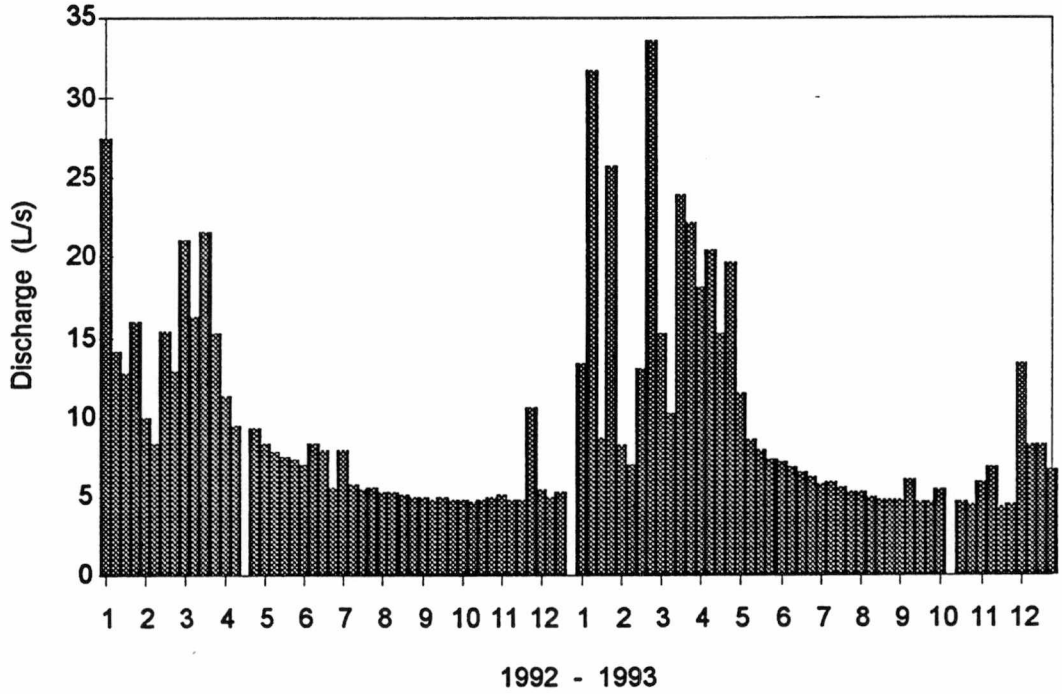
35
30
25
20
15
10
5
0
Discharge (L/s)
1 2 3 4 5 6 7 8 9 10 11 12 1 2 3 4 5 6 7 8 9 10 11 12
1992 - 1993

marked by sudden increases in discharge, are more prevalent during the winter and early months. Although there are many storm events during the summer months, canopy interception and low soil moisture content due to high rates of evapotranspiration prevent large increases in stream discharge at this time.

Instantaneous stream samples collected once a month at site WB60 were analyzed for their oxygen isotope composition. The oxygen isotopic signature of stream water varied little over a one-year period ($\delta^{18}O$ = -5.9‰ to -6.1‰). The average oxygen isotope composition was -6.0‰, and all of the variability seen in Figure 5 (maximum difference of 0.14‰) is within the analytical error of the analysis ($\pm$0.5‰).

Two Tennessee rivers, the French Broad River near Knoxville and the Tennessee River at Watts Bar Dam (tailwater) were sampled by the U.S. Geological Survey every three months beginning October 1984 through July 1985 (Kendall, unpublished data). The Clinch River at Melton Hill Dam (tailwater) was sampled every two months beginning October, 1984, through August, 1987. The oxygen and hydrogen isotopic compositions of the river water are illustrated on Figure 3. The samples fall around the global meteoric water line, with some samples falling just above the line with decreasing $\delta^{18}O$. The isotopic composition of the surface water samples falls within the scatter of winter precipitation samples (Fig. 3).

Figure 5. Oxygen isotope composition of stream water sampled monthly from stream site WB60.

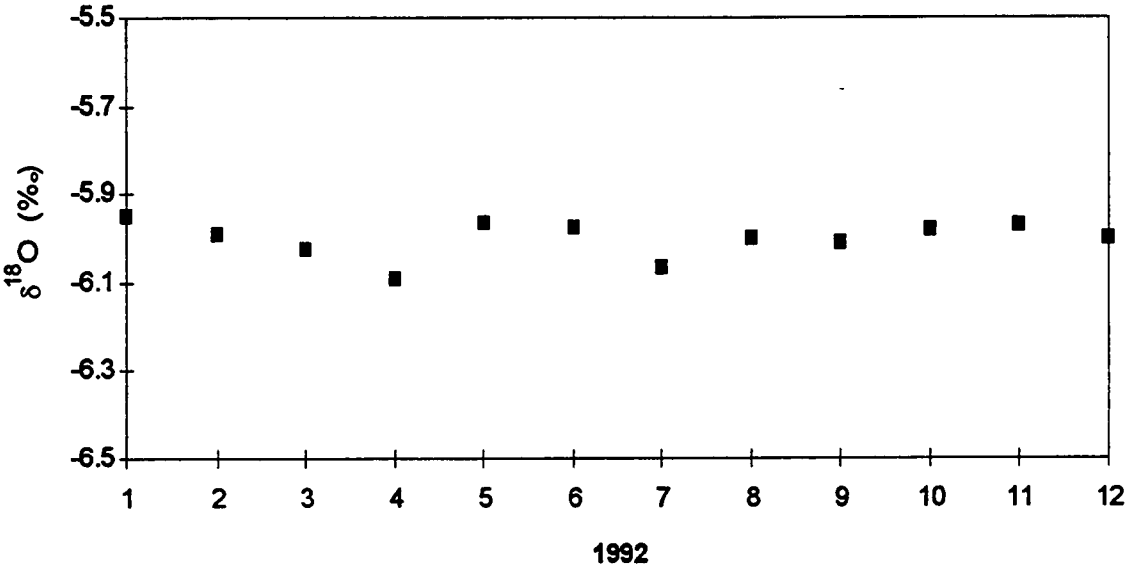
-5.5
-5.7
-5.9
-6.1
-6.3
-6.5
δ18O (‰)
1
2
3
4
5
6
7
8
9
10
11
12
1992

Vadose water

During augering and coring of the 30 m deep borehole in December, 1991, several potential flow zones (saturated zones) were observed by the drilling team and recorded by D. Lietzke (unpublished data). The first potential flow zone was noticed within 1.52 - 2.13 m depth, consisting of perched water above a chert bed (A; Fig. 6a). A second perched flow zone was found within 5.18 - 5.79 m depth (B; Fig. 6a). It was approximately 15 cm thick, occurring above a 0.95 cm saturated chert zone and fine-grained red and yellow saturated sandstone. The third flow zone (C) was intersected during augering from 7.32 - 8.23 m depth. Within the section cored below this depth (8.23 - 8.84 m), there were three flow zones (D) associated with 1.27 cm chert zones separated by massive red clay saprolite. The upper two flow zones contain white deoxidized clay, the lower zone contains black Mn oxides. While augering from 8.84 m to 10.67 m, a major flow zone was intercepted (E; Fig. 6a). While removing the drill stems to prepare for coring, it was noticed that 4.88 m of the drill stem was muddy. This would indicate that the corehole filled some 4.88 m above a depth of 10.67 m with water from the intercepted flow zone. Additional flow zones associated with chert beds were located within 10.67 - 11.28 m depth (F), and 13.11 - 13.72 m depth (G). By 14.63 m depth, there was no standing water in the hole. An additional

Figure 6. Borehole (W7) a) saturated zones; b) soil moisture; and c) $\delta^{18}O$ signature with depth.

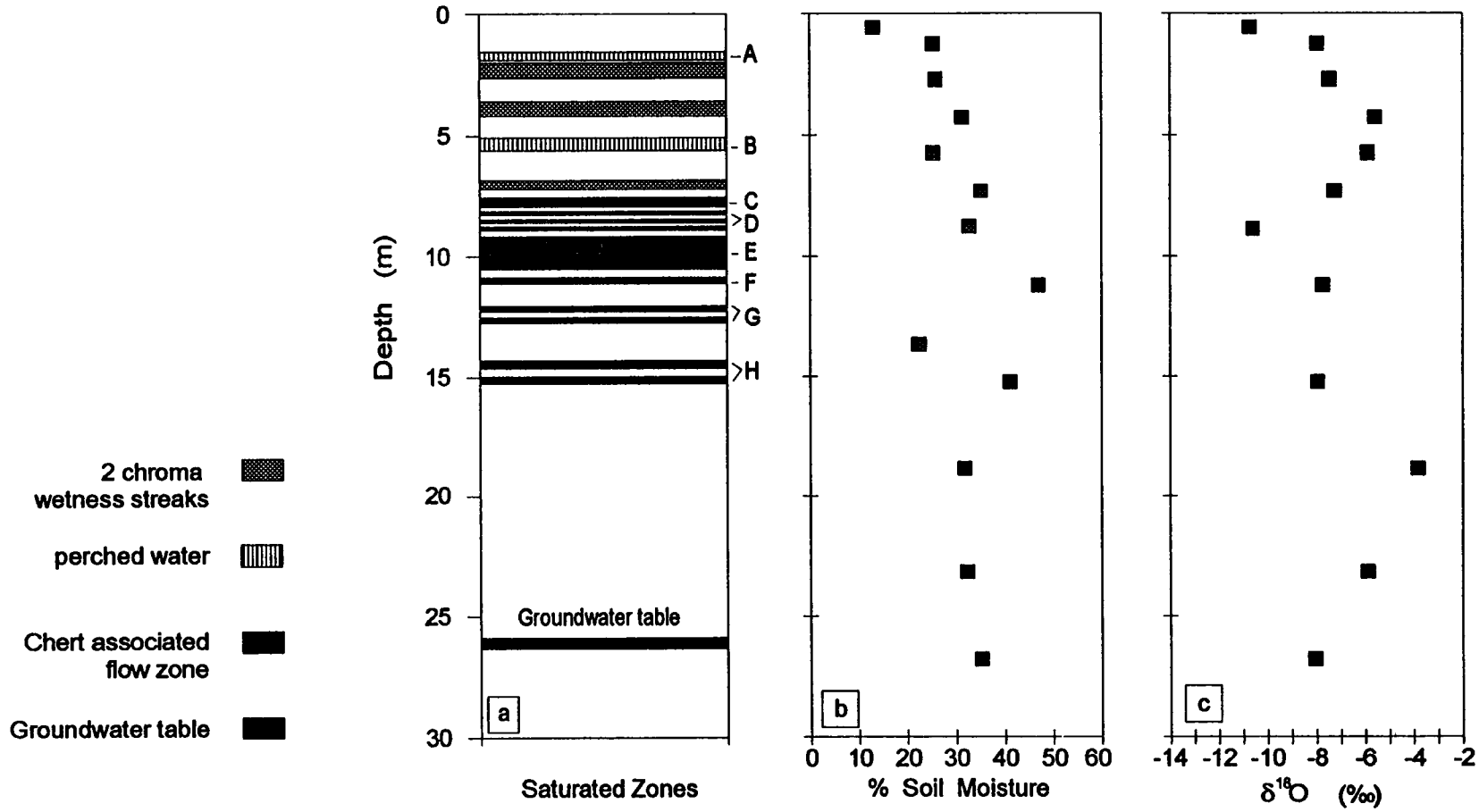
2 chroma wetness streaks
perched water
Chert associated flow zone
Groundwater table
Depth (m)
0
5
10
15
20
25
30
A
B
C
D
E
F
G
H
Groundwater table
a
Saturated Zones
b
0 10 20 30 40 50 60
% Soil Moisture
c
-14 -12 -10 -8 -6 -4 -2
δ18O (‰)

two flow zones were located within 14.63 - 15.24 m depth (H). No other saturated zones were detected below 15.24 m depth. This borehole (W7) was completed and cased to 26.7 m and screened from 26.74 m to 28.26 m depth. The depth to the water table in the borehole averages 26.14 m, well below the major flow zone intercepted just above 10.67 m. It is safe to assume, therefore, that this intercepted zone is a perched flow zone, not the regional groundwater table. Despite the evidence of several saturated zones, there is no direct evidence which, if any are major flow zones (perhaps with the exception of zone E).

The moisture content of the upper two zones of perched water (within 5.79 m depth) were nearly identical (Fig. 6b). Other soils sampled within this depth had similar moisture content, although one soil associated with two chromo flow zones had a greater moisture content. (Chromo describes the degree of graying in soil color indicative of the presence of flowing water.) Similar to this zone, the moisture content of underlying core (5.79 - 7.32 m) was higher due to moist clay and two chromo flow zones. With the exception of the interval 13.11 - 13.72 m, relatively high soil moisture content was associated with corresponding flow zones. Because the moisture within the fragmented chert zones was not easily collected during sampling, the moisture content of the cores is predominately a result of the clays associated with the chert zones. Thus,

although the core at 13.11 - 13.72 m depth contains chert associated flow zones, it may have a low moisture content due to the loss of intergranular chert moisture. No flow zones were logged below 15.24 m depth, and below 24.39 m depth was not logged by the soil scientist. Based on the above core, it can be assumed that the relatively high soil moisture content of samples below 14.63 m depth are associated with either saturated or water bearing-zones.

Oxygen isotopic signatures varied with depth in the 30 m deep bore hole (Fig. 6c). Soil water in surface soils within the bore hole are more depleted than that in underlying soils and saprolite, possibly because of the winter precipitation that might have affected this zone. The most enriched soils occurred within 18.29 - 18.90 m depth ($\delta^{18}O$ = -3.9‰), the most depleted were at the surface ($\delta^{18}O$ = -10.7‰), and at 8.23 - 8.84 m depth ($\delta^{18}O$ = -10.7‰). Surface soils have low values of both soil moisture and $\delta^{18}O$. A direct correlation of moisture content and oxygen isotope composition exists to a depth of 5.79 m (Fig. 6c). Between 5.79 m and 18.9 m depth, no correlation exits. The three samples collected at and below 18.9 m depth indicate a negative correlation between soil moisture and isotopic composition. This observed negative correlation might be a result of the larger interval between soil samples at this depth compared to shallower samples.

Groundwater

Groundwater levels in four wells (PS8, W5, W6, W7) fluctuated seasonally between February 1992 and May 1993, the magnitude of variation being dependent on well depth (Fig. 7), except in W7. The water level within the shallow well (PS8) located near the perennial stream exhibited the least seasonal variation (Fig 7; Table 1). Wells W5, W6, and W7 are located higher in the watershed (Fig. 2). Although W7 is the deepest of the wells, it fluctuated less than the other deep wells (W5, W6; Fig. 7; Table 1). Water levels increased in all four wells during the winter months as a result of precipitation recharging the groundwater system.

The average oxygen isotope compositions of groundwater sampled from wells PS8, W5 and W6 between February, 1992, and April, 1993, were essentially equal (Fig 8). Thus, the average oxygen isotope signature of groundwater within Walker Branch Watershed is -6.0‰. For all the wells combined, the average summer and winter oxygen isotope signatures were -5.9‰ and -6.1‰, respectively. Oxygen isotope ratios showed the most variation in the shallow well (PS8; Table 2) suggesting more rapid turnover of groundwater at the near stream site. Groundwater samples from W5 showed no significant variability. Groundwater was sampled from well W7 in April, July, August, and December 1992, and March of 1993. These samples were obtained using a bailer. The average oxygen isotope

Figure 7. Depth to the water table in four groundwater wells (PS8, W5, W6, and W7).

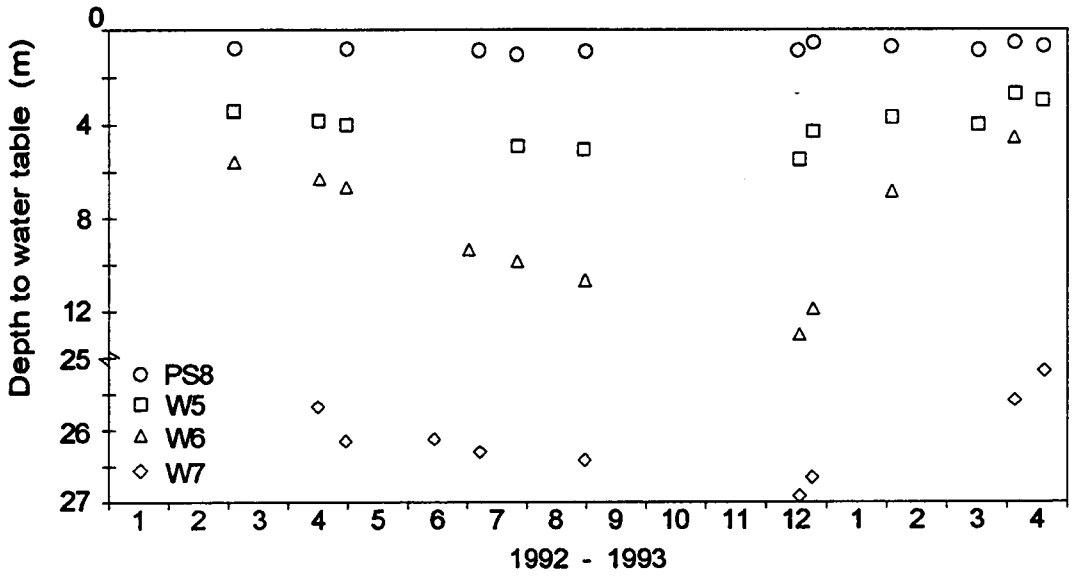
Depth to water table (m)
0
4
8
12
25
26
27
PS8
W5
W6
W7
1 2 3 4 5 6 7 8 9 10 11 12 1 2 3 4
1992 - 1993

Table 1. Average annual, summer and winter depths to the water table in four groundwater wells.

Well	Average depth to the water table (m)		
	Annual	Summer	Winter
PS8	0.779	0.949	0.693
W5	3.698	5.139	3.636
W6	8.489	10.754	6.978
W7	26.108	26.374	25.776

Figure 8. Oxygen isotope signature of groundwater sampled from three wells (PS8, W5, and W6).

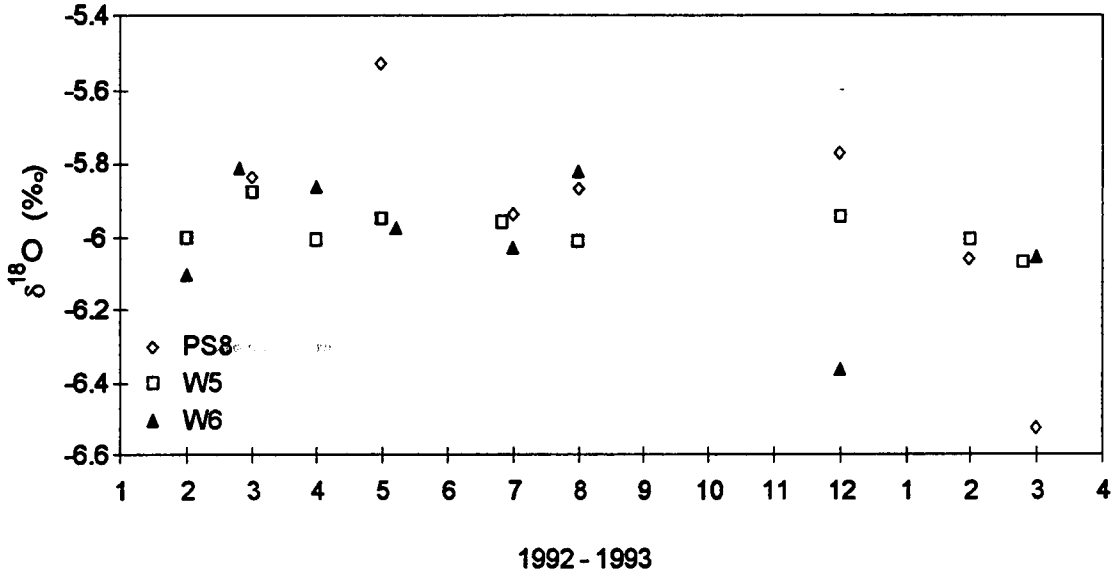
-5.4
-5.6
-5.8
-6
-6.2
-6.4
-6.6
δ18O (‰)
PS8
W5
W6
1
2
3
4
5
6
7
8
9
10
11
12
1
2
3
4
1992 - 1993

Table 2. Range and mean annual values of oxygen isotope ratios for groundwater wells and springs. The most negative (depleted) and positive (enriched) isotopic ratios were of winter and summer samples, respectively.

Well/Spring	$\delta^{18}O$ (‰)		Date of the most	
	Range	Mean	Depleted	Enriched
PS8	-5.5 to -6.5	-6.0	March 1993	April 1992
W5	–5.9 to -6.1	-6.0	March 1993	March 1992
W6	-5.8 to -6.5	-6.1	December 1992	March 1992
W7	-5.9 to -6.2	-6.0	December 1992	April 1993
S3	-6.0 to -6.4	-6.1	December 1992	July 1992
S4	-5.6 to -6.4	-6.0	December 1992	May 1992

composition of these samples was -6.0‰, with one sample being more negative ($\delta^{18}O$ = -7.2‰; Appendix A).

Groundwater springs S3 and S4 were sampled monthly. The average oxygen isotope ratio for these groundwater springs from January 1992 to December 1992 was -6.1‰ (Fig. 9). The average winter and summer signatures were -6.2‰ and -6.0‰ (Table 2). Although these differences in oxygen isotope composition fall within the analytical error of isotope analysis, the same seasonal trends were observed in wells (Fig. 8). For both groundwater wells and springs, winter samples had the most depleted and summer samples the most enriched stable oxygen isotope ratios (Table 2). The greater range in isotopic ratios observed at spring S4 than spring S3 (Table 2) is consistent with greater variability in flow rate at S4 and probably reflects greater variation in the rate and composition of groundwater recharge to this subsurface pool.

Samples from December 15 - 19, 1992 storm

Storm description

One storm event (December 15 - 19, 1992) was intensively sampled for oxygen-18 and silica in order to determine sources of stream runoff generated by relatively large precipitation events in the West Fork of Walker Branch Watershed. Precipitation began at 11:43 p.m. on December

Figure 9. Oxygen isotope signature of groundwater sampled from two groundwater springs (S3 and S4).

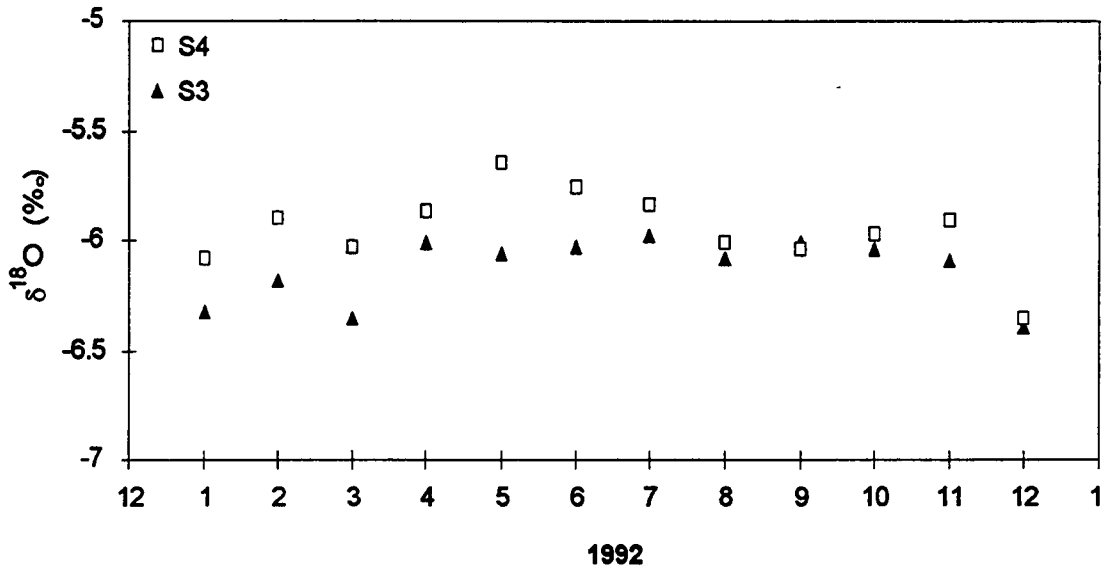
S4
S3
-5
-5.5
-6
-6.5
-7
δ18O (‰)
12
1
2
3
4
5
6
7
8
9
10
11
12
1
1992

15, and ended by 6:37 am December 16. The amount of rainfall in this event measured at the ridge crest was 1.48 cm (1.73 cm of throughfall was measured near the stream channel). In the latter stages of rainfall, stream flow began to increase at the base of the watershed (at WB0), but no flow was present in the ephemeral stream sites until approximately 8:00 am on December 17 (Fig. 10). Following an almost 14 hour intermission, a second storm brought 2.77 cm of rain (2.80 cm measured throughfall) beginning at 8:54 p.m., December 16, and continuing through 12:24 p.m. on December 17.

Rainfall increments (Fig. 10a) were determined from the precipitation weighing-recorder chart. The average rainfall intensities of the two events were very similar (first event 0.21 cm/hr; second event 0.29 cm/hr). The most intense rainfall during the first event occurred between the hours of 1:38 am and 2:21 am on December 16 (Fig. 10a), at a rate of 0.47 cm/hr. The rainfall intensity lessened only slightly until 4:11 am on December 16, after which it began to rapidly decline. The maximum rainfall intensity during the second event wasn't reached as rapidly as in the first event. The second event was characterized by a longer period of relatively intense precipitation, proportional to its greater volume of rainfall. The most intense portion of the event occurred between 1:28 am and 2:17 am on December 17, at a rate of 0.82 cm/hr.

Figure 10. Storm a) rainfall intensity; and b) stream flow measured at one perennial stream site (WB0) and one ephemeral site (WBT440) on December 15 - 19, 1992. Discharge was generated from the two storm events. The first event began at 11:43 p.m. December 15 and continued to 9:23 am December 16, totaling 1.73 cm. The second event began at 8:54 p.m. December 16 and continued to 12:24 p.m. December 17, totaling 2.69 cm. Baseflow has been subtracted from the stream hydrographs.

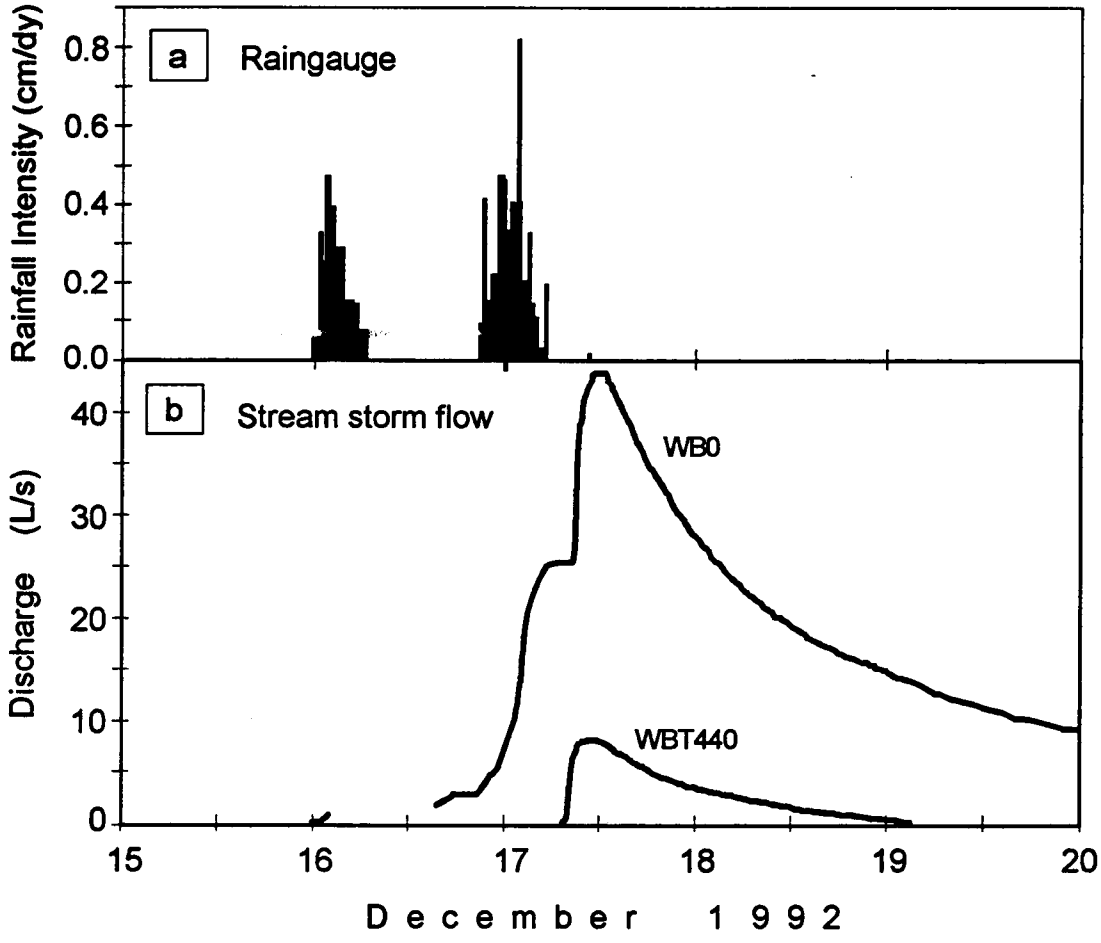
a
Raingauge
Rainfall Intensity (cm/dy)
0.8
0.6
0.4
0.2
0.0
b
Stream storm flow
WB0
WBT440
Discharge (L/s)
40
30
20
10
0
15
16
17
18
19
20
D e c e m b e r 1 9 9 2

Throughfall

The sequential rain sampler split the precipitation from the two storm events into three portions: the first event was sampled as a whole, and the second event was captured in two portions. The first split of the second event represents throughfall collected between 8:54 p.m. on December 16 and ~2:00 am on December 17, totaling 1.70 cm. The second split represents throughfall which fell from ~2:00 am to 12:24 p.m. on December 17, totaling 1.10 cm.

Bulk throughfall samples from the first rain event had oxygen and hydrogen isotope signatures of -5.7‰ and -22‰, respectively (Table 3; Appendix A). Throughfall collected in the sequential sampler during this first event had isotopic compositions ($\delta^{18}O$ = -4.6‰, δD = -18‰) that were somewhat less depleted than that from the bulk sampler (Table 3). The most likely explanation for the difference is the loss of some late event water within the tubing of the sequential sampler after the bag filled. The unsampled later portion of the storm event was most likely isotopically lighter than earlier event water, causing an apparent enrichment in the sampled portion relative to the cumulative event water. The silica concentration within the sequential sample was equal to that of the bulk sample (1.18 ppm; Table 3). This relatively large silica concentration in throughfall can be attributed to the placement of quartz wool in the rainfall

Table 3. Oxygen and hydrogen isotopic composition and silica concentration of two rainfall events.

Throughfall Event	Sampler	Volume cm	$\delta^{18}O$ (‰)	δD (‰)	Si (ppm)
1	bulk	1.73	-5.7	-22	1.18
	sequential	1.73	-4.6	-18	1.18
2	bulk	2.80	-9.2	-69	0.00
	sequential 1	1.70	-9.3	-61	0.00
	sequential 2	1.10	-10.4	-69	0.00

sampler to filter litter. Previous research indicates a silica concentration of 0.02 - 0.05 ppm in local throughfall (Mulholland, personal communication; Wilson et al., 1991b).

Bulk throughfall collected from the second event (2.80 cm) had signatures of $\delta^{18}O$ = -9.2‰ and δD = -69‰ (Table 3). The two sequential samples representing the second event, had oxygen and hydrogen isotope signatures of -9.3‰ and -61‰ (1.70 cm), and -10.4‰ and -69‰ (1.10 cm), respectively (Table 3). There is general agreement between the bulk and sequential throughfall samples for the second storm event, indicating that no apparent loss of sample occurred within the tubing of the sequential sampler. Silica was absent (Si = 0.00 ppm) in these bulk and sequential samples (Table 3).

Surface water

Discharge at the base of the watershed (WB0) increased with the initial rain event, and then leveled off before rising again with the second rain event (Fig. 10b). Discharge increased slightly at 1:05 am, December 16, twenty-two minutes after initiation of the storm event. Although the stream flow response to the first rain event was not recorded from 2:05 am to 3:40 p.m. on December 16, it likely was very little. As a result of the second rain event, stream discharge began to increase rapidly at

about 10:00 p.m. on December 16 and leveled off temporarily at approximately 5:40 am, December 17. The stream hydrograph reached a maximum of 48.79 L/s at 11:35 on December 17. After reaching this peak in surface flow, it leveled off for one and a half hours before gradually decreasing over the next several days.

Flow at the ephemeral stream sites was not initiated until the second precipitation event. Stream flow at site WBT360 was indicated by automatic collection of the first sample at 8:30 am on December 17 (Fig. 10b). Due to the sampling interval at this site, the estimated time of initial flow would be between the hours of 7:00 and 8:30 am, December 17. Stream flow at site WBT440 was first recorded at ~8:00 am (Fig. 11a). Samples were actually collected as early as 6:45 am (Fig. 11b, c), however, these first few sample bottles were partially filled with air, indicating that stream flow did not fill the width of the flume. The placement of the sampling and recording devices account for the differences in the timing of samples collected versus the recorded hour discharge began. Discharge at ephemeral stream site WBT440 rapidly reached a peak of 8.15 L/s at 11:00 am on December 17, and gradually decreased until 3:00 am December 18 when flow ceased (Fig. 11a).

The oxygen isotope composition of stream flow at the base of the watershed (WB60) was -6.0‰ on December 15, and -6.0‰ on December

Figure 11. Stream a) discharge; b) oxygen isotopic compositions; and c) silica concentrations measured at two stream sites (WB0 and WBT440) during a December 15 - 19, 1992 storm event.

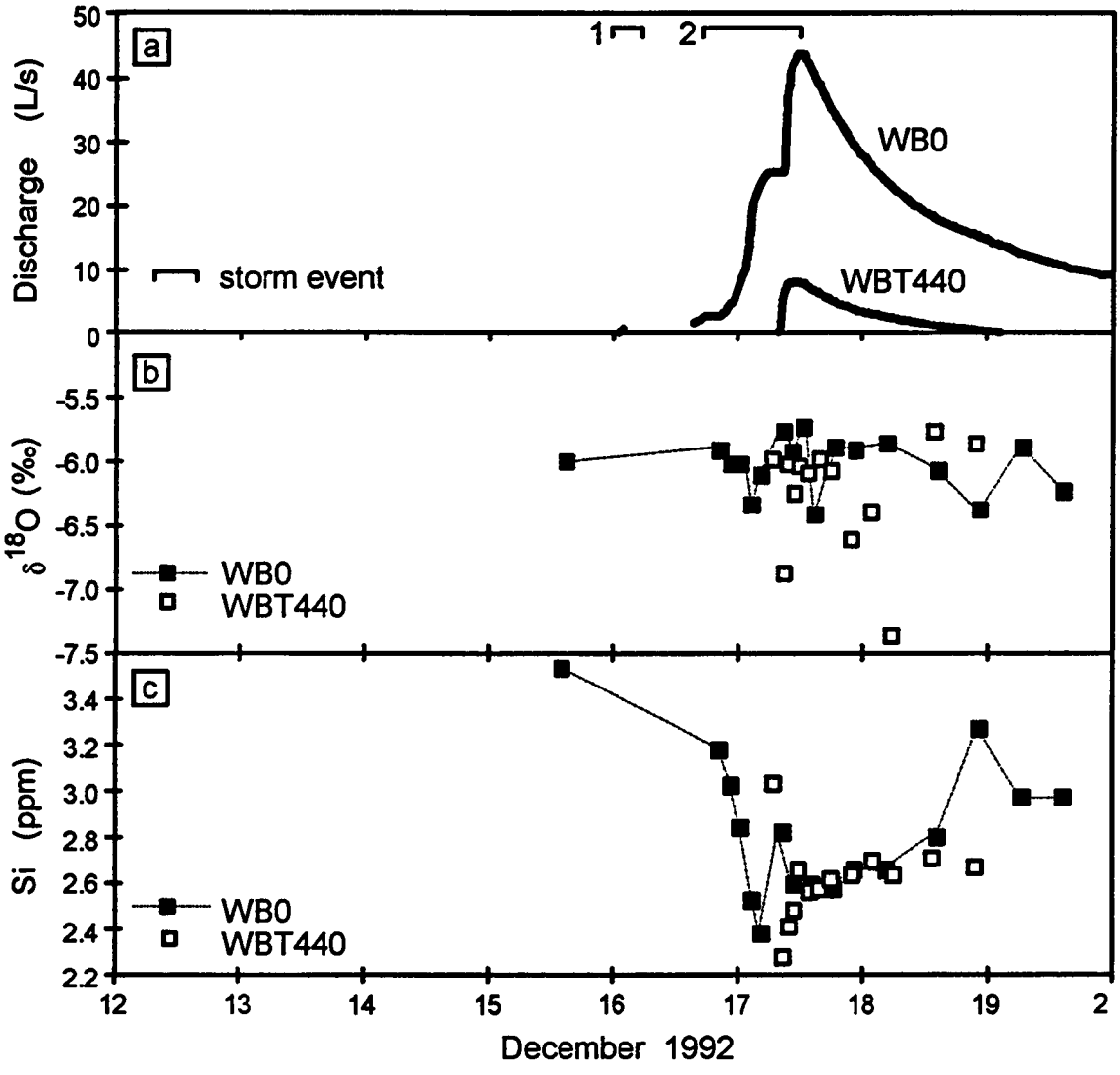
a
b
c
1
2
WB0
WBT440
storm event
Discharge (L/s)
50
40
30
20
10
0
$\delta^{18}O$ (‰)
-5.5
-6.0
-6.5
-7.0
-7.5
WB0
WBT440
Si (ppm)
3.4
3.2
3.0
2.8
2.6
2.4
2.2
WB0
WBT440
12
13
14
15
16
17
18
19
2
December 1992

16 prior to the storm (Fig. 11b). During the entire storm event, the oxygen isotope signature of stream flow at site WB60 fluctuated between -5.7‰ and -6.4‰ (Appendix A). Most of the variation in oxygen composition, including the most negative value, occurred in the first half of the day on the 17th (early in the storm on the rising portion of the hydrograph). Post-storm stream flow had an oxygen isotope signature similar to pre-event water (-6.2‰). The oxygen isotope composition of stream flow through site WB300 varied (from -6.6‰ to -6.2‰) throughout the storm event (Appendix A), but within the analytical error of the analyses (±0.5‰). Initially, the oxygen isotope composition of ephemeral flow through site WBT440 remained fairly constant ($\delta^{18}O$ = -6.1‰; Fig. 11b), with the exception of the second sample. During the descending portion of the hydrograph (late December 17 - early December 18), the oxygen isotope composition became lighter (-7.4‰), and then returned to -5.9‰ before flow stopped.

At both WB60 and WBT440 sites, the silica content of stream flow was initially high, decreased rapidly, and then gradually increased (Fig. 11c). At site WB60 silica concentrations were relatively high prior to the first rain event (3.53 ppm), and decreased afterward despite only a small increase in flow (3.18 ppm). During the second rain event, the silica concentration decreased rapidly to a low of 2.38 ppm, and then increased

on the descending portion of the hydrograph to a final value of 2.97 ppm. Similar to site WB60, silica in stream flow at site WBT440 was initially high 3.03 ppm, rapidly decreased to 2.28 ppm, and then gradually increased to a final 2.66 ppm (Fig. 11c).

Vadose water

The hour at which flow was initiated at the subsurface weir site is unknown because of mechanical failure of the automatic sampler at this site. The first grab samples were collected at ~11:00 am on December 17. Subsurface flow at this site ended by the afternoon of December 17.

Soil samples taken both pre- and post-event from five sites located in the vicinity of the borehole W7 show similar compositional trends in oxygen, hydrogen, and silica (Table 4). Pre-event A-soil horizon samples are relatively enriched in ^{18}O, and slightly depleted in deuterium compared to B-horizon soils (Table 4; Fig. 12d). Post-event, A-horizon soil shifts towards more negative $\delta^{18}O$ values, while becoming slightly enriched in deuterium. The B horizon soils become more enriched in oxygen after the event. Post-event deuterium trends are difficult to determine based on the limited number of analyses.

Pre-event silica concentrations in soil horizon A are consistently greater than B horizon soils (Table 4; Fig. 12e). Post-event, the silica

Table 4. Average oxygen and hydrogen isotopic compositions and silica concentrations in surface soil horizons (A and B) sampled in December 1992.

		December 15 1992		December 19 1992	
		A horizon	B horizon	A horizon	B horizon
$\delta^{18}O$	ave	-6.0	-7.0	-7.0	-5.7
(‰)	range	-6.6 to -4.9	-7.3 to -6.7	-7.7 to -6.2	-5.9 to -5.5
δD	ave	-35	-29	-35	-28
(‰)	range	-42 to -25	-40 to -20	-40 to -33	-34 to -27
Si	ave	3.02	0.50	2.87	1.57
(ppm)	range	2.22 to 4.28	0.30 to 0.75	2.22 to 3.98	0.03 to 3.10

Figure 12. Stream discharge at two stream sites (a) is compared to groundwater levels in four wells (b), discharge at four springs (c), oxygen isotope compositions (d) and silica concentrations (e) of three wells, four springs, and soil water samples, during a December 15 - 19, 1992 storm event.

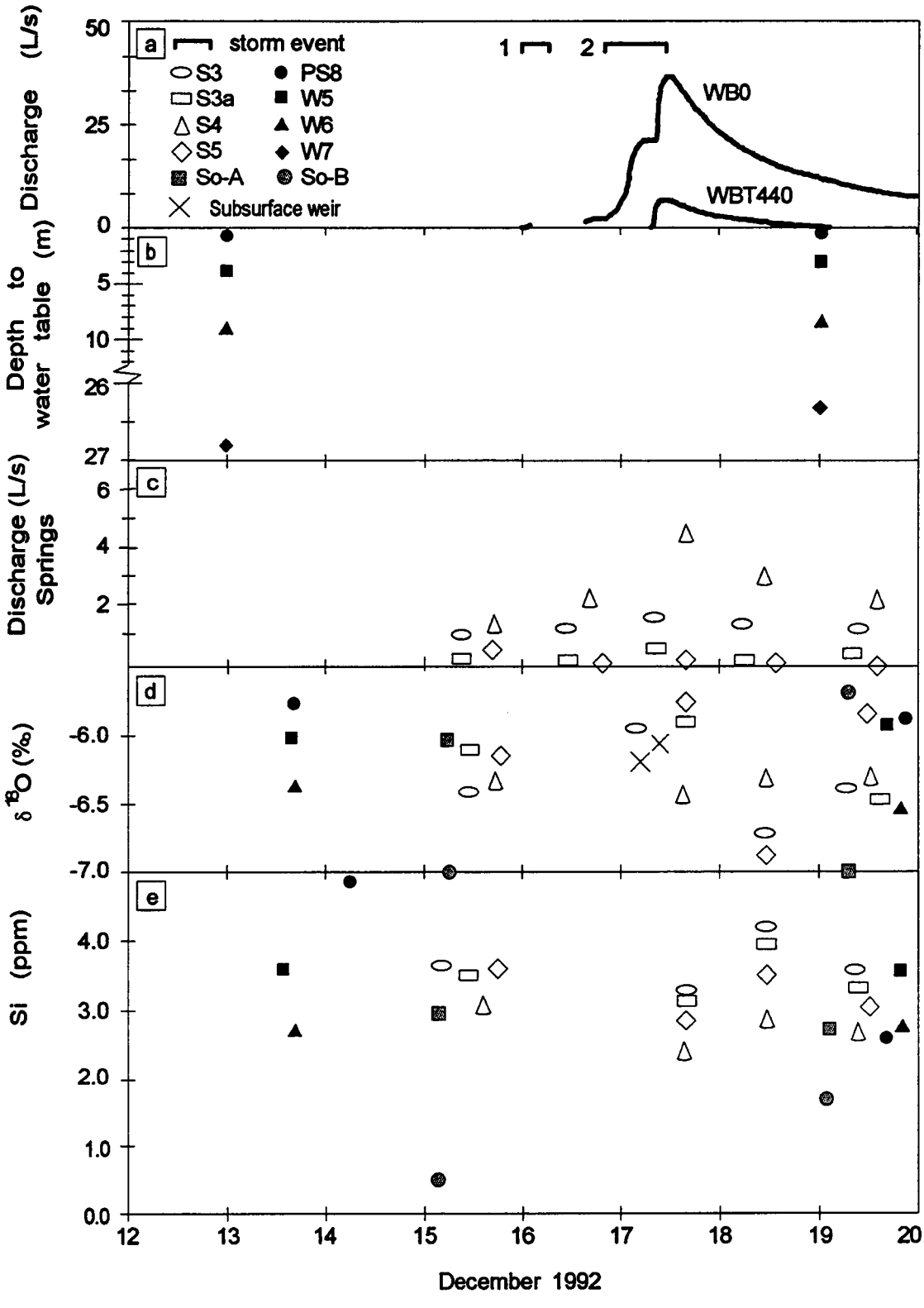
a
storm event
1
2
S3
S3a
S4
S5
So-A
PS8
W5
W6
W7
So-B
Subsurface weir
WB0
WBT440
Discharge (L/s)
50
25
0
b
Depth to water table (m)
5
10
26
27
c
Discharge (L/s) Springs
6
4
2
d
δ18O (‰)
-6.0
-6.5
-7.0
e
Si (ppm)
4.0
3.0
2.0
1.0
0.0
12
13
14
15
16
17
18
19
20
December 1992

concentrations decrease in the A horizon (Table 4; Fig. 12e) and increase markedly in the B horizon. The silica concentration of B-horizon soil water was usually less than 1 ppm. This is unlike that measured by Mulholland (personal communication), and Wilson and others (1991b), which indicate an average silica concentration between 2 and 3 ppm.

Groundwater

Water levels rose by 0.180 - 1.142 m in all four groundwater wells due to the December 15 - 19 storm event (Table 5). Unlike the relatively flat seasonal trends in water level seen in the shallow well (PS8; Fig. 7), water levels in PS8 were significantly affected by the storm event (Fig. 12b). This is most likely due to the expansion of the stream channel during the event, and the existence of several storm-generated groundwater springs in the vicinity of this well. In fact, the well casing was surrounded by ephemeral spring flow.

Flow increased in all four groundwater springs during the event (Fig. 12c). Flow in spring S4 located near the shallow well (PS8) increased most, with a maximum discharge increase of 4.31 L/s above baseflow conditions (1.98 L/s). The maximum measured spring flow occurred at nearly the same time as peak stream discharge on December 17. On the basis of daily spring discharge measurements, groundwater from these four

Table 5. Depth to the water table in four wells prior to and after a storm event.

Well name	Depth to the water table (m) Dec. 13 1992	Dec. 19 1992
PS8	0.914	0.560
W5	5.482	5.302
W6	13.074	11.932
W7	26.902	26.660

springs collectively contributed a minimum of 4 L/s and a maximum of 10 L/s to the stream hydrograph at site WBO.

Groundwater sampled from three wells was apparently unaffected isotopically by the storm event within the sampling interval (Fig. 12d). Possible isotopic variations during the event could not be observed because of the nature of the sampling equipment used. The shallow well (PS8) had an average oxygen signature of -5.8‰. Groundwater sampled from W5 and W6 had average oxygen signatures of -5.9‰, and -6.5‰, respectively. Silica concentrations remained fairly constant in wells W5 and W6 (Fig. 12e). The silica concentration in the shallow well (PS8) greatly decreased after the event (from 4.87 to 2.63 ppm; Fig. 12e). The silica concentration of groundwater samples collected once a month over 2 years indicate an average silica concentration of 3.7 ppm (Mulholland, personal communication).

The oxygen isotope composition of samples from three groundwater springs (S3, S3a, S5) varied in response to the storm event. The $\delta^{18}O$ values of groundwater at these sites became more positive from December 15 to 17, more negative from December 17 to 18, and more positive again from December 18 to 19 (Fig. 12d). In contrast, the oxygen composition of groundwater sampled at spring site S4 remained essentially constant throughout the event (Fig. 12d). Springs sites S3 and S3a had similar

isotopic compositions and discharge patterns each day sampled (Fig. 12c, d), although discharge from spring S3 was consistently 1.50 L/s higher. It can be assumed that, because of their isotopic and discharge similarities and proximity to each other, they are fed by the same fracture system. Spring site S5, with one exception on December 18, was the most enriched in oxygen-18 ($\delta^{18}O$ = -6.2‰). Spring S5 forms a relatively wide, flat, and slow-moving pool above the flume. This pool provides a large surface area for evaporation of the spring water upstream from the sampling point. Enriched isotopic compositions may result from such evaporation.

The silica concentration in samples from groundwater springs S3, S3a, S4, and S5 varied in response to the storm event, with each spring experiencing similar temporal trends of dilution or concentration (Fig. 12e). From December 15 to 17, the silica concentration in the springs decreased. From December 17 to 18, it increased; from December 18 to 19, they decreased once again. Silica concentrations in springs S3 and S3a were greater than in the other two springs (~3.17 ppm), with S4 being the most dilute (~3.06 ppm). Spring S4 and the adjacent shallow well (PS8) do not share the same pre-event silica content (S4 = 3.06 ppm, PS8 = 4.87 ppm). This difference may be a result of an inaccurate analysis of the pre-event silica concentration in water from well PS8. Their post-event

silica concentrations are similar (S4 = 2.69 ppm, PS8 = 2.63 ppm).

Hydrograph separation

Three storm flowpaths have previously been identified in the West Fork of Walker Branch Watershed through hydrologic and chemical (Ca and SO_4) measurements (Mulholland et al., 1990; Mulholland, 1993). These flowpaths include: 1) groundwater flow through bedrock which supplies much of the base flow to the perennial stream, 2) saturated soil flow just above the bedrock-soil interface which contributes both to base flow and storm flow, and 3) a perched saturation zone within the upper soil horizon that supplies flow only during storm events. The contribution of new (precipitated) water along each of these flowpaths was not considered in the three component model applied, although new water could be important in the perched flowpath and possibly the deeper saturated soil flowpath.

Storm flow end-member mixing calculations

The general approach to hydrograph separation based on an end-member mixing model is to determine the end-members that potentially produce storm flow, using oxygen and hydrogen isotope ratios, or selected ion concentrations. This is done by solving a set of mixing equations for

the fractional contribution of each end-member to stream flow at any time. The two-component mass balance mixing equations are as follows:

$$Q_t = Q_o + Q_n$$

and:

$$Q_o/Q_t = [(C_t - C_n)/(C_o - C_n)]$$

where Q is discharge, C is the tracer concentration, and the subscripts t, n, and o refer to the total, new, and old water components, respectively (Sklash and Farvolden, 1979; Ingraham et al., 1991). For these equations, "new" water is event precipitation and "old" water includes both groundwater and soil moisture present before the event (Sklash and Farvolden, 1979; Pearce et al., 1986; Sklash et al., 1986; Bottomley et al., 1986). Only a single tracer (isotope or solute) is needed to solve these equations since there are only two unknowns (Q_o and Q_n).

A more recently proposed three end-member model considers the separate contribution of soil water and groundwater to "old" waters (Pearce et al., 1986; DeWalle et al., 1988; Christophersen et al., 1990; Hooper et al., 1990). In this case,

$$Q_t = Q_p + Q_s + Q_{gw}$$

and:

$$Q_s/Q_t = [(C_t - C_{gw})/(C_s - C_{gw})] - Q_p/Q_t[(C_p - C_{gw})/(C_s - C_{gw})]$$

where Q and C are as above and the subscripts t, p, s, and gw represent total stream flow, event precipitation, old soil water, and old groundwater components (DeWalle et al., 1988). Solution of the three end-member equation requires two independent tracers (isotopes and/or solutes) (Sklash and Farvolden, 1979). Because oxygen and hydrogen experience similar temperature-dependent fractionation, and their isotopic ratios are correlated, they cannot be considered independent tracers. However, a conservative chemical constituent such as Si may be used as a second tracer.

Two end-member model

The separations performed for WB0 using $\delta^{18}O$ yielded a "new" water (precipitation) contribution of 1% of the total storm flow volume (7.2 x 10^6 L). The maximum "new" water contribution at any time for which we have water samples was 12% (Table 6), occurring within the

Table 6. The percentage of new water, soil water, and groundwater contributed to total storm flow at stream site WB0, including the maximum contribution to stream flow at a sampled interval. Two and three component model results are compared.

Model	Tracer	Comments	Component	Total (%)	Max. (%)
two component	$\delta^{18}O$	incremental new water	new water	1	12
		independent rainfall events	new water	<1	12
	Si	measured Si, new = 0.02 ppm	new water	5	15
		"background" Si new = 0.02 ppm	new water	16	26
three component	$\delta^{18}O$ and Si	measured Si incremental new water	new water soil water groundwater	5 50 45	32 71
		measured Si, new = 0.02 ppm independent new	new water soil water groundwater	<1 48 52	5 54
		"background" Si incremental new water	new water soil water groundwater	3 52 46	9 66
		"background" Si independent new water	new water soil water groundwater	2 52 46	5 68

first few hours of storm flow in the morning of December 16 (Fig. 13a, b). The results of the separations indicate that the contribution of precipitation to total stream flow was significant only during the period of rain. At the height of stream flow at site WB0 on December 17, the "new" water contribution had declined to 1%.

New water contributed 5 - 16% of the total stream flow at site WB0 when calculated using measured and "background" silica as a tracer (Table 6). The maximum "new" water contribution was 15% (measured silica) to 26% ("background" silica), occurring at the first peak in stream flow (Fig. 13c, d, respectively). This estimate is slightly greater than that determined from the application of oxygen-18 as a tracer (Table 6). At the height of stream flow at site WB0, the "new" water contribution based on Si concentration was 7% (measured) or 19% ("background"). The results of the separation performed using "background" silica indicated a new water contribution greater than that determined from the other two end-member separations (Table 6).

The application of oxygen-18 as a hydrograph component tracer at the ephemeral stream site WBT440 also indicates the dominance of the "old" water contribution to stream flow (Table 7; Fig. 14). New water contributed 3 - 6% of the total stream flow volume (19,927 L) at site WBT440 based on hydrograph separations using the isotopic composition

Figure 13. Two end-member hydrograph separations of stream flow at perennial stream site WB0 to identify old versus new water. An incremental new water hydrograph separation method using oxygen as a tracer (a) is compared to an independent new water method using oxygen (b), a method using measured silica tracer concentrations (c); and one using background silica tracer concentrations (d).

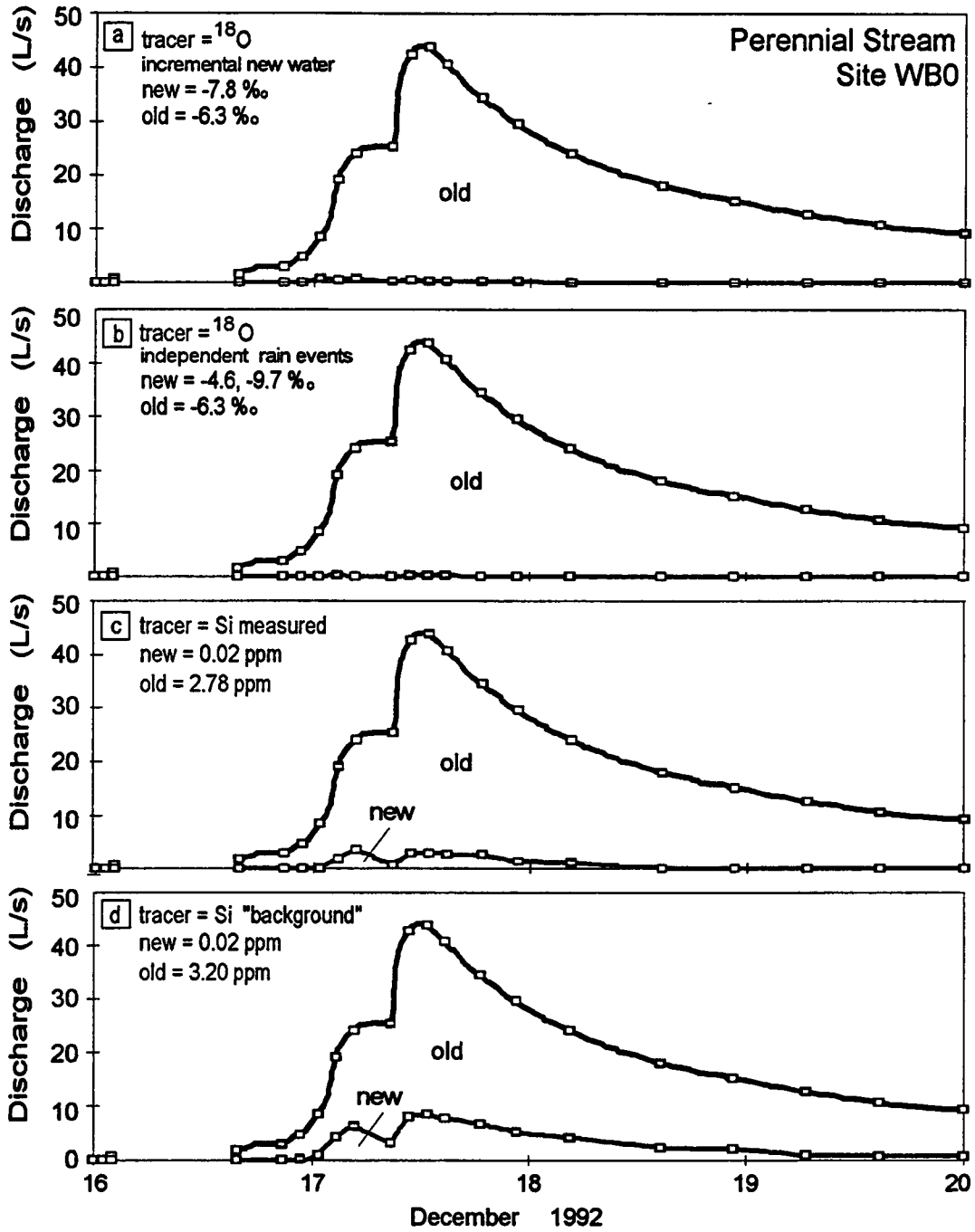
a tracer = ^{18}O
incremental new water
new = -7.8 ‰
old = -6.3 ‰
Perennial Stream
Site WB0
old
b tracer = ^{18}O
independent rain events
new = -4.6, -9.7 ‰
old = -6.3 ‰
old
c tracer = Si measured
new = 0.02 ppm
old = 2.78 ppm
old
new
d tracer = Si "background"
new = 0.02 ppm
old = 3.20 ppm
old
new
Discharge (L/s)
0
10
20
30
40
50
16
17
18
19
20
December 1992

Table 7. The percentage of new water, soil water, and groundwater contributed to total storm flow at ephemeral stream site WBT440, including the maximum contribution to stream flow at a sampled interval. Two and three component model results are compared.

Model	Tracer	Comments	Component	Total (%)	Max. (%)
two component	$\delta^{18}O$	incremental new water	new water	6	8
		independent rainfall events	new water	3	3
	Si	measured Si, new = 0.02 ppm	new water	8	18
		"background" Si new = 0.02 ppm	new water	19	29
three component	$\delta^{18}O$ and Si	measured Si incremental new water	new water soil water groundwater	6 45 48	11 71
		measured Si, new = 0.02 ppm independent new	new water soil water groundwater	2 52 45	3 59
		"background" Si incremental new water	new water soil water groundwater	7 78 15	14 59
		"background" Si independent new water	new water soil water groundwater	4 96 0	17 100 14

Figure 14. Two end-member hydrograph separations of stream flow at perennial stream site WBT440 to identify old versus new water. An incremental new water hydrograph separation method using oxygen as a tracer (a) is compared to an independent new water method using oxygen (b), a method using measured silica tracer concentrations (c); and one using background silica tracer concentrations (d).

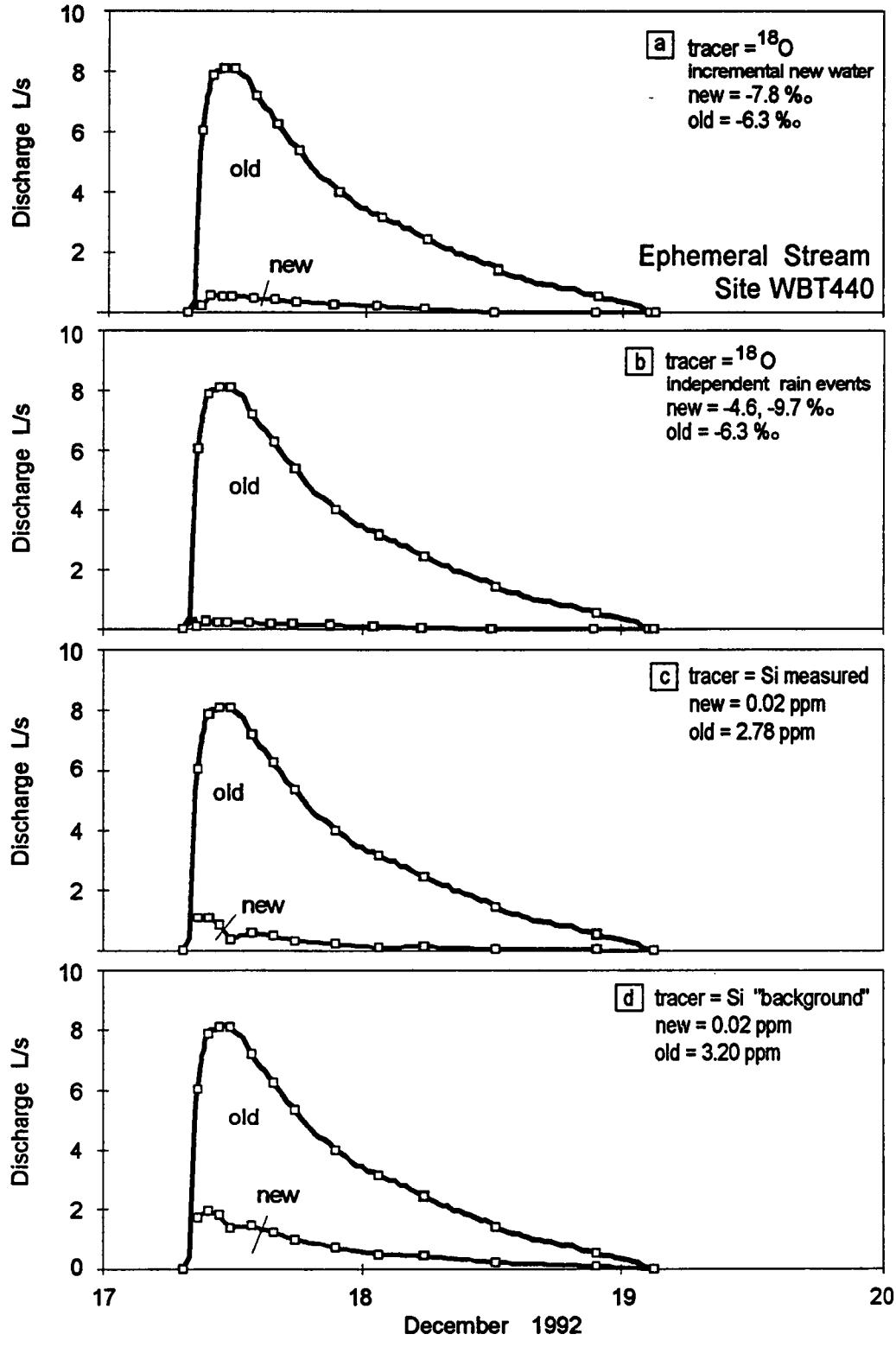
a tracer = 18O
incremental new water
new = -7.8 ‰
old = -6.3 ‰
Ephemeral Stream
Site WBT440
b tracer = 18O
independent rain events
new = -4.6, -9.7 ‰
old = -6.3 ‰
c tracer = Si measured
new = 0.02 ppm
old = 2.78 ppm
d tracer = Si "background"
new = 0.02 ppm
old = 3.20 ppm
old
new
Discharge L/s
0
2
4
6
8
10
17
18
19
20
December 1992

of the second rainfall event, and an incremental-weighted average of the isotopic composition of both rainfall events combined (Fig. 14b, a, respectively). The maximum "new" water contribution was calculated as 3% (second rainfall composition) to 8% (weighted average of both rainfall events' isotopic composition), occurring near the peak of stream flow (Table 7; Fig. 14b, a, respectively). The period in which the "new" water contribution was greatest was during and shortly after the period of rainfall on December 17.

The stream flow separation for WBT440 calculated using silica as a tracer yielded a greater estimate (8% measured, 19% "background") for the new water contribution to total stream flow (Table 7; Fig. 14c, d, respectively). The maximum new water contribution to stream flow was calculated at 18 - 29%, as stream flow first began at the ephemeral stream site (Table 7; Fig. 14c, d). The results of the hydrograph separations for stream site WBT440 using measured silica and a combined oxygen isotopic composition of both rainfall events were similar. The separation performed using "background" silica concentrations for old water was most unlike the results obtained by separations using other tracer concentrations (measured silica or either oxygen solution).

Three end-member model

The three end-member mixing model simultaneously considers the $\delta^{18}O$ composition and silica concentration of waters to determine the individual contributions of groundwater (wells and springs), soil water (A and B soil horizons), and throughfall. Pre-event oxygen isotope tracer concentrations for both groundwater and soil water were determined from samples of each collected before the event (Appendix B). Groundwater samples were from three wells and four springs; soil water samples were of the A and B soil horizons. The pre-event oxygen-18 compositions of groundwater and soil water were $\delta^{18}O$ = -6.1‰ (± 0.3‰, n=7), and $\delta^{18}O$ = -6.5‰ (± 1.2‰, n=8), respectively (Appendix B).

Four three end-member separations were performed for each stream site. The first separation used the incremental volume-weighted throughfall averages applied in the two end-member model ($\delta^{18}O$ = -7.8‰ and Si = 0.56 ppm). The old soil (1.78 ppm) and groundwater (3.56 ppm) silica concentrations applied in both the first and second hydrograph separations were an average of measured values. A new water silica concentration of 0.02 ppm was applied in the second separation method. This value was based on the silica concentrations in precipitation measured in previous research. The $\delta^{18}O$ composition of the first rainfall event was applied only to the time when the second rainfall event began (separate new water

compositions). The third separation method used "background" silica concentrations (soil water 2.7 ppm and groundwater 3.7 ppm), a new water Si concentration of 0.02 ppm, and an incremental volume-weighted throughfall $\delta^{18}O$ composition (combined rainfall events). The final separation method used "background" silica concentrations, new water Si = 0.02 ppm, and two separate new water $\delta^{18}O$ compositions. Each solution assumed that groundwater and soil water retained their pre-event isotopic ratios and silica concentrations during the event.

Three end-member separations using measured tracer concentrations

The first application of the three end-member model used the measured "new" and "old" water tracer concentrations. The tracer concentration of samples from three wells and four springs was used to compute the groundwater tracer concentration (Appendix B). The soil water tracer concentration was the average of the tracer concentrations in A and B soil horizon samples.

The solution to the three end-member model, using measured tracer concentrations, indicates that precipitation contributed 5%, soil water 50%, and groundwater 45% to the total stream flow at perennial site WB0 (Table 6; Fig. 15a). The maximum "new" water contribution of 32% (Table 6), occurred as the second rain event began. Soil water rapidly increased

Figure 15. Three end-member hydrograph separations of stream flow at perennial stream site WB0 using oxygen and silica to distinguish between new water, soil water, and groundwater. The separation methods are (a) incremental new water oxygen isotopic compositions and measured silica concentrations; (b) independent new water and measured silica concentrations; (c) incremental new water and background silica concentrations; and (d) independent new water and background silica concentrations.

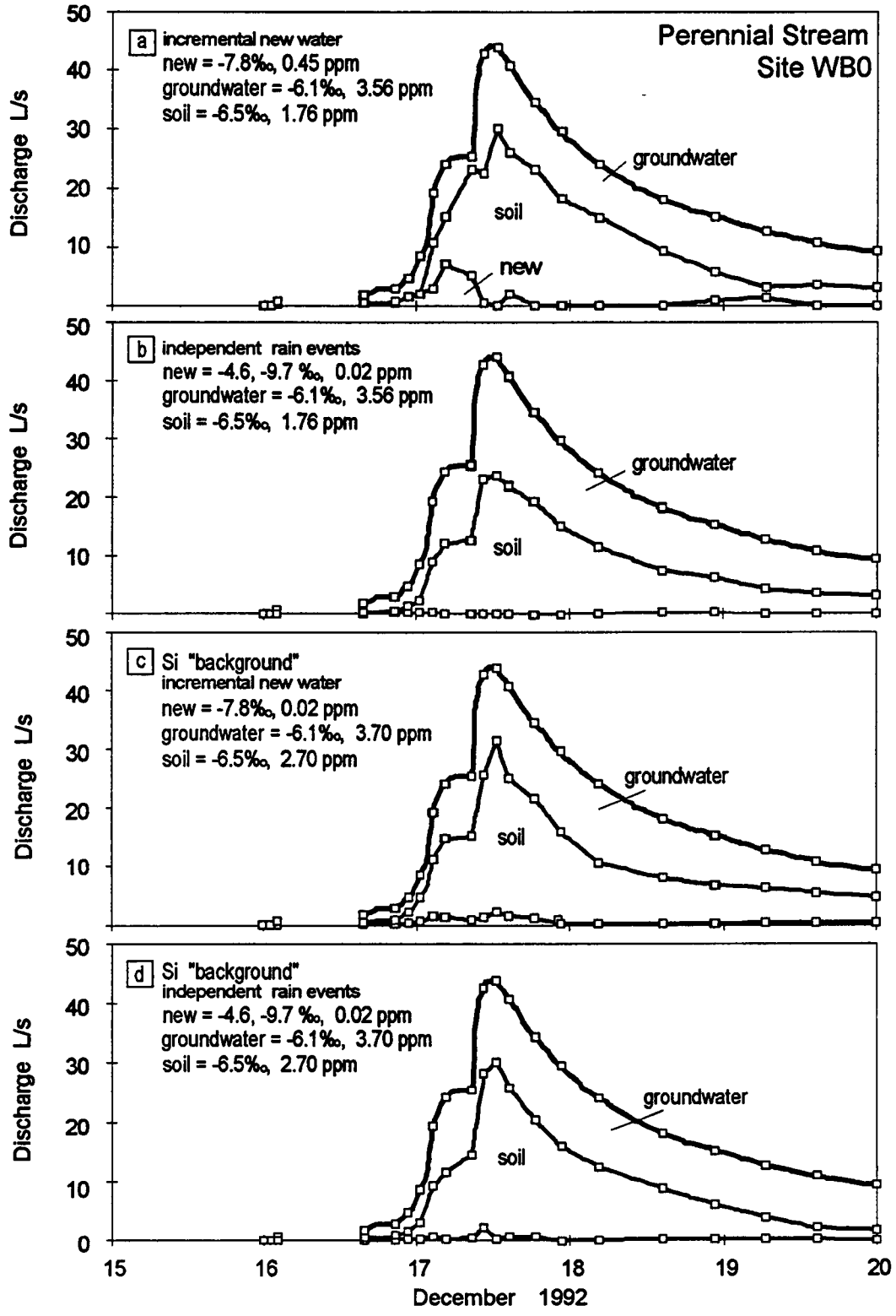
Perennial Stream
Site WB0
a incremental new water
new = -7.8‰, 0.45 ppm
groundwater = -6.1‰, 3.56 ppm
soil = -6.5‰, 1.76 ppm
groundwater
soil
new
b independent rain events
new = -4.6, -9.7 ‰, 0.02 ppm
groundwater = -6.1‰, 3.56 ppm
soil = -6.5‰, 1.76 ppm
groundwater
soil
c Si "background"
incremental new water
new = -7.8‰, 0.02 ppm
groundwater = -6.1‰, 3.70 ppm
soil = -6.5‰, 2.70 ppm
groundwater
soil
d Si "background"
independent rain events
new = -4.6, -9.7 ‰, 0.02 ppm
groundwater = -6.1‰, 3.70 ppm
soil = -6.5‰, 2.70 ppm
groundwater
soil
Discharge L/s
0
10
20
30
40
50
15
16
17
18
19
20
December 1992

to a maximum contribution of 71% between peaks in storm stream flow. Soil water usually contributed no less than 33% of storm flow. The maximum groundwater contribution was 79%, occurring prior to the second rain event. The minimum groundwater contribution was 9%, occurring as soil water reached its maximum contribution between peaks in stream flow.

Groundwater dominated storm stream flow at ephemeral site WBT440 (Fig. 16a). The solution to the three end-member model at this site indicates that precipitation contributed 6%, soil water 45%, and groundwater 48% to the total stream flow. Precipitation reached a maximum contribution of 11% (Table 7) during the peak in stream flow; 5 hours after the second rain event ended. The maximum soil water contribution of 71% was determined from the first ephemeral stream sample collected. Groundwater contributed a minimum of 29% while soil water reached its peak contribution, and a maximum of 57% at 2:40 am on December 18.

Three end-member separations using measured Si concentrations, 0.02 ppm new water Si, and separate rainfall events

The second separation method applied real silica concentrations to old soil water (1.78 ppm) and groundwater (3.56 ppm), a new water Si

Figure 16. Three end-member hydrograph separations of stream flow at perennial stream site WBT440 using oxygen and silica to distinguish between new water, soil water, and groundwater. The separation methods are (a) incremental new water oxygen isotopic compositions and measured silica concentrations; (b) independent new water and measured silica concentrations; (c) incremental new water and background silica concentrations; and (d) independent new water and background silica concentrations.

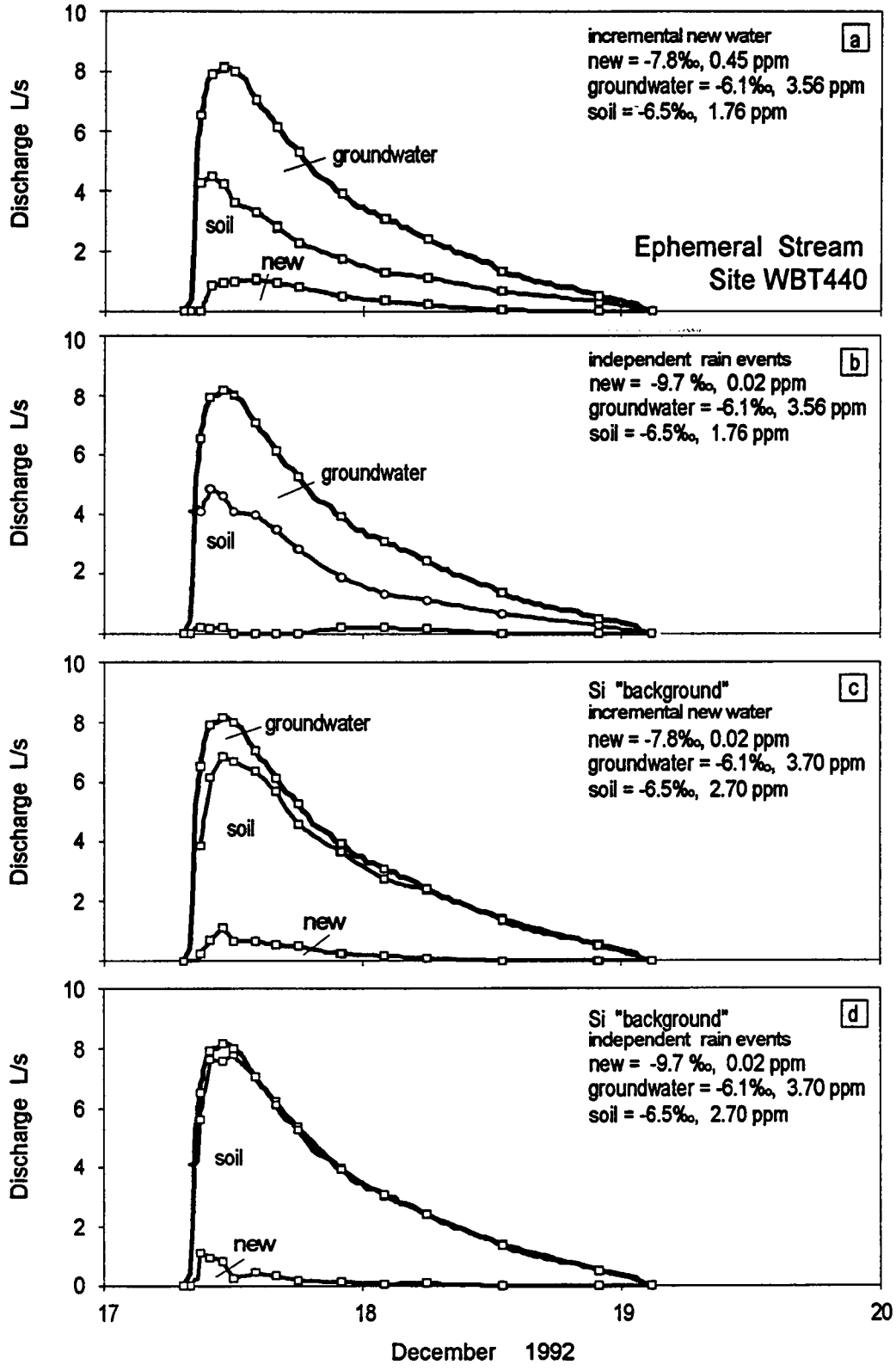
Discharge L/s
10
8
6
4
2
0
incremental new water
new = -7.8‰, 0.45 ppm
groundwater = -6.1‰, 3.56 ppm
soil = -6.5‰, 1.76 ppm
a
groundwater
soil
new
Ephemeral Stream
Site WBT440
independent rain events
new = -9.7 ‰, 0.02 ppm
groundwater = -6.1‰, 3.56 ppm
soil = -6.5‰, 1.76 ppm
b
Si "background"
incremental new water
new = -7.8‰, 0.02 ppm
groundwater = -6.1‰, 3.70 ppm
soil = -6.5‰, 2.70 ppm
c
Si "background"
independent rain events
new = -9.7 ‰, 0.02 ppm
groundwater = -6.1‰, 3.70 ppm
soil = -6.5‰, 2.70 ppm
d
17
18
19
20
December 1992

concentration of 0.02 ppm, and assumed two separate rainfall events. The $\delta^{18}O$ composition of the first rainfall event was applied only up to the time when the second rainfall event began, after which time only the composition of the second rainfall event was applied.

The solution to the second hydrograph separation indicated that new water, soil water and groundwater contributed $\ll 1\%$, 48%, and 52%, respectively to the total stream flow at site WB0 (Table 6; Fig. 15b). The maximum new water contribution was determined to be 5% of stream flow as the second rainfall event began. Soil water reached a maximum of 55% of stream flow at the height of flow. According to this hydrograph solution, groundwater and soil water contributed nearly equally to the stream storm flow (Table 6).

The total new water, soil and groundwater contributions to storm stream flow at site WBT440 were 2%, 52%, and 45%, respectively (Table 7), using the above mentioned tracer concentrations. The maximum new water contribution was 3%, occurring as stream flow first began. The contribution of soil water and groundwater were essentially equal during the height of stream flow (Figure 16b). Groundwater contributed no less than 37% and no more than 57% to storm stream flow at any sampled interval.

Three end-member separations using background Si concentrations

The third three end-member mixing model applied measured oxygen isotopic ratios, and background silica concentrations of event precipitation (0.02 ppm), soil water (2.70 ppm), and groundwater (3.7 ppm) determined from previous research by Mulholland (personal communication) and Wilson and others (1991b). This method used an incremental volume-weighted new water $\delta^{18}O$ composition which combined the values of both rainfall events through time.

This application of the three end-member mixing model indicates that new water contributed 3%, soil water 52%, and groundwater 46% to the total stream flow at site WB0 (Table 6). The maximum new water contribution was 9% (Table 6), occurring prior to the initial peak in stream flow (Fig. 15c). The soil water contribution to stream flow was approximately 66% during peak stream flow (Fig. 15c). It was least during the first few hours of stream storm flow, and remained greater than 40% after the peak in stream flow. Groundwater dominated stream flow at the beginning and end of the sampling interval, with soil water dominating stream flow between these times (Fig. 15c). The minimum contribution of groundwater (29%) occurred at the same time that soil water reached its maximum.

Soil water dominated the hydrograph at ephemeral stream site

WBT440 (Fig. 16c). Here, new water contributed 7%, soil water 78%, and groundwater 15% of the total stream flow (Table 7). The maximum new water contribution was determined to be 14% of stream flow, occurring during the peak in ephemeral stream flow (Fig. 16c). The soil water contribution was greatest during the last sampled intervals (98%), and least as flow first began (59%). The groundwater contribution was as little as 1%, and never exceeded 36% (during the first hours of ephemeral flow).

Three end-member separations using independent throughfall events

The third end-member separation method used background silica concentrations and measured oxygen isotope compositions for event precipitation, soil water, and groundwater (see *Three end-member separation using background Si concentrations* for tracer concentrations). However, the tracer concentrations of each precipitation event were applied to the model independently of each other. The tracer concentrations of the first rainfall were used only up to the moment the second rainfall began. With the onset of the second rainfall, the tracer concentrations of "new" water applied to the model were those of the second rainfall event only.

The solution to the end-member separation identifying two distinct

rainfall events indicates that new water, soil water and groundwater contributed 2%, 52%, and 46% of total stream storm flow at stream site WB0, respectively (Table 6). New water contributed a maximum of 5% to stream flow during the first hours in which the second rainfall event began (Fig. 15d). Soil water dominated the storm hydrograph during hours in which peak flow occurred (Fig. 15d). The maximum contribution to stream flow was 68%, occurring at the peak in flow. The groundwater contribution was least during this time (31%), and never exceeded 89% (first hours of stream flow).

Soil water dominated the storm hydrograph at the ephemeral stream site WBT440 using separate "new" water tracer concentrations (Fig. 16d). Soil water contributed an average of 96%, "new" water an average of 4%, and groundwater an average of $<1\%$ to the total ephemeral stream flow (Table 7). Soil water contributed no less than 70% to the stream flow at any sampled interval. The "new" water contribution represented the second rainfall event only, since the first event had ended before ephemeral stream flow began. The results of this separation are unlike the results of all other separations.

All of the three end-member separations performed for stream flow at site WB0 had similar results, with soil water and groundwater contributing nearly equally to the total stream storm flow (45 - 52%). The

new water contribution to stream flow was $<<1$ to 5% as a result of the three end-member hydrograph separations. The new water contribution to stream flow determined in this model was similar to that of two end-member separations, with the two end-member separation using "background" silica concentrations being greater (16%).

The results of the three end-member separations performed for stream storm flow at site WBT440 varied from 2% to 7% new water, with the soil water contribution ranging from 45% to 96%, and groundwater 0% to 48%. The results of the two end-member separations are similar to those of the three end-member separations (3% to 8%), with the exception of the two end-member separation using "background" silica concentrations (19%). The results of the "background" silica two end-member separations for stream flow at sites WB0 and WBT440 are unlike the results of the three end-member hydrograph separations.

VI. Discussion

The purpose of this study was to evaluate the sources of groundwater recharge and surface discharge in the West Fork of Walker Branch Watershed. This was done through tracer analysis of watershed hydrology at regular intervals over time and during one storm event. In the following section (**Annual conditions**) the 1) type and quantity of water recharging and discharging the watershed, and 2) significance of soil water moisture and oxygen isotope profiles with depth are examined. Conclusions are drawn concerning the role and timing of new water, soil water and groundwater in storm-generated runoff in the subsequent section on the **December 15 - 19, 1992 storm**.

Annual conditions

Throughfall

A local meteoric water line having a slightly steeper slope ($\delta^{18}O = 9.08\delta D + 17$) than the global meteoric water line was defined using 43 throughfall samples collected over 16 months. The local meteoric water line describes the isotopic composition of precipitation over only a limited sampling interval. The oxygen and hydrogen isotopic compositions of local throughfall lie within the scatter of the global line (Craig, 1961b), and therefore, the presently defined local meteoric water line is likely not

different from the global meteoric water line. Thus, the global meteoric water line should continue to be used to describe local precipitation.

The local meteoric water line was established with throughfall samples to describe the isotopic composition of recharge within the watershed, and the surrounding region. Open rainfall was not collected during this study, therefore the difference between precipitation and throughfall cannot be evaluated at this time. Future studies comparing open rainfall and throughfall would be useful in understanding the effects of the forest canopy on both the isotopic composition and volume of meteoric water recharging the watershed.

The isotopic composition of water recharging the watershed is volume dependent, therefore, a volume-weighted average isotopic signature should be used. This weighted average is calculated using the equation:

$$WA = \Sigma(v*\delta)/\Sigma v$$

(Dansgaard, 1964; Yurtsever and Gat, 1981), where WA equals weighted average, v is the volume of precipitation from an individual event, and δ is the isotopic composition of an individual event. Volume-weighted summer monthly isotope averages are fairly constant ($\delta^{18}O$ = -4.2 ±1.6‰, δD = -21 ±11‰) whereas winter precipitation varies significantly from month to month ($\delta^{18}O$ = -7.6 ±3.5‰, δD = -49 ±24‰; Figure 17). The unweighted and volume-weighted $\delta^{18}O$ and δD annual, summer and winter

Figure 17. Volume weighted average monthly oxygen and hydrogen isotope compositions of throughfall in Walker Branch Watershed (line). Spikes represent the precipitation thickness of each event; dots represent the oxygen isotopic composition of individual events.

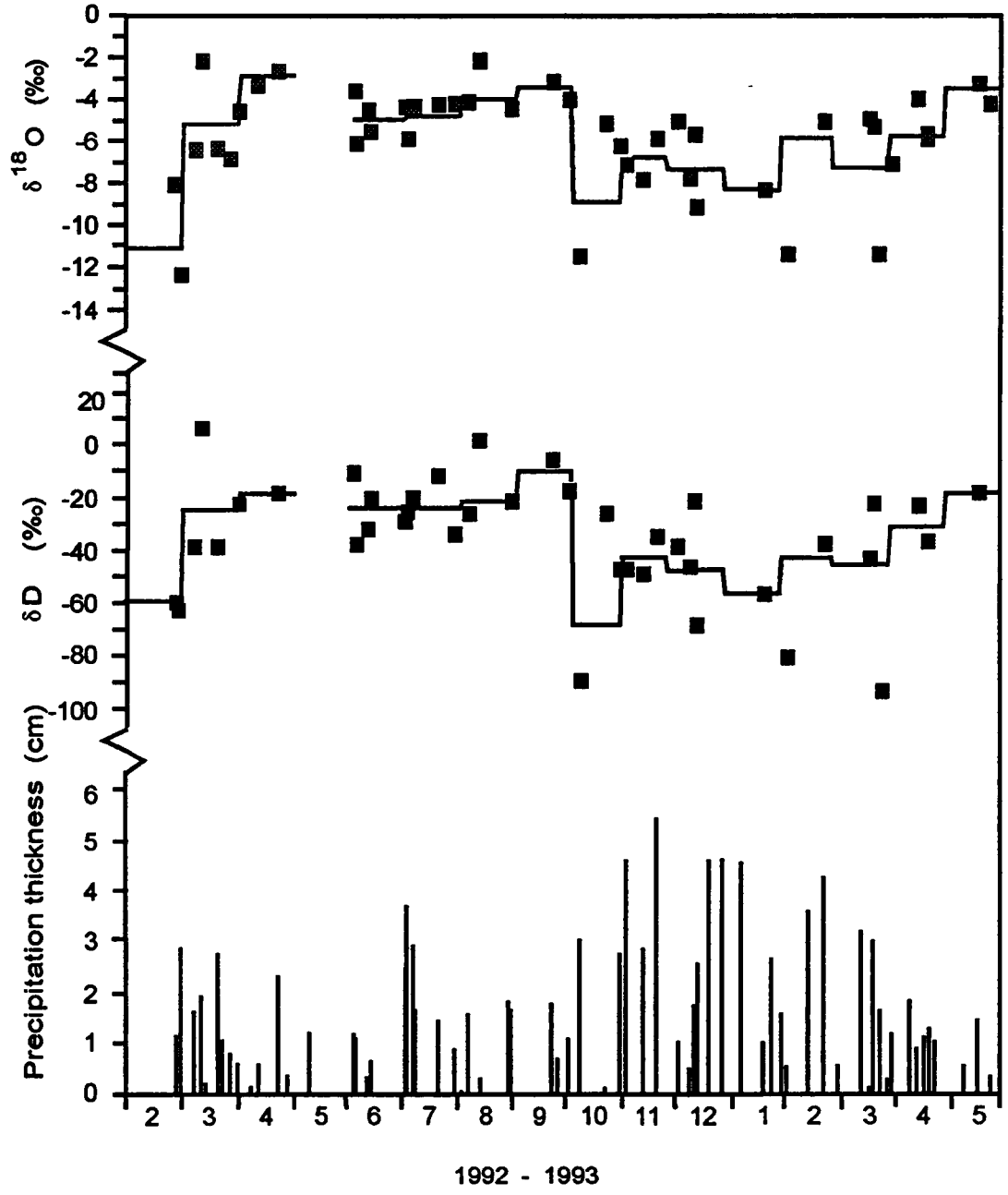
δ 18O (‰)
0
-2
-4
-6
-8
-10
-12
-14
δD (‰)
20
0
-20
-40
-60
-80
-100
Precipitation thickness (cm)
6
5
4
3
2
1
0
2 3 4 5 6 7 8 9 10 11 12 1 2 3 4 5
1992 - 1993

averages are similar (Table 8). Recent studies indicate that only portions of a rainfall event are responsible for groundwater recharge, not the entire volume of rainfall infiltrating the ground surface (Nativ, personal communication).

Vadose water

The auger and core sampling method employed to sample the soil column in the bore hole (W7; Fig. 2) allows for the examination of discrete portions of the soil column but is inadequate to determine whether individual portions of the column are in fact lateral or vertical flow zones. Although this method was employed, the abundant presence of zones containing high soil moisture within a soil matrix having low hydraulic conductivity support the idea of preferred subsurface pathways recharging deeper groundwater. Intersecting fragmented chert zones act as macropores to quickly facilitate infiltration to greater depths. At shallower depths, root channels, worm burrows, and other macropores act to channel water downslope at shallow depths in response to storm events. Shallow subsurface flow was observed during this study, and in many previous hydrologic studies of the Walker Branch Watershed since the installation of the subsurface weir. Previous solute studies in the 0.47 ha subcatchment of the Walker Branch Watershed (Jardine et al., 1990; Luxmoore et al.,

Table 8. Average and volume-weighted average oxygen and hydrogen isotopic composition of throughfall.

	Average		Volume-weighted average	
	$\delta^{18}O$ (‰)	δD (‰)	$\delta^{18}O$ (‰)	δD (‰)
Annual	-5.6	-34	-5.7	-33
Winter	-7.6	-49	-7.0	-47
Summer	-4.2	-21	-4.2	-20

1990; Mulholland et al., 1990; Mulholland 1993) indicate that infiltrating rainfall quickly flows through meso- and macro- pores, bypassing much of the soil matrix.

The low soil moisture content (13.3%) and relatively depleted oxygen isotope composition ($\delta^{18}O$ = -10.7‰), in soils of the top 0.61 m of the bore hole (0 - 0.61 m) would indicate that evaporation, which would cause a relative enrichment in heavy isotopes, is less significant than the movement of recently infiltrated waters to greater depths. Previous studies (Jardine et al., 1990; Luxmoore et al., 1990; Mulholland, 1990; Wilson et al, 1990) have determined that shallow subsurface flowpaths facilitate flow to the stream channel as a result of relatively large rain events (depending on the preceding soil moisture conditions), whereas, deeper subsurface flowpaths continuously supply the underlying groundwater table (Mulholland et al., 1990; Mulholland, 1993; Wilson et al., 1991a). Variations in oxygen isotope signatures with depth probably represent a combination of: 1) mixing of infiltrated water with water held in meso- and micro- pores, and 2) infiltrated waters which bypassed the soil matrix through macro- or mesopores, allowing less mixing to occur with soil moisture.

The significance of the soil moisture profile, logging of saturated soil horizons, and the oxygen isotopic composition of soil horizons with depth

is dependent on the timing of the emplacement of the bore hole, as well as the interconnected nature of the numerous soil horizons. The mobility of soil water within different soil horizons may differ, therefore, caution should be exercised when interpreting the variability of oxygen isotopic compositions with depth. Additionally, the seasonal timing of the bore hole soil sampling should be considered when any translation from winter soil moisture or oxygen isotopic composition profiles to that of summer are being made. Finally, the borehole samples obtained during December 1991 represent the soil moisture content and oxygen isotopic composition of a limited spatial distance.

Surface water and groundwater

Winter precipitation recharging the groundwater system in the Walker Branch Watershed and the surrounding region largely determines the isotopic composition of groundwater discharging to streams. The isotopic composition of groundwater recharge should approximate the average winter precipitation signature, due to the greater volume of winter precipitation available for recharge (lower rates of evapotranspiration). Indeed, the annual isotopic composition of groundwater ($\delta^{18}O$ = -6.0‰) and surface water ($\delta^{18}O$ = -6.0‰) sampled in the Walker Branch Watershed reflect winter precipitation compositions ($\delta^{18}O$ = -7.0‰;

volume-weighted $\delta^{18}O$ = -7.6‰) more closely than summer precipitation (unweighted and volume-weighted $\delta^{18}O$ = -4.2‰). Three East Tennessee rivers sampled by Kendall (unpublished data) have average annual isotopic signatures ($\delta^{18}O$ = -6.4‰, δD = -39‰) similar to surface water sampled in the Walker Branch Watershed. The 1.6‰ difference between the average annual compositions of stream flow and groundwater, and volume-weighted winter throughfall supports the conclusion that winter precipitation is the dominant, but not only, source of groundwater recharge. The isotopic composition of baseflow and throughfall are consistent with a minor contribution of summer precipitation to groundwater recharge within the watershed. Evaporation of infiltrated winter precipitation within the soil column could also account for the relative enrichment of the baseflow oxygen isotope composition.

December 15 - 19, 1992 storm

Throughfall

Although the calibration of the sequential throughfall collector was such that the two precipitation events were separated into only three portions, decreases in $\delta^{18}O$ and δD throughout the event were detected. Mulholland (unpublished data) has also measured progressive declines in the $\delta^{18}O$ content of throughfall during storms in the Walker Branch

Watershed. Unlike the suggestion of using several rainfall collectors (Kendall and McDonnell, 1993), throughfall collected at one site in the Walker Branch Watershed is believed to be representative of precipitation occurring over this relatively small watershed (38.4 ha). The depletion of oxygen and hydrogen isotopic ratios measured in throughfall throughout this event indicates the importance of sequential rainfall sampling, especially in the application of environmental isotopes or water chemistry to water evolution studies. Sequential rainfall sampling allows for more precise quantitative solutions to hydrograph separations. Only that portion of a rain event that has reached the ground surface is incorporated into the model at any point in time.

An estimate of the volume of direct channel rainfall can be determined for both rainfall events assuming an equal throughfall distribution. Direct channel precipitation from the first event (~25,950 L) and second event (~42,000 L) totaled ~67,950 L (channel area = 1500 m^2; Mulholland, 1993). Direct channel precipitation therefore accounts for a very small portion of the total stream flow.

Surface water

There were two responses in stream flow at site WBO. First, direct channel precipitation from the first rainfall event immediately caused a

slight increase in flow. Second, a much greater increase in stream flow occurred as a result of the second rain event, approximately 18 hours after the first precipitation event ended. This rise in stream flow occurred during the hours of precipitation. Stream flow increased again and reached maximum discharge as flow through the ephemeral stream sites began. The relatively quick response of the watershed to the second rainfall event is likely related to the saturated watershed conditions following the first event.

Direct channel interception from the first rain event had little effect on the oxygen isotopic composition and silica concentration of stream water at site WB0, whereas direct channel interception from the second event decreased the $\delta^{18}O$ value of stream water. The oxygen isotope composition of stream water was unaffected by direct channel interception of the first event because of their similar compositions (rain $\delta^{18}O$ = -5.7‰; stream flow $\delta^{18}O$ = -6.0‰), and dilution of silica in stream flow was minimal (0.51 ppm). Direct channel precipitation of the second event temporarily resulted in a more negative oxygen isotope composition of stream water ($\delta^{18}O$ = -6.3‰).

Due to the timing of the rainfall events and the onset of ephemeral stream flow at stream site WBT440, it is assumed that discharge at this site was mainly in response to the second rain event. Previous studies

(Mulholland 1990; 1993) indicate that both stream sites WB0 and WBT440 respond nearly simultaneously to large precipitation events. In this case, it can be concluded that the first rain event created saturated conditions within the watershed, after which time the second rain event caused ephemeral flow to begin at stream site WBT440 and produced the large response in flow at WB0.

Similar to stream flow at site WB60, precipitation initially affected the isotopic composition and silica concentration of stream water at site WBT440. Although the second rainfall event was nearly over when ephemeral stream flow began (Fig. 11a), the flushing of new water caused a momentary decrease in the $\delta^{18}O$ value (-6.9‰) and a sharp decline in the silica concentration (0.75 ppm difference) of stream flow at site WBT440 one hour after flow began (Fig. 11b, c). After this time, the oxygen isotope composition of the stream water returned to a -6.0‰ value, typical of annual groundwater and surface water. The silica concentration also increased, but it remained diluted compared to the first sample's concentration.

The persistence of low silica concentrations in stream flow at sites WB0 and WBT440 supports the hypothesis that soil water, rather than precipitation, was a major contributor to stream flow. The rapid decline in stream water silica concentration as stream flow increased at site WB0 (to

a minimal 2.38 ppm) and WBT440 (minimal 2.28 ppm) related to the first and second rain events, would indicate that soil water (average Si = 1.76 ppm) was a major contributor to stream flow. The silica concentration in stream flow increased momentarily between the stream flow peaks resulting from the two rain events. The dilution of the silica concentration in stream flow at both sites can only be partially accounted for by direct channel precipitation (volume-weighted Si = 0.45 ppm; 0.02 ppm background levels) of both rainfall events. Direct channel precipitation over the entire stream channel amounted to a total volume of approximately 67,950 L (channel area = 1500 m^2). Direct channel precipitation from the second rain event (~42,000 L) could account for ~2% of the increase in stream flow during the hours in which the rain fell (42,000 L of direct channel precipitation; stream flow increase of 31.09 L/s over 15.5 hrs).

Vadose water

Throughfall which infiltrated the ground surface caused a depletion in the ^{18}O value of the A-horizon soil water. Post-event B horizon soil water was more enriched in ^{18}O ($\delta^{18}O$ = -5.7‰) than pre-event soil water ($\delta^{18}O$ = -7.0‰); whereas, post-event A horizon soil water was more depleted (pre-event $\delta^{18}O$ = -6.0‰; post-event $\delta^{18}O$ = -7.0‰). The enrichment of B

horizon soil water and depletion of A horizon soil water may be caused by infiltration of more depleted precipitation (volume-weighted average $\delta^{18}O$ = -7.3‰) displacing some A-horizon soil moisture into the underlying B horizon and diluting what remains within the A horizon. Two scenarios exist with the post-event B-horizon soil moisture becoming: a) more enriched than that of pre-event A horizon; and b) enriched, but less than that of pre-event A horizon waters (Table 2). This is probably due to the amount of mixing which occurs during displacement of A horizon soil moisture into the B horizon.

The dissolution of silica controlled the silica concentration in surface soils after both rainfall events. Dissolution of silica from micro- and meso-pores in shallow surface soils was induced by the introduction of infiltrating throughfall having a low silica concentration (volume-weighted average of 0.56 ppm; background level = 0.02 ppm). Wilson and others (1991b) determined that meso- and micro- pores of surface soils sampled in a 0.47 ha subcatchment of the Walker Branch Watershed, were capable of supplying a semi-infinite source of solutes to water within macropores. The maximum difference between averaged pre- and post- event soils during this study was 0.29 ppm, occurring in the B horizon. The A horizon soils experienced only a 0.08 ppm difference in silica concentration.

The silica concentration of groundwater and surface water might be

controlled by silica concentrations in soil water. The range of individual soil concentrations (0.03 - 4.28 ppm) bounds that of groundwater wells and springs (2.44 - 4.18 ppm), with one exclusion that will be discussed in the next section.

Groundwater

Dissolution of silica from siliceous dolomite and chert may account for the high silica concentration (4.87 ppm) in one shallow well (PS8) prior to the storm event (Fig. 12e). Although soil silica concentrations may determine the silica concentration of groundwater, in a catchment consisting of siliceous dolomite with occasional chert beds, the local dissolution of silica from these sources may occur concurrently. The ultimate silica concentration in any water would be controlled by equilibrium reactions under certain pH and temperature conditions. (Amorphous silica has a solubility product constant of 2×10^{-3} at 25 ^{0}C (Drever, 1988).) The silica concentration in this well was diluted as a result of the storm event (2.63 ppm) similar to the dilution of silica in subsurface (Wilson et al., 1991b) and surface water during increased flow. Presumably, as the rate of groundwater flow decreases, the dissolution of silica would again cause an increase in silica content. The silica concentrations in the other two sampled wells were essentially unaffected

by the storm event during the sampled period (Fig. 12e). The average silica concentrations in groundwater wells before and after the event were 3.14 ppm (excluding PS8) and 3.00 ppm, respectively. This agrees with the range of groundwater silica concentrations of 3 - 4 ppm observed by Mulholland (personnel communication) over a 2 year period.

Hydrograph separations using two and three end-member models

Due to the timing of the rainfall events versus the increase in stream flow, the limited number of sequential throughfall samples had no negative effect on the results of the end-member models. The application of either an incremental, or an average weighted mean (McDonnell et al., 1990) for the tracer composition of throughfall throughout the event yielded the same results.

The results of eight individual hydrograph separations for new water (precipitation), soil water, and groundwater at each stream site can readily be compared. The four two-end-member (old versus new water) separation methods used were: 1) ^{18}O as a tracer, incremental new water tracer concentration; 2) ^{18}O as a tracer, separate or independent rainfall tracer concentrations; 3) measured Si concentrations as a tracer; and 4) background Si concentrations as a tracer. The four three end-member (new, old soil water, old groundwater) separation methods used were:

1) combined new water and measured Si tracer concentrations; 2) independent new water tracer concentrations and measured silica concentrations (0.02 ppm new water substituted); 3) combined new water tracer concentration and background Si concentrations; and 4)independent rainfall tracer concentrations and background silica concentrations. As previously stated, the background silica concentrations were determined from previous research performed in the Walker Branch Watershed. These silica concentrations are believed to be more representative of the "background" silica concentrations in each of these waters.

Precipitation

Event precipitation (new water) accounted for only a small portion of the stream flow resulting from the two rain events. Eight individual hydrograph separations performed for each stream site indicate that precipitation contributed 1 - 16% of the total stream flow at stream site WBO, and 2 - 19% of the total stream flow at site WBT440. Most of this contribution occurred during the hours in which the second rain event occurred (20:54 December 16 through 12:24 December 17), and after subsurface flow began in the subsurface weir (observed at ~11:00 am on December 17). The maximum individual new water contribution to stream flow at stream site WBO (5 - 32%) and stream site WBT440 (3 - 29%)

occurred just prior to or at the peak in stream discharge. The largest average new water contributions to total stream flow at both sites was a result of the separations performed using background silica concentrations. The results of the other separations agreed more closely to each other.

Vadose water

Vadose water was determined to be a significant component of storm-generated stream flow. The soil water contribution to stream flow measured at site WBO was greatest during peak stream flow, and increased during times of increasing stream flow. The soil water contribution at stream site WBT440 was greatest as ephemeral stream flow began and reached its peak at this site, and then the soil water contribution declined. The decline in the soil water contribution to stream flow at both stream sites could be attributed to 1) the declining effect of shallow subsurface flow as infiltration of precipitation ended; and/or 2) the increasing influence of deeper soil water flowpaths resulting in a greater groundwater contribution (documented in similar studies in Walker Branch Watershed by Mulholland et al., 1990; Wilson et al., 1990, Wilson et al., 1991a).

Results of the three end-member models disagreed on the soil water contribution to total stream flow. The average soil water contribution determined ranged from 48 - 52% of the total stream flow at site WBO,

and 40 - 96% at site WBT440. The largest soil water contribution determined for stream site WBT440 (96%) was the result of the separation using independent rainfall events and background silica concentrations. The results of the other three separations performed at this site range more closely (45 - 78% of the total stream flow). The maximum soil water contributions determined ranged from 66 - 71% at stream site WB0, and 59 - 100% at site WBT440. The results of these separations indicate that soil water was a significant contributor to storm stream flow and dominated the storm hydrograph during some of the periods sampled. The separations performed at stream site WBT440 indicate that soil water contributed slightly more to this stream location than to site WB0. This difference can be explained by the greater number of groundwater outlets to the stream channel below stream site WBT440, supplying the lower portions of the stream with larger quantities of groundwater.

Groundwater

Some of the groundwater contribution to stream flow may to attributed to groundwater "ridging" near the stream channel. The volume of groundwater discharging to the stream over the duration of the event cannot be quantified without continuous water table-level monitoring in several wells located near the stream channel. It can, however, be

concluded that groundwater ridging would be more significant in the lower portions of the stream channel where the water table is closer to the stream channel elevation. The significant role of groundwater throughout the storm event at both stream sites supports the theory of a deeper preferred subsurface flowpath recharging the groundwater system.

The four applications of the three component model yield slightly different implications to the role of groundwater as a storm flow component. The average groundwater contribution to stream flow was greater at stream site WB0 (45 - 52%) than at site WBT440 (0 - 50%). Thus, groundwater was a significant contributor to storm stream flow at both stream sites. The results of the separations performed for stream flow at site WBT440 using measured silica concentrations were consistent with the results of the four separations performed for site WB0. The results of the three component models applying background silica concentrations at site WBT440 were more variable. Generally, the groundwater contribution to stream flow at both sites decreased while flow increased, and then increased again after the peak in stream discharge, when the soil water contribution was greatest.

Model limitations

It is important to address the limitations of the hydrograph separations. The similarity of $\delta^{18}O$ values in pre-storm groundwater and soil water compositions make three component hydrograph separations difficult to perform. The similarity of end-member contributions resulting from the two component model using silica as a tracer, however, would indicate that, although this assumption was not met for oxygen, it had little effect on the results of the separations.

Pre-storm soil water tracer concentrations are fair representations of soil water flowing through macropores along the shallow subsurface flowpath, but may not be representative of subsurface flow along deep flowpaths. The surface soil samples collected were from within 1 m depth, and therefore are not absolute representations of the entire soil column. Deep soil water was not represented in the pre-storm tracer concentrations, although soil moisture at greater depth may be an important contributor to subsurface flow along deep flowpaths. The tracer concentrations in the soil water represented are fair representations of soil water (2 m depth) believed to contribute to the shallow storm flow zone.

Oxygen isotope compositions and silica concentrations of subsurface flow throughout the event and silica concentrations with depth in the 30 m deep borehole would have been extremely useful in substantiating the role

of preferred subsurface flowpaths, and the amount of mixing that occurs along the flowpath. The three water samples collected from the subsurface weir on December 17 had oxygen isotope compositions of -6.3‰, the same as the average pre-storm surface soil signatures (Appendix A). It is unknown, due to mechanical failure of the automatic sampler (battery died with no replacement battery available), whether the composition of soil waters flowing through the subsurface weir changed or remained constant during the event. It could be assumed, based on the dilution of silica in subsurface flow during previous storm events within this site (Wilson et al., 1991b), that the silica concentration would have declined during the event as recently infiltrated waters initiated subsurface flow.

Comparison to other watersheds

The results of an isotopic characterization of precipitation, soil water and groundwater occurring within the Georgia Piedmont (Wenner et al., 1991) are similar to the results presented for the Walker Branch Watershed. The oxygen isotopic composition of precipitation, soil water and groundwater are slightly more positive within the watershed studied in the Georgia Piedmont (~1‰). However, the seasonal trends observed in the two watersheds were similar. Within both watersheds, the isotopic

composition of groundwater remains fairly constant throughout the calendar year. Within the Georgia Piedmont watershed, the composition of summer stream water was more enriched (0.5‰) relative to the groundwater supplying it because of evaporation affecting water ponded above the sampling site.

The results of the hydrograph separations performed for storm stream flow in the West Fork of the Walker Branch Watershed are similar to several watersheds in which either "old" water macropore flow and/or the development of a perched water table occurs within the unsaturated zone. Storm flow generation within the Maimai catchment in New Zealand is most similar to Walker Branch. Within the Maimai catchment macropore flow is initiated after a perched water table develops (McDonnell, 1990). Within both watersheds, soil water is significant in generating storm flow.

The dominance of old water in storm hydrographs in the Walker Branch and Maimai watersheds, as well as catchments in the Georgia Piedmont (Wenner et al., 1991) and the Tawhai State Forest, Westland, New Zealand (Pearce et al., 1986), do not explain the rapid flushing of new water via macropore flow. Instead, the recently infiltrated new water must quickly lose its isotopic identity by mixing with the significantly larger volume of soil water before reaching the stream channel (Wenner et al., 1991). Thus within these watersheds, the water transported through

macropores must be largely old soil water, but possibly including some new event water that has isotopic and/or chemical compositions similar to that of the soil water.

Literature Cited

Adar, E. M., A. Karnieli, B. Z. Sandler, A. S. Issar, M. Wolf, L. Landsman, and K. Rozanski, A mechanical sequential rain sampler for isotopic and chemical analyses, IAEA Contract No. 5542/RO/RB, Final Report, 1991.

Bottomley, D. J., D. Craig and L. M. Johnston, Oxygen-18 studies of snowmelt runoff in a small Precambrian shield watershed: Implications for streamwater acidification in acid-sensitive terrain, J. Hydrol., 88, 213-234, 1986.

Christophersen, N., C. Neal, R. P. Hooper, R. D. Vogt and S. Anderson. Modelling streamwater chemistry as a mixture of soilwater end-members - a step towards second-generation acidification models, J. Hydrol., 116, 307-320, 1990.

Craig, H., Standards for reporting concentrations of D and delta 18O in natural waters, Science, 133, 1833-1834, 1961a.

---------- Isotopic variations in meteoric waters, Science, 133, 1702-1703, 1961b.

Crider, D. V., Structural and stratigraphic effects on geomorphology and groundwater movement in Knox Dolostone terrain, M.S. Thesis, University of Tennessee, Knoxville, Tennessee, 1981.

Dansgaard, W., Stable isotopes in precipitation, Tellus, XVI, 436-468, 1964.

DeWalle, D. R., B. R. Swistock and W. E. Sharpe, Three-component tracer model for stormflow on a small Appalachian forested catchment, J. Hydrol., 104, 301-310, 1988.

Drever, J. I., The geochemistry of natural waters, 2nd ed., Prentice Hall, New Jersey, 437p., 1988.

Dutton, A. R. and W. W. Sympkins, Isotopic evidence for paleohydrologic evolution of groundwater flow paths, Great Plains, Geology, 7, 653-656, 1989.

Epstein, S., and T. Mayeda, Variation of 18O content of waters from natural sources, Geochim. Cosmochim. Acta, 4, 213-224, 1953.

Freeze, R. A., Streamflow generation, Rev. Geophys. Space Phys., 12, 627-647, 1974.

Fritz, P., J. A. Cherry, K. U. Weyer, and M. G. Sklash, Storm runoff analyses using environmental isotopes and major ions, in Interpretation of Environmental Isotope and Hydrochemical Data in Groundwater Hydrology, IAEA, Vienna, 111p., 1976.

Gardner, W. H., Water Content, in Methods of Soil Analysis, ed. C.A. Black, pp. 82-125, American Society of Agronomy, Wisconsin, 1965.

Gat J. R., and Y. Tzur, Modification of the isotopic composition of rainwater by processes which occur before groundwater recharge, in Isotopes in Hydrology, IAEA, Vienna, 49-60, 1967.

Genereux, D., H. Hemond, and P. Mulholland, Field studies of streamflow generation using natural and injected tracers on Bickford and Walker Branch Watershed, ORNL/TM-12018, Oak Ridge National Laboratory, Oak Ridge, Tennessee, 1992.

Godfrey, J.D., The deuterium content of hydrous minerals from the Early Cambrian, Sierra Nevada and Yosemite National Park, Geochim. Cosmochim. Acta, 26, 1215-1245, 1962.

Hatcher, R. D. Jr., P. J. Lemiszki, R. B. Dreier, R. H. Ketelle, R. R. Lee, D. A. Lietzke, W. M. McMaster, J. L. Foreman, and S. Y. Lee, Status report on the geology of the Oak Ridge Reservation, ORNL/TM-12074, Oak Ridge National Laboratory, Oak Ridge, Tennessee, 1992.

Hewlett, J. D., Principles of forest hydrology, The University of Georgia Press, Athens, 183p., 1982.

Hewlett, J. D., and A. R. Hibbert, Moisture and energy conditions within a sloping soil mass during drainage, J. Geophys. Res., 68, 1081-1087, 1963.

Hewlett, J. D., and A. R. Hibbert, Factors affecting the response of small watersheds to precipitation in humid areas, in Forest Hydrology, ed. W. E. Sopper and H. W. Lull, Pergamon Press, Oxford, 275-290, 1967.

Hinton, M. J., S. L. Schiff, and M. C. English, Examining the contributions of glacial till water to storm runoff using two- and three-component hydrograph separations, Water Resour. Res., 30, 983-993, 1994.

Hirata, T., and K. Muraoka, The relation between water migration and chemical processes in a forest ecosystem, in Tracers in Hydrology, 31-40, IAHS, 215, 1993.

Hooper, R. P., N. Christophersen and N. E. Peters, Modelling streamwater chemistry as a mixture of soilwater end-members - an application to the Panola Mountain catchment, Georgia, U.S.A., J. Hydrol., 116, 321-343, 1990.

Hooper, R. P., and C. A. Shoemaker, A comparison of chemical and isotopic hydrograph separation, Water Resour. Res., 22, 1444-1454, 1986.

Horton, R. E., The role of infiltration in the hydrological cycle, Amer. Geophys. Union, Trans., 14, 446-460, 1933.

Ingraham, N. L., B. F. Lyles, R. L. Jacobson and J. W. Hess, Stable isotope study of precipitation and spring discharge in southern Nevada, J. Hydrol., 125, 243-258, 1991.

Jardine, P. M., G. V. Wilson, and R. J. Luxmoore, Unsaturated solute transport through a forest soil during rain storm events, Geoderma, 46, 103-118, 1990.

Kendall, C., unpublished data, U. S. Geological Survey, Menlo Park.

Kendall, C., and J. J. McDonnell, Effect of intrastorm isotopic heterogeneities of rainfall, soil water, and groundwater on runoff modelling, in Tracers in Hydrology (Proc. of the Yokohama Symp. 1993), pp. 41-48, IAHS, 215, 1993.

Kennedy, V. C., Silica variation in stream water with time and discharge, Adv. Chem. Ser., 106, 94-130, 1971.

Kennedy, V. C., C. Kendall, G. W. Zellweger, T. A. Wyerman and R. J. Avanzino, Determination of the components of stormwater using water chemistry and environmental isotopes, Mattole River Basin, California, J. Hydrol., 84, 107-140, 1986.

Ketelle, R. H., and D. D. Huff, Site characterization of the West Chestnut Ridge site, ORNL/TM-9229, Oak Ridge National Laboratory, Oak Ridge, Tennessee, 1984.

Lee, S. Y., O. C. Kopp, and D. A. Lietzke, Mineralogical characterization of West Chestnut Ridge soils, ORNL/TM-9361, Oak Ridge National Laboratory, Oak Ridge, Tennessee, 1984.

Lietzke, D. A., unpublished data, Lietzke Soil Services, Rutledge, Tennessee.

Lietzke, D. A., R. H. Ketelle, and R. R. Lee, Soils and geomorphology of the East Chestnut Ridge site, ORNL/TM-11364, Oak Ridge National Laboratory, Oak Ridge, Tennessee, 1989.

Lietzke, D. A., Soils of Walker Branch Watershed, ORNL/TM-11724, Oak Ridge National Laboratory, Oak Ridge, Tennessee, 1990.

Likens, G. E., H. Bormann, R. S. Pierce, J. S. Eaton, and N. M. Johnson, Biogeochemistry of a forested ecosystem, 146 pp., Springer-Verlag, New York, 1977.

Luxmoore, R. J., T. Grizzard, and M. R. Patterson, Hydraulic properties of Fullerton cherty silt loam, Soil Sci. Soc. Amer. J 45, 692-298, 1981.

Luxmoore, R. J., and C. H. Abner, Environmental Sciences Division field facilities for subsurface transport research, DOE/ER-0329, U. S. Dept. of Energy, Washington, D. C., 1987.

Luxmoore, R.J., and D.D. Huff, Water, in Analysis of biogeochemical cycling processes in Walker Branch Watershed, ed., D.W. Johnson and I. Van Hook, pp. 164-196, Springer-Verlag, New York, 1989.

Luxmoore, R. J., P. M. Jardine, G. V. Wilson, J. R. Jones and L. W. Zelazny, Physical and chemical controls of preferred path flow through a forested hillslope, Geoderma, 46, 139-154, 1990.

McDonnell, J. J., A rational for old water discharge through macropores in a steep, humid catchment, Water Resour. Res., 11, 2821-2832, 1990.

McDonnell, J. J., M. Bonell, M. K. Stewart, and A. J. Pearce, Deuterium variations in storm rainfall: Implications for stream hydrograph separation, Water Resour. Res., 26, 455-458, 1990.

McKeaque, J. A., and M. G. Cline, Silica in soil solutions, 1, The form and concentration of dissolved silica in aqueous extracts of some soils, Can. J. Soil Sci., 43, 70-82, 1963.

McMaster, W. M., Hydrologic data for the Oak Ridge area, Tennessee, U. S. Geological Survey Water Supply Paper 1839-N, U. S. Government Printing Office, Washington, D. C., 1967.

Mosley, M. P., Streamflow generation in a forested watershed, New Zealand, Water Resour. Res., 15, 795-806, 1979.

Mulholland, P. J., G. V. Wilson and P. M. Jardine, Hydrogeochemical response of a forested watershed to storms: effects of preferential flow along shallow and deep pathways, Water Resour. Res., 26, 3021-3036, 1990.

Mulholland, P. J., Hydrometric and stream chemistry evidence of three storm flowpaths in Walker Branch Watershed, J. of Hydrol., 151, 291-316, 1993.

Nativ, R. and R. Riggio, Precipitation in the southern high plains: meteorologic and isotopic features, J. Geophys. Res., 22, 559-564, 1990.

Nativ, R., and D. A. Smith, Hydrogeology and geochemistry of the Ogallala aquifer, Southern High Plains, J. Hydrol., 91, 217-253, 1987.

Pearce, A. J., and L. K. Rowe, Rainfall interception in a multistoried evergreen mixed forest: estimates using Gash's analytical method, J. Hydrol., 49, 341-353, 1981.

Pearce, A. J., M. K. Stewart and M. G. Sklash, Storm runoff generation in humid headwater catchments 1. Where does the water come from?, Water Resour. Res., 22, 1263-1272, 1986.

Peters, L. N., D. F. Grigal, J. W. Curlin, and W. J. Selvidge, Walker Branch Watershed report: chemical, physical, and morphological properties of the soils of Walker Branch Watershed, ORNL/TM-2968, Oak Ridge National Laboratory, Oak Ridge, Tennessee, 1970.

Ragan, R. M., An experimental investigation of partial-area contributions, Intern. Assoc. Sci. Hydrol. Gen. Assembly, Berne, Publ. 76, pp. 241-249, 1968.

Revesz, K. and P. H. Woods, A method to extract soil water for stable isotope analysis, J. Hydrol., 115, 397-406, 1990.

Shimada, Y., N. Ohte, and N. Tokuchi, A dissolved silica budget for a temperate forested basin, in Tracers in Hydrology (Proc. of the Yokohama Symp. 1993, pp. 23-30, IAHS, 215, 1993.

Sklash, M. G., R. N. Farvolden, and P. Fritz, A conceptual model of watershed response to rainfall developed through the use of oxygen-18 as a natural tracer, Can. J. Earth Sci., 13, 271-283, 1976.

Sklash, M. G. and R. N. Farvolden, The role of groundwater in storm runoff, J. Hydrol., 43, 45-65, 1979.

Sklash, M. G., M. K. Stewart and A. J. Pearce, Storm runoff generation in humid headwater catchments 2. A case study of hillslope and low-order stream response, Water Resour. Res., 22, 1273-1282, 1986.

Solomon, D. K., G. K. Moore, L. E. Toran, R. B. Dreier, and W. M. McMaster, A hydrologic framework for the Oak Ridge Reservation, Status Report, ORNL/TM-12026, Oak Ridge National Laboratory, 1992.

Space, M. L., N. L. Ingraham and J. W. Hess, The use of stable isotopes in quantifying groundwater discharge to a partially diverted creek, J. Hydrol., 129, 175-193, 1991.

Stewart, M. K. and J. J. McDonnell, Modeling base flow soil water residence times from deuterium concentrations, Water Resour. Res., 27, 2681-2693, 1991.

TVA, Upper Bear Creek experimental project: a continuous daily streamflow model, Research Paper No. 8, Tennessee Valley Authority, Knoxville, Tennessee, 1972.

Vennemann, T. W., and J. R. O'Neil, A simple and inexpensive method of hydrogen isotope and water analyses of minerals and rocks based on zinc reagent, Chem. Geology, 103, 227-234, 1993.

Whipkey, R. Z., Subsurface stormflow from forested slopes, Bull Intern. Assoc. Sci. Hydrol., 10, 74-85, 1965.

Wenner, D. B., P. D. Ketcham, and J. F. Dowd, Stable isotopic compositions of waters in a small Piedmont watershed, in Stable isotope geochemistry: a tribute to Samuel Epstein, ed., H. P. Taylor, Jr., J. R. O'Neil, and I. R. Kaplan, pp. 195-203, The Geochemistry Society, Special Paper No.3, 1991.

Wilson, G. V., and R. J. Luxmoore, Infiltration, macroporosity, and mesoporosity distributions on two forested watersheds, Soil Sci. Soc. Am. J., 52, 329-335, 1988.

Wilson, G. V., J. Alfonsi, and P. M., Jardine, Spatial variability of saturated hydraulic conductivity of the subsoil of two forested watersheds, Soil Sci. Soc. Am. J., 53, 679-685, 1989.

Wilson, G. V., P. M. Jardine, R. J. Luxmoore, and J. R. Jones, Hydrology of a forested watershed during storm events, Geoderma, 46, 119-138, 1990.

Wilson, G. V., P. M. Jardine, R. J. Luxmoore, L. W. Zelanzny, D. A. Lietzke and D. E. Todd, Hydrogeochemical processes controlling subsurface transport from an upper subcatchment of Walker Branch Watershed during storm events. 1. Hydrologic transport processes, J. Hydrol. 123, 297-316, 1991a.

Wilson, G. V., P. M. Jardine, R. J. Luxmoore, L. W. Zelazny, D. E. Todd and D. A. Lietzke, Hydrogeochemical processes controlling subsurface transport from an upper catchment of Walker Branch watershed during storm events. 2. Solute transport processes, J. Hydrol., 123, 317-336, 1991b.

Yurtsever, Y., and J. R. Gat, Stable isotope hydrology. Deuterium and oxygen-18 in the water cycle, IAEA, Vienna Tech. Rept. 210, Chap. 6., 1981.

Zimmermann, U., K. O. Munnich, W. Roether, W. Kreutz, K. Schubach, and O. Siegel, Tracers determine movement of soil moisture and evapotranspiration, Science, 152, 346-347, 1966.

Zimmermann, U., D. Enhalt, and K.O. Munnich, Soil water movement and evapotranspiration: changes in the isotopic composition of the water, in Isotopes in Hydrology (Proc. Symp. Vienna, 1966), 567p., IAEA, Vienna, 1967.

Appendices

Appendix A: Oxygen and hydrogen isotopic compositions and solute concentrations in throughfall, surface water, soil water, and groundwater samples. Included are volumes of throughfall samples, and the date/time (storm samples) of samples collected. Analytical methods described in text.

Sample	Date	Time	Volume (cm)	Depth (m)	^{18}O (‰)	^{2}H (‰)	Si ppm	Al ppm	B ppm	Ba ppm	Ca ppm	Cd ppm	Co ppm	Cr ppm	Cu ppm
Bulk	2/26/92		1.10		-8.0	-60									
Throughfall	2/26/92				-8.1										
	2/28/92		2.85		-12.3										
	3/7/92		1.65		-6.4	-39									
	3/11/92		1.92		-2.2	+7									
	3/13/92		0.22												
	3/20/92		2.74		-6.4	-39									
	3/22/92		10.40												
	3/26/92		0.80		-6.8										
	3/31/92		0.60		-4.5	-23									
	4/7/92		0.17												
	4/11/92		0.60		-3.4										
	4/22/92		2.30		-2.7	-19									
	4/29/92		0.38												
	5/9/92		1.21												
	6/3/92		1.18		-3.7	-11									
	6/4/93		1.10		-6.1	-38									
	6/10/92		0.33		-4.6	-32									
	6/12/92		0.66		-5.5	-21									
	7/1/92		2.46		-4.3	-29									
	7/2/92		3.68		-5.9	-26									
	7/5/92		2.91		-4.4	-20									
	7/6/92		1.65												
	7/19/92		1.43		-4.3	-12									
	7/28/92		0.91		-4.2	-34									
	7/31/92		0.07		-3.1										
	8/4/92		1.56		-4.1	-27									
	8/11/92		0.33		-2.2	+1									
	8/27/92		1.81		-5.6										
	8/28/92		1.65		-4.3	-21									
	9/20/92		1.78		-3.1	-6									
	9/23/92		1.71		-4.0										
	9/29/92		1.10		-4.0	-18									
	10/5/92		3.02		-11.5	-90									
	10/19/92		0.14		-5.2	-26									

Appendix A: continued

Sample	Date	Time	Fe ppm	K ppm	Mg ppm	Mn ppm	Mo ppm	Na ppm	Ni ppm	P ppm	Pb ppm	Sr ppm	Zn ppm
Bulk	2/26/92												
Throughfall	2/26/92												
	2/28/92												
	3/7/92												
	3/11/92												
	3/13/92												
	3/20/92												
	3/22/92												
	3/26/92												
	3/31/92												
	4/7/92												
	4/11/92												
	4/22/92												
	4/29/92												
	5/9/92												
	6/3/92												
	6/4/93												
	6/10/92												
	6/12/92												
	7/1/92												
	7/2/92												
	7/5/92												
	7/6/92												
	7/19/92												
	7/28/92												
	7/31/92												
	8/4/92												
	8/11/92												
	8/27/92												
	8/28/92												
	9/20/92												
	9/23/92												
	9/29/92												
	10/5/92												
	10/19/92												

Appendix A: continued

Sample	Date	Time	Volume (cm)	Depth (m)	^{18}O (‰)	^{2}H (‰)	Si ppm	Al ppm	B ppm	Ba ppm	Ca ppm	Cd ppm	Co ppm	Cr ppm	Cu ppm
Bulk	10/31/92		2.74		-6.3	-48									
Throughfall	11/4/92		4.58		-7.1	-47									
	11/13/92		2.83		-7.8	-50									
	11/25/92		5.43		-5.9	-35									
	12/7/92		1.04		-5.1	-39									
	12/13/92		0.55		-7.8	-46	0.15	0.00	0.70	0.01	2.55	0.00	0.00	0.00	0.00
	12/16/92		1.73		-5.7	-22	1.18	0.00	0.99	0.01	1.67	0.00	0.00	0.00	0.02
	12/17/92		2.69		-9.2	-69	0.00	0.06	0.21	0.01	0.71	0.00	0.00	0.00	0.02
	1/10/93		13.71												
	1/15/93		0.02												
	1/22/93		0.99		-8.3	-57									
	1/27/93		2.63												
	2/2/93		1.56												
	2/4/93		0.55		-11.3	-81									
	2/16/93		3.57												
	2/24/93		4.25		-5.1	-38									
	3/4/93		0.55												
	3/17/93		3.15												
	3/21/93		0.10		-4.9	-43									
	3/23/93		3.16		-5.4	-22									
	3/27/93		1.57		-11.4	-94									
	3/31/93		0.32												
	4/2/93		1.19		-7.1										
	4/13/93		1.82												
	4/16/93		0.89		-4.0	-23									
	4/21/93		1.12		-5.7										
	4/22/93		1.28		-5.9	-37									
	4/28/93		1.06												
	5/12/93		0.59												
	5/19/93		1.48		-3.3	-19									
	5/26/93		0.36		-4.2										
	6/2/93		1.35		-2.8										
	6/16/93		1.20												
	7/5/93		1.16												
Sequential	12/16/92		1.73		-4.6	-18	1.18	0.04	0.87	0.01	1.38	0.00	0.00	0.00	0.01
Throughfall	12/17/92		1.70		-9.3	-61	0.00	0.00	0.86	0.03	0.72	0.01	0.00	0.00	0.01

Appendix A: continued

Sample	Date	Time	Fe ppm	K ppm	Mg ppm	Mn ppm	Mo ppm	Na ppm	Ni ppm	P ppm	Pb ppm	Sr ppm	Zn ppm
Bulk	10/31/92												
Throughfall	11/4/92												
	11/13/92												
	11/25/92												
	12/7/92												
	12/13/92		0.00	2.79	0.40	0.00	0.00	0.92	0.07	0.00	0.02	0.00	0.06
	12/16/92		0.00	5.94	0.34	0.31	0.00	2.75	1.36	0.00	0.00	0.00	0.06
	12/17/92		0.00	1.34	0.19	0.00	0.00	0.58	0.00	0.00	0.01	0.00	0.16
	1/10/93												
	1/15/93												
	1/22/93												
	1/27/93												
	2/2/93												
	2/4/93												
	2/16/93												
	2/24/93												
	3/4/93												
	3/17/93												
	3/21/93												
	3/23/93												
	3/27/93												
	3/31/93												
	4/2/93												
	4/13/93												
	4/16/93												
	4/21/93												
	4/22/93												
	4/28/93												
	5/12/93												
	5/19/93												
	5/26/93												
	6/2/93												
	6/16/93												
	7/5/93												
Sequential	12/16/92		0.00	1.56	0.28	0.00	0.00	1.48	0.00	0.00	0.00	0.00	0.09
Throughfall	12/17/92		0.00	1.39	0.28	0.00	0.00	1.48	0.00	0.00	0.00	0.00	0.09

Appendix A: continued

Sample	Date	Time	Volume (cm)	Depth (m)	^{18}O (‰)	^{2}H (‰)	Si ppm	Al ppm	B ppm	Ba ppm	Ca ppm	Cd ppm	Co ppm	Cr ppm	Cu ppm
	12/17/92		1.10		-10.4	-69	0.00	0.00	0.80	0.03	0.36	0.00	0.00	0.00	0.01
WB60	1/20/92				-5.9										
	2/18/92				-6.0										
	3/16/92				-6.0										
	4/22/92				-6.1										
	5/19/92				-6.0										
	6/23/92				-6.0										
	7/21/92				-6.1										
	8/18/92				-6.0										
	9/15/92				-6.0										
	10/20/92				-6.0										
	11/10/92				-6.0										
	12/15/92	14:55			-6.0		3.53	0.06	0.00	0.03	26.97	0.00	0.00	0.02	0.00
	12/16/92	20:35			-5.9		3.18	0.05	0.00	0.03	24.22	0.00	0.00	0.00	0.00
	12/16/92	22:35			-6.0		3.03	0.07	0.00	0.02	22.51	0.00	0.00	0.00	0.00
	12/17/92	0:35			-6.0		2.84	0.04	0.00	0.03	20.61	0.00	0.00	0.00	0.00
	12/17/92	2:35			-6.3		2.52	0.03	0.00	0.02	18.60	0.00	0.00	0.00	0.00
	12/17/92	4:35			-6.1		2.38	0.03	0.00	0.02	16.87	0.00	0.00	0.00	0.00
	12/17/92	8:35			-5.8		2.82	0.06	0.00	0.02	14.71	0.00	0.00	0.00	0.00
	12/17/92	10:35			-5.9		2.60	0.10	0.00	0.02	11.00	0.00	0.00	0.00	0.00
	12/17/92	12:35			-5.7		0.00	0.04	0.00	0.00	4.03	0.00	0.00	0.00	0.00
	12/17/92	14:35			-6.4		2.59	0.07	0.00	0.02	9.64	0.00	0.00	0.00	0.00
	12/17/92	18:35			-5.9		2.57	0.10	0.00	0.01	9.28	0.00	0.00	0.00	0.00
	12/17/92	22:35			-5.9		2.65	0.04	0.00	0.01	9.47	0.00	0.00	0.00	0.00
	12/18/92	4:35			-5.9		2.65	0.04	0.00	0.02	9.90	0.00	0.00	0.00	0.00
	12/18/92	14:35			-6.1		2.80	0.04	0.00	0.02	10.94	0.01	0.00	0.00	0.00
	12/18/92	22:38			-6.4		3.27	0.00	0.96	0.02	17.43	0.00	0.00	0.00	0.00
WB60	12/19/92	6:38			-5.9		2.97	0.02	0.00	0.03	12.37	0.00	0.00	0.00	0.00
	12/19/92	14:38			-6.2		2.97	0.01	0.00	0.02	12.94	0.00	0.00	0.00	0.00
WB300	12/15/92				-6.6										
	12/17/92	22:00			-6.2										
	12/18/92	22:00			-6.4										
	12/19/92	14:00			-6.6										
WBT360	12/17/92	8:30			-6.5										
WBT440	12/17/92	6:45			-6.0		3.03	0.00	0.72	0.02	3.84	0.00	0.00	0.00	0.00
	12/17/92	8:45			-6.9		2.28	0.03	1.04	0.02	6.96	0.00	0.00	0.00	0.00

Appendix A: continued

Sample	Date	Time	Fe ppm	K ppm	Mg ppm	Mn ppm	Mo ppm	Na ppm	Ni ppm	P ppm	Pb ppm	Sr ppm	Zn ppm
	12/17/92		0.00	1.09	0.08	0.01	0.00	1.08	0.00	0.00	0.04	0.00	0.36
WB60	1/20/92												
	2/18/92												
	3/16/92												
	4/22/92												
	5/19/92												
	6/23/92												
	7/21/92												
	8/18/92												
	9/15/92												
	10/20/92												
	11/10/92												
	12/15/92	14:55	0.00	1.03	15.83	0.01	0.03	0.49	0.00	0.00	0.00	0.02	0.02
	12/16/92	20:35	0.00	1.16	13.70	0.03	0.00	0.36	0.00	0.00	0.00	0.02	0.00
	12/16/92	22:35	0.00	0.86	12.97	0.00	0.00	0.38	0.00	0.00	0.00	0.02	0.00
	12/17/92	0:35	0.00	0.79	11.98	0.01	0.00	0.07	0.00	0.00	0.00	0.02	0.00
	12/17/92	2:35	0.00	1.30	10.57	0.01	0.00	0.16	0.00	0.00	0.00	0.02	0.00
	12/17/92	4:35	0.00	0.61	9.74	0.00	0.00	0.29	0.00	0.00	0.00	0.02	0.00
	12/17/92	8:35	0.00	0.63	8.70	0.11	0.00	0.31	0.00	0.00	0.00	0.01	0.00
	12/17/92	10:35	0.04	1.54	6.28	0.08	0.00	0.11	0.00	0.00	0.00	0.01	0.00
	12/17/92	12:35	0.00	1.09	1.81	0.04	0.00	0.06	0.00	0.00	0.02	0.00	0.00
	12/17/92	14:35	0.03	1.33	5.35	0.06	0.00	0.32	0.00	0.00	0.00	0.01	0.00
	12/17/92	18:35	0.00	1.10	5.19	0.02	0.00	0.45	0.00	0.00	0.00	0.01	0.00
	12/17/92	22:35	0.00	1.14	5.45	0.00	0.00	0.19	0.00	0.00	0.00	0.01	0.00
	12/18/92	4:35	0.02	1.35	5.71	0.01	0.00	0.25	0.01	0.00	0.00	0.02	0.00
	12/18/92	14:35	0.01	1.79	6.37	0.03	0.00	0.37	0.02	0.00	0.00	0.01	0.00
	12/18/92	22:38	0.00	1.08	7.04	0.03	0.00	1.82	0.04	0.00	0.00	0.02	0.14
WB60	12/19/92	6:38	0.00	1.27	7.28	0.01	0.00	0.26	0.00	0.00	0.00	0.02	0.00
	12/19/92	14:38	0.00	1.57	7.78	0.00	0.00	0.32	0.00	0.00	0.00	0.02	0.00
WB300	12/15/92												
	12/17/92	22:00											
	12/18/92	22:00											
	12/19/92	14:00											
WBT360	12/17/92	8:30											
WBT440	12/17/92	6:45	0.03	1.84	1.38	0.00	0.00	1.52	0.00	0.00	0.00	0.01	0.05
	12/17/92	8:45	0.01	2.33	0.71	0.02	0.00	2.02	0.01	0.00	0.00	0.01	0.26

Appendix A: continued

Sample	Date	Time	Volume (cm)	Depth (m)	^{18}O (‰)	^{2}H (‰)	Si ppm	Al ppm	B ppm	Ba ppm	Ca ppm	Cd ppm	Co ppm	Cr ppm	Cu ppm
	12/17/92	9:45			-6.0		2.41	0.03	1.16	0.03	7.40	0.00	0.00	0.00	0.00
	12/17/92	10:45			-6.3		2.49	0.00	1.10	0.03	9.55	0.01	0.00	0.00	0.00
	12/17/92	11:45			-6.0		2.65	0.00	1.20	0.03	10.12	0.00	0.00	0.00	0.01
	12/17/92	13:45			-6.1		2.56	0.00	1.16	0.03	10.08	0.00	0.00	0.02	0.00
	12/17/92	15:45			-6.0		2.57	0.03	1.27	0.03	5.75	0.00	0.00	0.03	0.00
	12/17/92	17:45			-6.1		2.62	0.00	1.06	0.03	5.60	0.00	0.00	0.00	0.00
	12/17/92	21:45			-6.6		2.64	0.00	1.05	0.03	5.71	0.00	0.00	0.00	0.04
	12/18/92	1:45			-6.4		2.70	0.00	1.38	0.02	5.25	0.00	0.00	0.00	0.01
	12/18/92	5:45			-7.4		2.64	0.00	1.14	0.03	6.23	0.00	0.00	0.00	0.00
	12/18/92	13:45			-5.8		2.71	0.00	1.04	0.02	6.42	0.00	0.00	0.00	0.00
	12/18/92	21:45			-5.8		2.66	0.00	0.00	0.03	1.13	0.00	0.00	0.00	0.02
Borehole	12/18/91			0.61	10.7										
	12/18/91			1.24	-7.9										
	12/18/91			2.74	-7.5										
	12/18/91			4.27	-5.6										
	12/18/91			5.79	-5.9										
	12/18/91			7.32	-7.2										
	12/18/91			8.84	-10.6										
	12/18/91			11.28	-7.7										
	12/18/91			13.72											
	12/19/91			15.24	-8.0										
	12/19/91			18.90	-3.8										
	12/19/91			23.17	-5.9										
	12/20/91			26.83	-8.0										
So1-A	12/15/92	15:15			-4.9		4.28	0.58	0.00	0.15	12.56	0.01	0.00	0.00	0.02
So1-B	12/15/92	15:30			-7.2										
So1-A	12/19/92	15:05			-6.3		3.98	0.88	0.00	0.16	7.51	0.02	0.00	0.00	0.04
So1-B	12/19/92	15:15			-5.7		0.03	0.07	0.13	0.02	15.10	0.29	0.00	0.00	0.33
So2-A	12/15/92	15:45			-5.9		2.76	0.43	0.00	0.34	23.63	0.01	0.00	0.00	0.05
So2-B	12/15/92	16:00			-6.8										
So2-A	12/19/92	15:45			-7.0		2.22	0.35	0.00	0.14	9.51	0.00	0.00	0.00	0.02
So3-A	12/15/92	16:15			-6.5		2.73	1.18	0.00	0.18	20.62	0.00	0.00	0.00	0.06
So3-B	12/15/92	16:25			-6.7		0.30	0.66	0.25	0.14	16.88	0.15	0.00	0.00	0.46
So3-A	12/19/92	16:15			-7.7		2.42	0.80	0.00	0.10	9.24	0.01	0.00	0.00	0.04
So3-B	12/19/92	15:25			-5.8										
So4-A	12/15/92	16:45			-6.6		3.10	0.66	0.00	0.30	4.08	0.00	0.00	0.00	0.05

Appendix A: continued

Sample	Date	Time	Fe ppm	K ppm	Mg ppm	Mn ppm	Mo ppm	Na ppm	Ni ppm	P ppm	Pb ppm	Sr ppm	Zn ppm
	12/17/92	9:45	0.04	2.22	0.71	0.02	0.00	2.07	0.00	0.00	0.00	0.02	0.33
	12/17/92	10:45	0.02	1.93	0.73	0.02	0.00	2.05	0.02	0.00	0.00	0.02	0.35
	12/17/92	11:45	0.02	1.99	0.73	0.02	0.00	2.06	0.01	0.00	0.00	0.02	0.34
	12/17/92	13:45	0.00	1.91	0.73	0.02	0.00	1.97	0.04	0.00	0.00	0.02	0.32
	12/17/92	15:45	0.14	1.82	0.69	0.02	0.00	2.23	0.00	0.00	0.00	0.01	0.25
	12/17/92	17:45	0.03	2.16	0.72	0.02	0.00	1.88	0.00	0.00	0.00	0.02	0.35
	12/17/92	21:45	0.00	1.88	0.66	0.00	0.01	1.95	0.00	0.00	0.01	0.01	0.16
	12/18/92	1:45	0.00	2.03	0.70	0.01	0.00	2.40	0.00	0.00	0.00	0.01	0.17
	12/18/92	5:45	0.00	2.01	0.71	0.02	0.00	2.20	0.00	0.00	0.00	0.01	0.26
	12/18/92	13:45	0.00	1.99	0.70	0.02	0.01	1.70	0.00	0.00	0.00	0.01	0.21
	12/18/92	21:45	0.00	1.94	0.63	0.01	0.00	0.50	0.00	0.00	0.00	0.01	0.00
Borehole	12/18/91												
	12/18/91												
	12/18/91												
	12/18/91												
	12/18/91												
	12/18/91												
	12/18/91												
	12/18/91												
	12/18/91												
	12/19/91												
	12/19/91												
	12/19/91												
	12/20/91												
So1-A	12/15/92	15:15	0.00	13.17	2.57	0.41	0.00	6.33	1.33	0.00	0.00	0.06	0.14
So1-B	12/15/92	15:30											
So1-A	12/19/92	15:05	0.04	8.11	1.98	0.34	0.00	1.21	0.43	0.00	0.00	0.04	0.09
So1-B	12/19/92	15:15	0.00	12.52	4.17	0.68	0.01	29.92	1.54	0.00	0.06	0.04	0.13
So2-A	12/15/92	15:45	0.03	16.90	5.94	0.10	0.00	2.12	0.14	0.00	0.04	0.15	0.14
So2-B	12/15/92	16:00											
So2-A	12/19/92	15:45	0.01	9.13	2.42	0.07	0.00	0.91	0.13	0.00	0.05	0.06	0.15
So3-A	12/15/92	16:15	0.15	7.55	4.75	0.32	0.00	3.29	0.95	0.00	0.10	0.11	0.21
So3-B	12/15/92	16:25	0.00	13.87	5.75	0.56	0.00	39.25	1.87	0.00	0.06	0.06	0.59
So3-A	12/19/92	16:15	0.12	8.07	2.47	0.18	0.00	1.41	0.12	0.00	0.04	0.05	0.06
So3-B	12/19/92	15:25											
So4-A	12/15/92	16:45	0.00	6.10	1.49	0.73	0.00	2.85	0.84	0.00	0.06	0.03	0.11

Appendix A: continued

Sample	Date	Time	Volume (cm)	Depth (m)	^{18}O (‰)	^{2}H (‰)	Si ppm	Al ppm	B ppm	Ba ppm	Ca ppm	Cd ppm	Cd ppm	Cr ppm	Cu ppm
So4-B	12/15/92	16:55			-7.3		0.45	0.29	0.31	0.04	22.99	0.45	0.00	0.00	0.72
So4-A	12/19/92	16:45			-6.9		3.10	0.80	0.00	0.20	5.18	0.03	0.00	0.00	0.05
So4-B	12/19/92	16:55			-5.5										
So5-A	12/15/92	17:15					2.21	0.77	0.00	0.07	4.57	0.06	0.00	0.00	0.09
So-5B	12/15/92	17:25					0.75	0.31	0.10	0.04	11.23	0.08	0.00	0.00	0.31
SUBWEIR	12/17/92	11:30			-6.4										
	12/17/92	12:15			-6.3										
	12/17/92	16:50			-6.1										
PS8	2/28/92	17:45		0.700											
	3/4/92	13:05		0.802	-5.8										
	4/29/92	3:55		0.778	-5.6										
	4/29/92	4:02			-5.5										
	7/5/92	16:35		0.914	-5.4										
	7/5/92	16:50			-5.7										
	7/5/92	17:10			-5.9										
	7/24/92	11:35		1.020											
	8/27/92	13:00		0.988	-5.9										
	12/13/92	15:40		0.914	-5.9										
	12/13/92	15:55			-5.8		4.87	1.07	0.00	0.04	9.89	0.00	0.00	0.00	0.01
	12/19/92	14:15		0.560	-5.9		2.63	0.00	0.00	0.01	2.78	0.00	0.00	0.00	0.00
	1/28/93	14:20		0.683											
	3/12/93	13:45		0.884	-6.1										
	3/12/93	14:00			-6.1										
	3/30/93	15:00		0.607	-6.5										
	4/15/93	15:15		0.647											
W5	2/24/92	10:00		3.700	-6.0										
	2/24/92	10:05			-5.9										
	2/24/92	10:10			-6.0										
	2/24/92	10:15			-6.0										
	2/24/92	10:20			-5.9										
	2/24/92	10:30			-6.0										
	3/4/92	13:45		3.502	-5.9										
	3/4/92	14:05			-5.9										
	4/15/92	12:36		3.816	-6.0										
	4/15/92	12:45			-6.0										
	4/15/92	12:50			-6.0										

Appendix A: continued

Sample	Date	Time	Fe ppm	K ppm	Mg ppm	Mn ppm	Mo ppm	Na ppm	Ni ppm	P ppm	Pb ppm	Sr ppm	Zn ppm
So4-B	12/15/92	16:55	0.00	17.62	7.42	1.06	0.00	43.97	3.83	0.00	0.05	0.07	0.53
So4-A	12/19/92	16:45	0.00	8.43	1.80	0.48	0.00	2.01	0.51	0.00	0.04	0.03	0.14
So4-B	12/19/92	16:55											
So5-A	12/15/92	17:15	0.04	4.80	1.41	0.22	0.00	5.52	0.71	0.00	0.04	0.03	0.39
So-5B	12/15/92	17:25	0.00	12.03	3.46	0.31	0.00	21.32	1.36	0.00	0.05	0.04	0.14
SUBWEIR	12/17/92	11:30											
	12/17/92	12:15											
	12/17/92	16:50											
PS8	2/28/92	17:45											
	3/4/92	13:05											
	4/29/92	3:55											
	4/29/92	4:02											
	7/5/92	16:35											
	7/5/92	16:50											
	7/5/92	17:10											
	7/24/92	11:35											
	8/27/92	13:00											
	12/13/92	15:40											
	12/13/92	15:55	0.61	1.44	6.22	0.12	0.00	0.64	0.00	0.00	0.01	0.02	0.02
	12/19/92	14:15	0.00	2.48	1.59	0.00	0.00	0.42	0.00	0.00	0.00	0.01	0.00
	1/28/93	14:20											
	3/12/93	13:45											
	3/12/93	14:00											
	3/30/93	15:00											
	4/15/93	15:15											
W5	2/24/92	10:00											
	2/24/92	10:05											
	2/24/92	10:10											
	2/24/92	10:15											
	2/24/92	10:20											
	2/24/92	10:30											
	3/4/92	13:45											
	3/4/92	14:05											
	4/15/92	12:36											
	4/15/92	12:45											
	4/15/92	12:50											

Appendix A: continued

Sample	Date	Time	Volume (cm)	Depth (m)	^{18}O (‰)	^{2}H (‰)	Si ppm	Al ppm	B ppm	Ba ppm	Ca ppm	Cd ppm	Co ppm	Cr ppm	Cu ppm
	4/29/92	15:27		3.987	-5.8										
	4/29/92	15:42			-5.9										
	7/24/92	12:10		4.890	-6.0										
	8/27/92	13:40		5.046	-6.0										
	12/13/92	15:10		5.482	-6.0										
	12/13/92	15:35			-5.9		3.53	0.13	0.00	0.02	23.65	0.00	0.00	0.00	0.01
	12/19/92	13:40		4.302	-5.9		3.57	0.15	0.00	0.02	19.45	0.00	0.00	0.00	0.02
	1/28/93	11:45		3.738											
	3/12/93	13:20		4.048	-6.0										
	3/12/93	13:40			-6.0										
	3/30/93	15:30		2.735	-5.9										
	3/30/93	15:45			-6.1										
	4/15/93	15:40		2.957											
W6	2/24/92	11:00		8.490	-6.0										
	2/24/92	11:15			-6.2										
	2/24/92	11:30			-6.1										
	3/4/92	14:30		5.541	-8.6										
	3/4/92	14:35			-5.8										
	4/15/92	11:00		6.282	-5.7										
W6	4/15/92	11:20			-5.9										
	4/15/92	11:40			-5.8										
	4/15/92	11:50			-5.9										
	4/29/92	12:30		6.721	-5.8										
	4/29/92	13:24			-6.0										
	6/29/92	17:40		9.341											
	7/24/92	12:50		9.904	-6.0										
	8/27/92	14:40		10.698	-5.8										
	12/13/92	16:50		13.074	-6.4		2.75	0.03	0.00	0.01	1.38	0.01	0.00	0.00	0.02
	12/19/92	15:30		11.932	-6.5		2.82	0.08	0.00	0.01	1.57	0.00	0.00	0.00	0.03
	1/28/93	12:06		6.823											
	3/30/93	17:15		4.569	-6.1										
W7	4/15/92	12:05		25.674											
	4/29/92	12:00		26.157	-5.9										
	6/12/92	17:45		26.114											
	7/5/92	16:45		26.288	-5.9										
	8/27/92	15:00		26.408	-6.0										

Appendix A: continued

Sample	Date	Time	Fe ppm	K ppm	Mg ppm	Mn ppm	Mo ppm	Na ppm	Ni ppm	P ppm	Pb ppm	Sr ppm	Zn ppm
	4/29/92	15:27											
	4/29/92	15:42											
	7/24/92	12:10											
	8/27/92	13:40											
	12/13/92	15:10											
	12/13/92	15:35	0.00	1.48	13.71	0.05	0.00	0.42	0.03	0.00	0.03	0.02	0.00
	12/19/92	13:40	0.00	1.60	11.37	0.01	0.00	0.52	0.03	0.00	0.00	0.01	0.00
	1/28/93	11:45											
	3/12/93	13:20											
	3/12/93	13:40											
	3/30/93	15:30											
	3/30/93	15:45											
	4/15/93	15:40											
W6	2/24/92	11:00											
	2/24/92	11:15											
	2/24/92	11:30											
	3/4/92	14:30											
	3/4/92	14:35											
	4/15/92	11:00											
W6	4/15/92	11:20											
	4/15/92	11:40											
	4/15/92	11:50											
	4/29/92	12:30											
	4/29/92	13:24											
	6/29/92	17:40											
	7/24/92	12:50											
	8/27/92	14:40											
	12/13/92	16:50	0.31	1.57	0.49	0.15	0.00	0.95	0.02	0.00	0.07	0.01	0.03
	12/19/92	15:30	0.08	2.22	0.76	0.11	0.00	0.68	0.03	0.00	0.04	0.01	0.00
	1/28/93	12:06											
	3/30/93	17:15											
W7	4/15/92	12:05											
	4/29/92	12:00											
	6/12/92	17:45											
	7/5/92	16:45											
	8/27/92	15:00											

Appendix A: continued

Sample	Date	Time	Volume (cm)	Depth (m)	^{18}O (‰)	^{2}H (‰)	Si ppm	Al ppm	B ppm	Ba ppm	Ca ppm	Cd ppm	Co ppm	Cr ppm	Cu ppm
	12/13/92	17:10		26.902	-6.2										
	12/19/92	15:50		26.660											
	1/28/93	14:40		25.860											
	3/30/93	17:30		25.600	-6.1										
	4/15/93	13:00		25.170											
S3	1/20/92				-6.3										
	2/18/92				-6.2										
	3/16/92				-6.4										
	4/22/92				-6.0										
	5/19/92				-6.1										
	6/23/92				-6.0										
	7/21/92				-6.0										
	8/18/92				-6.1										
	9/15/92				-6.0										
	10/20/92				-6.0										
	11/10/92														
	12/15/92	14:15			-6.4		3.61	0.06	0.00	0.03	28.07	0.01	0.00	0.00	0.00
	12/17/92	15:53			-5.9		3.26	0.01	0.00	0.02	20.93	0.00	0.00	0.00	0.00
	12/18/92	11:10			-6.7		4.18	0.04	0.85	0.03	29.87	0.00	0.00	0.00	0.01
	12/19/92	14:45			-6.4		3.54	0.05	0.00	0.03	27.42	0.00	0.00	0.00	0.01
S3a	12/15/92	14:16			-6.1		3.55	0.07	0.00	0.03	26.36	0.00	0.00	0.00	0.02
	12/17/92	15:52			-5.9		3.17	0.05	0.00	0.02	16.54	0.00	0.00	0.00	0.00
	12/18/92	11:11					3.97	0.03	0.84	0.02	25.49	0.00	0.00	0.00	0.00
	12/19/92	14:47			-6.4		3.35	0.02	0.00	0.02	24.14	0.00	0.00	0.00	0.03
S4	1/20/92				-6.1										
	2/18/92				-5.9										
	3/16/92				-6.0										
	4/22/92				-5.9										
	5/19/92				-5.6										
	6/23/92				-5.8										
	7/21/92				-5.8										
	8/18/92				-6.0										
	9/15/92				-6.0										
S4	10/20/92				-6.0										
	11/10/92				-5.9										
	12/15/92	14:30			-6.4		3.06	0.02	0.00	0.03	23.29	0.00	0.00	0.00	0.00

Appendix A: continued

Sample	Date	Time	Fe ppm	K ppm	Mg ppm	Mn ppm	Mo ppm	Na ppm	Ni ppm	P ppm	Pb ppm	Sr ppm	Zn ppm
	12/13/92	17:10											
	12/19/92	15:50											
	1/28/93	14:40											
	3/30/93	17:30											
	4/15/93	13:00											
S3	1/20/92												
	2/18/92												
	3/16/92												
	4/22/92												
	5/19/92												
	6/23/92												
	7/21/92												
	8/18/92												
	9/15/92												
	10/20/92												
	11/10/92												
	12/15/92	14:15	0.00	1.94	16.78	0.00	0.01	0.41	0.00	0.00	0.01	0.02	0.04
	12/17/92	15:53	0.00	1.59	12.28	0.00	0.01	0.43	0.00	0.00	0.00	0.02	0.04
	12/18/92	11:10	0.00	2.42	14.75	0.00	0.00	1.80	0.00	0.00	0.00	0.02	0.24
	12/19/92	14:45	0.00	2.39	16.37	0.00	0.00	0.36	0.00	0.00	0.00	0.02	0.00
S3a	12/15/92	14:16	0.00	2.32	15.58	0.00	0.00	0.32	0.00	0.00	0.02	0.02	0.00
	12/17/92	15:52	0.00	2.41	10.09	0.00	0.00	0.10	0.00	0.00	0.00	0.01	0.04
	12/18/92	11:11	0.00	2.25	13.16	0.00	0.00	1.68	0.01	0.00	0.00	0.02	0.27
	12/19/92	14:47	0.00	1.77	14.06	0.00	0.00	0.40	0.00	0.00	0.00	0.02	0.00
S4	1/20/92												
	2/18/92												
	3/16/92												
	4/22/92												
	5/19/92												
	6/23/92												
	7/21/92												
	8/18/92												
	9/15/92												
S4	10/20/92												
	11/10/92												
	12/15/92	14:30	0.00	1.77	13.65	0.00	0.00	0.69	0.01	0.00	0.00	0.02	0.00

Appendix A: continued

Sample	Date	Time	Volume (cm)	Depth (m)	^{18}O (‰)	^{2}H (‰)	Si ppm	Al ppm	B ppm	Ba ppm	Ca ppm	Cd ppm	Co ppm	Cr ppm	Cu ppm
	12/17/92	15:22			-6.4		2.44	0.00	0.00	0.02	5.82	0.00	0.00	0.00	0.03
	12/18/92	11:20			-6.3		2.88	0.00	1.06	0.01	9.67	0.00	0.00	0.00	0.01
	12/19/92	14:20			-6.3		2.69	0.03	0.00	0.01	6.56	0.00	0.00	0.00	0.00
S5	12/15/92	14:40			-6.2		3.59	0.02	1.01	0.01	20.78	0.00	0.00	0.00	0.01
	12/17/92	15:45			-5.8		2.87	0.01	0.00	0.01	10.57	0.00	0.00	0.00	0.02
	12/18/92	11:25			-6.9		3.51	0.00	1.08	0.01	15.05	0.00	0.00	0.00	0.00
	12/19/92	14:17			-5.8		3.05	0.00	0.00	0.01	9.77	0.01	0.00	0.00	0.02

Appendix A: continued

Sample	Date	Time	Fe	K	Mg	Mn	Mo	Na	Ni	P	Pb	Sr	Zn
			ppm	ppm	ppm	ppm	ppm	ppm	ppm	ppm	ppm	ppm	ppm
	12/17/92	15:22	0.00	1.75	3.02	0.00	0.00	0.49	0.00	0.00	0.00	0.01	0.04
	12/18/92	11:20	0.00	1.48	3.17	0.00	0.00	2.02	0.00	0.00	0.00	0.01	0.21
	12/19/92	14:20	0.00	1.54	3.52	0.00	0.00	0.60	0.00	0.00	0.00	0.01	0.00
S5	12/15/92	14:40	0.00	1.51	9.01	0.00	0.00	1.92	0.00	0.00	0.00	0.02	0.27
	12/17/92	15:45	0.00	2.58	6.21	0.00	0.00	0.66	0.00	0.00	0.00	0.01	0.04
	12/18/92	11:25	0.00	1.61	5.75	0.00	0.00	2.05	0.03	0.00	0.00	0.01	0.22
	12/19/92	14:17	0.00	2.11	5.72	0.00	0.00	0.48	0.01	0.00	0.00	0.01	0.00

Appendix B: Determination of tracer concentrations used in hydrograph separation models.

Throughfall:

Throughfall tracer concentrations were applied as weighted incremental averages in some of the hydrograph separation models. Incremental weighted averages were determined as the average of the concentrations of rainfall collected up to the moment in time that the sample was collected. Rainfall which had not yet reached the ground surface was not incorporated into the calculation. For example, using oxygen isotopic compositions of rainfall:

Date	Precip. Vol. (cm)	$\delta^{18}O$ (‰)	Vol.X $\delta^{18}O$	Inc. Wtd. Ave
12/16/92	1.73	-4.6	-8.0	-4.6
12/17/92	1.70	-9.3	-15.8	-6.9
12/17/92	1.10	-10.4	-11.4	-7.8

For some of the separations performed, the first and second rainfall events were considered separately from each other. In this case, the tracer concentration of new water was -4.6 ‰ until the second rainfall event occurred. At the moment the second rainfall event began, the new water tracer concentration was determined as the weighted average of the concentration of rainfall from the second event. Thus, the tracer concentration applied with the onset of the second rainfall event was -9.7‰; ([1.70 cm X -9.3‰] + [1.70 cm X -10.4‰])/(1.70 + 1.10 cm).

Groundwater:

Groundwater tracer concentrations were determined by first separately calculating an average concentration for samples collected from wells and springs before the event. The average tracer concentration of groundwater was then computed as the average of groundwater sampled from wells and springs. This method prevented the favoring of groundwater sampled from springs (a greater number of samples were collected from springs than from wells). An example is provided using $\delta^{18}O$ (‰).

Appendix B continued.

Wells	$\delta^{18}O$ (‰)	Springs	$\delta^{18}O$ (‰)
PS8	-5.8	S3	-6.4
W5	-5.9	S3a	-6.1
W6	-6.4	S4	-6.4
		S5	-6.2
Averages	-6.0		-6.3

Groundwater Average = -6.1‰ (-6.0 + -6.3)/2

Soil Water:

The average tracer concentration of soil water was determined the same way as that of groundwater. For soil water the average tracer compositions of water extracted from the A and B soil horizons were computed first. Second, the average of both sources of soil water was determined. This method allowed for the equal representation of water occurring in both soil horizons. For the silica averages, this method prevented the favoring of A-horizon soil water over water occurring in the B horizon. This is important since the lack of some silica analysis of B horizon soils was due to insufficient sample size, not to the lack of water present. An example follows using $\delta^{18}O$ (‰).

A Horizon	$\delta^{18}O$ (‰)	B Horizon	$\delta^{18}O$ (‰)
1	-4.9	1	-7.2
2	-5.9	2	-6.8
3	-6.5	3	-6.7
4	-6.6	4	-7.3
Average	-6.0		-7.0

Soil water average = -6.5‰ (-6.0 + -7.0)/2

Old water tracer concentrations applied to the two-endmember model:

Pre-event "old" water was determined as the average tracer concentration of soil water and groundwater occurring prior to the rainfall event. These averages were determined by first averaging the pre-event tracer concentrations of soil water and groundwater separately as shown above. An average of the two was then computed. Calculating the

Appendix B continued.

averages in this manner prevented the favoring of one type of water. An example of the method used to determine pre-event tracer concentrations of "old" water using $\delta^{18}O$ (‰) follows.

Groundwater Average = -6.1‰ (above)
Soil water average = -6.5‰ (above)

Average "old" water $\delta^{18}O$ = -6.3‰ = (-6.1 + -6.5)/2

Vita

Amy Lynn Halleran was born on May 14, 1968 somewhere in Beaver County Pennsylvania. When she was four years old, her father, John, and mother, Virginia, packed their belongings, the five children, numerous pets, and all of Amy's rocks and moved to Pittsford, New York. She managed to graduate from Pittsford Sutherland High School in May 1986 and attended college at the State University of New York College at Geneseo the following fall. Under the guidance of Dr. P. D. Boger, she became a geology major, an adult, and was introduced to her future husband, but not necessarily in that order. Amy attended field camp at the University of Indiana in the summer of 1990 and graduated from S. U. N. Y. - Geneseo the following December. She spent the summer of 1991 working at the U. S. Geological Survey Water Resources Research office in Orlando, Florida as a National Association of Geology Teachers Summer Internship awardee. It was this experience that swayed Amy to prefer studying water over rocks. In August of 1991 Amy began graduate work at the University of Tennessee - Knoxville. During her last two years attending UT, she held a Research Assistantship in the Environmental Sciences Division at the Oak Ridge National Laboratory. Immediately after completing her Master's thesis defense in October 1994, Amy began full-time employment at ORNL. She has aspirations for a Ph.D, and other neat stuff, too.